United States
Environmental Protection
Agency

Municipal Environmental Research
Laboratory
Cincinnati OH 45268

EPA-600/2-80-098
August 1980

Research and Development

Design Considerations for a Thermal Decomposition Analytical System

RESEARCH REPORTING SERIES

Research reports of the Office of Research and Development, U.S. Environmental Protection Agency, have been grouped into nine series. These nine broad categories were established to facilitate further development and application of environmental technology. Elimination of traditional grouping was consciously planned to foster technology transfer and a maximum interface in related fields. The nine series are:

1. Environmental Health Effects Research
2. Environmental Protection Technology
3. Ecological Research
4. Environmental Monitoring
5. Socioeconomic Environmental Studies
6. Scientific and Technical Assessment Reports (STAR)
7. Interagency Energy-Environment Research and Development
8. "Special" Reports
9. Miscellaneous Reports

This report has been assigned to the ENVIRONMENTAL PROTECTION TECHNOLOGY series. This series describes research performed to develop and demonstrate instrumentation, equipment, and methodology to repair or prevent environmental degradation from point and non-point sources of pollution. This work provides the new or improved technology required for the control and treatment of pollution sources to meet environmental quality standards.

This document is available to the public through the National Technical Information Service, Springfield, Virginia 22161.

EPA-600/2-80-098
August 1980

DESIGN CONSIDERATIONS FOR A THERMAL DECOMPOSITION ANALYTICAL SYSTEM

by

Wayne A. Rubey
University of Dayton Research Institute
Dayton, Ohio 45469

Grant No. R805117-01-0

Project Officer

Richard A. Carnes
Solid and Hazardous Waste Research Division
Municipal Environmental Research Laboratory
Cincinnati, Ohio 45268

MUNICIPAL ENVIRONMENTAL RESEARCH LABORATORY
OFFICE OF RESEARCH AND DEVELOPMENT
U.S. ENVIRONMENTAL PROTECTION AGENCY
CINCINNATI, OHIO 45268

DISCLAIMER

This report has been reviewed by the Municipal Environmental Research Laboratory, U.S. Environmental Protection Agency, and approved for publication. Approval does not signify that the contents necessarily reflect the views and policies of the U.S. Environmental Protection Agency, nor does mention of trade names or commercial products constitute endorsement or recommendation for use.

FOREWORD

The U.S. Environmental Protection Agency was created because of increasing public and government concern about the dangers of pollution to the health and welfare of the American people. Noxious air, foul water, and spoiled land are tragic testimonies to the deterioration of our natural environment. The complexity of that environment and the interplay of its components require a concentrated and integrated attack on the problem.

Research and development is that necessary first step in problem solution; it involves defining the problem, measuring its impact, and searching for solutions. The Municipal Environmental Research Laboratory develops new and improved technology and systems to prevent, treat, and manage wastewater and solid and hazardous waste pollutant discharges from municipal and community sources, to preserve and treat public drinking water supplies, and to minimize the adverse economic, social, health, and aesthetic effects of pollution. This publication is one of the products of that research and provides a most vital communications link between the researcher and the user community.

The safe, permanent disposal of highly toxic organic wastes is vitally important. The study reported here presents a sophisticated laboratory system that has been designed and assembled to provide fundamental thermal decomposition data on a wide assortment of organic waste materials.

Francis T. Mayo, Director
Municipal Environmental Research
Laboratory

ABSTRACT

The safe, permanent disposal of highly toxic organic wastes is vitally important, and controlled high-temperature incineration is one of the most promising methods for achieving it. For safety reasons, the thermal decomposition properties of a toxic organic substance must be well established before large quantities are subjected to high-temperature incineration. However, there is a serious lack of basic experimental data concerning the thermal decomposition behavior of these organic materials.

In response to this need, a sophisticated laboratory system has been designed and assembled to provide fundamental thermal decomposition data on a wide assortment of organic materials. This thermal decomposition analytical system (TDAS) is a specially designed, closed, continuous system consisting of a versatile and fully instrumented thermal decomposition unit which is connected to dedicated in-line gas chromatography, mass spectrometry, and data reduction equipment. With the TDAS, a wide variety of organic samples can be subjected to analysis, including gases, liquids, solids, and even polymeric materials.

In the TDAS, precisely controlled thermal decompositions are conducted in a narrow-bore quartz tube reactor. The various thermal decomposition products are subsequently collected using a cryogenic adsorptive trap. After thermal desorption, the products are subjected to high-resolution gas chromatographic analysis, and identification of the various decomposition products is accomplished using in-line coupled mass spectrometry. A dedicated minicomputer is used for reducing the analytical data. From the product analyses obtained through a sequence of thermal exposures, the thermal decomposition properties for a given organic sample can be readily obtained.

The TDAS has been designed to generate fundamental thermal decomposition data rapidly, economically, and safely. These laboratory data should be instrumental in establishing acceptable criteria for controlled high-temperature incineration of toxic organic wastes.

This report was submitted in partial fulfillment of Grant No. R805117-01-0 by the University of Dayton Research Institute under the sponsorship of the U.S. Environmental Protection Agency. The report covers the period September 1, 1977 to April 15, 1979, and work was completed as of May 31, 1979.

CONTENTS

Foreword iii
Abstract iv
Figures vi
Tables ix
Abbreviations and Symbols x
Acknowledgments xiv

1. Introduction 1
2. Conclusions 4
3. Recommendations 5
4. System Precursors 6
5. Concept and Basic Design of TDAS 14
6. Thermal Decomposition Unit 20
   - Sample handling and insertion 24
   - Transport of sample and effluent products ... 29
   - Quartz tube reactor 30
   - Collection of effluent products 48
   - TDU instrumentation 50
7. Chromatographic Separation and Analysis 59
8. Mass Spectrometer with Dedicated Minicomputer and Associated Data Reduction Equipment 68
9. Utilization of the TDAS in Thermal Decomposition Studies 73

References 75
Bibliography 89
Appendices

A. Gas flow analysis: a detailed analysis of gas flow and dispersion in a narrow-bore circular cross section tube of folded configuration 91
   - Straight tube of circular cross section 93
   - Folded tube of circular cross section 102
B. Error analysis of mean residence time determination 109
C. Quartz tube reactor heat transfer analysis 112
D. TDAS transducer calibrations 123
E. Preparation of gas chromatographic open tubular columns 131
F. Application of thermal focusing and programmed temperature gas chromatography in the TDAS 139
G. Approximate costs of TDU components 142

FIGURES

Number		Page
1	Transport between adjacent analytical components ...	8
2	Schematics of the first generation discontinuous system	9
3	First generation thermal equipment	10
4	Variety of residence time distributions	12
5	Block diagram of TDAS	15
6	Simplified schematic of TDAS	16
7	Artist's rendering of assembled TDAS	18
8	Diagrams of the TDU	21
9	TDAS residence time distribution	23
10	Sample insertion assembly	25
11	Glass rod probe	27
12	Packed tube probe	27
13	Sample handling devices	28
14	Transport tubing tee connector	31
15	Heated transport lines	32
16	First generation reactor configuration	34
17	Proposed second generation reactor	34
18	Secondary flow and circular cross sectional flow path	36
19	Sectional view of furnace interior	38
20	Quartz tube reactor components	39

Number		Page
21	Assembled quartzware	40
22	Quartzware assembly in three-zone furnace	42
23	Detail of quartz tube reactor	43
24	Additional details of reactor assembly	45
25	Square wave profile of gas phase temperature versus time	46
26	Scanning electron microscope photographs of quartz surfaces	47
27	Schematic of collection trap assembly	51
28	Adsorption trap insert	52
29	TDU console and instrumentation modules	53
30	Interior of gas flow control module	55
31	Fundamental schematic of mass flow transducer	56
32	Pressure transducer schematic	58
33	Schematic of GC column installation	60
34	Glass OTC installation in modified Pye 104	61
35	Glass OTC separation of normal alkanes	63
36	Chromatographic separation of a complex mixture	64
37	Separation of complex chlorinated hydrocarbon mixture	65
38	LKB 2091 GCMS and TDU	69
39	Minicomputer for data reduction	71
40	Mass spectra searching terminal	72
A-1	Effect of residence time bandwidth	92
A-2	Quartz tube reactor data	105
A-3	Relative bandwidth as a function of mean residence time	108

Number		Page
C-1	Details of quartz tube reactor assembly	113
C-2	Simplified version of fine bore connecting tube	114
C-3	Graph of bulk temperature versus distance	120
C-4	Sketch of heat transfer condition	121
D-1	Mass flow transducer calibration	125
D-2	Calibration of transducer readout instrument	126
D-3	Calibration of $\bar{T}_2$ readout instrument	129
D-4	Calibration of temperature selector readout instrument	130
E-1	Capillary cleaning apparatus	133
E-2	Whisker-textured tubing bore	135
E-3	Apparatus for drying glass tube interior	136

TABLES

Number		Page
1	Sample Handling Modes	26
2	TDU Temperatures	33
A-1	Calculated Fluid Dynamic Values	106
D-1	Differential Pressure Transducer Calibration	124
D-2	Mass Flow Transducer Calibration	125
D-3	Calibration of HP-3465A Digital Multimeter	126
D-4	Reactor Temperature Measurements	127
D-5	Omega K-1 Thermocouple Chromel-Alumel	127
D-6	Calibration of Omega Digital Temperature	129
D-7	Calibration of Omega Digital Temperature Indicator Model 175, Type K	130

ABBREVIATIONS AND SYMBOLS

ABBREVIATIONS

AMP	-- operational amplifier
CHAZ	-- N-cyclohexyl-3-azetidinol
DDT	-- dichloro-diphenyl-trichloroethane
GC	-- gas chromatography
GLC	-- gas-liquid chromatography
GCMS	-- gas chromatography mass spectrometry
GCMS-COMP	-- gas chromatography mass spectrometry with dedicated computer
ID	-- inside diameter
MS	-- mass spectrometer
OD	-- outside diameter
OTC	-- open tubular column
PBB	-- polybrominated biphenyl
PCB	-- polychlorinated biphenyl
PGC	-- pyrolysis gas chromatography
PTGC	-- programmed temperature gas chromatography
RTD	-- resistance-temperature detector
TDAS	-- thermal decomposition analytical system
TDU	-- thermal decomposition unit
UV	-- ultraviolet
amu	-- atomic mass unit
eV	-- electron volt
kV	-- kilovolt
ms	-- milliseconds
mv	-- millivolts
tc	-- thermocouple
w	-- watts

SYMBOLS

A_m	-- cross-sectional area
C	-- concentration
$\bar{C}$	-- average radial concentration
D_e	-- effective diffusion coefficient
D_g	-- gas diffusion coefficient
F	-- flow

F_m -- mass flow
F_o -- outlet flow
K -- column permeability
L -- length
L_c -- total length of curved tubing
L_s -- total length of straight tubing
N_{Dn} -- Dean number
N_{Nu} -- Nusselt number
N_{Re} -- Reynolds number
N_{Sc} -- Schmidt number
P_s -- surface perimeter
R -- gas flow resistance
R_l -- resistance of transfer lines
R_n -- nth resistance
R_q -- resistance quartz tube assembly
R_r -- restrictor resistance
R_t -- resistance of trap
T -- temperature
T_b -- bulk temperature
T_o -- outlet temperature
T_s -- inner surface temperature
T_w -- outer wall temperature
T_2 -- average reactor temperature
V -- volume; also maximum velocity in Appendix A
V_o -- outlet volume
V_q -- volume of quartz tube
V_r -- reactor volume
V_t -- transition volume
V_2 -- volume at condition 2
c_p -- specific heat
$\bar{h}$ -- average convective heat transfer coefficient
k -- partition ratio
$\bar{k}$ -- average thermal conductivity
k_e -- average partition ratio at exit

k_i -- initial partition coefficient
m -- mass rate of flow
p -- pressure
p_d -- differential pressure
p_o -- outlet pressure
p_1 -- pressure at condition 1
p_2 -- pressure at condition 2
q -- rate of heat transfer
q_c -- rate of heat transfer by convection
q_k -- rate of heat flow by conduction
r -- radius
r_o -- inner tube radius
r_s -- radius of inner surface
r_w -- radius of outer wall surface
t -- time
t_r -- residence time
$\bar{t}_r$ -- average residence time
t_1 -- time coordinate
v -- velocity
$\bar{v}$ -- average velocity
v_e -- exit velocity
v_m -- mobile phase velocity
x -- coordinate
y -- coordinate
z -- distance and coordinate
z_1 -- revised coordinate
η -- fluid viscosity
θ -- cylindrical coordinate
λ -- coil to tube diameter ratio
ν -- kinematic viscosity
π -- geometric constant
ρ -- density
σ -- statistical standard deviation
σ_t -- time-based standard deviation

σ_z -- distance-based standard deviation

ϕ -- identity in Appendix A

ψ -- probability

ω -- flow profile parameter

ACKNOWLEDGMENTS

The author wishes to acknowledge the support and encouragement of the EPA Project Officers, R. A. Carnes of the Municipal Environmental Research Laboratory and L. Weitzman of the Industrial Environmental Research Laboratory. Thanks are also due to D. S. Duvall, the Principal Investigator for this grant and Head of the Environmental Sciences Division at the Research Institute. During the course of this research effort, many of my colleagues graciously offered suggestions and advice pertaining to the development of this system. Particular appreciation is extended to R. A. Grant for his exceptional scientific glass blowing and his many ideas concerning the fabrication of the system quartzware. We also wish to express our gratitude to J. A. Mescher for her consultation with respect to the mass spectrometry requirements, and to R. N. Ely, who assisted with the transducer installations and calibrations.

SECTION 1

INTRODUCTION

Thousands of organic compounds are used daily in our modern industrial society. Unfortunately, it seems that many of the more useful industrial chemicals also have associated toxicities of one form or another. Even though there are continual searches to find chemical substitutes that are less toxic, for the foreseeable future, there will be large quantities of toxic substances that must eventually be disposed of once they have fulfilled their intended industrial use.

Many procedures have been proposed for the disposal of toxic organic compounds (1,2). Some of these procedures are temporary; that is, they consist essentially of containment methods. Other methods are more permanent in nature, as they produce chemical changes in the substance with the intention of rendering the material safe. Of the various methods involved with changing the structure of the toxic organic molecule, chemical and thermal techniques have received the most attention (3). In addition to the straightforward chemical and thermal reaction procedures, special techniques such as microwave plasma detoxification (4,5) and molten salt decomposition methods (6) have been employed.

Controlled high-temperature incineration is one of the most promising methods for disposal of hazardous organic wastes. Both land-based incineration and incineration on ocean-going vessels have been utilized for the permanent disposal of organochlorine wastes (7) and large quantities of other types of organic industrial wastes (8). Incineration has also been employed for the disposal of various pesticide formulations (9). Although waste disposal by incineration at sea is expensive, it is receiving increased consideration (10).

Before methods can be developed for the immense variety of organic materials, precise information is needed concerning their thermal decomposition properties. Much remains to be learned about the thermal decomposition of these organic materials and the nature of the decomposition products formed. It is anticipated that this basic information can be obtained in the laboratory using very small quantities of sample--micrograms or less.

There are many advantages to generating fundamental thermal decomposition data in the laboratory. First, it is anticipated that these thermal decomposition experiments can be conducted safely in a properly equipped laboratory. There would be a much higher element of risk if the initial studies were conducted in larger throughput units. Second, data generated in the laboratory can be much more precise and comprehensive than thermal decomposition data generated in field-scale studies. Third, laboratory thermal decomposition data can be obtained economically and in a short period of time.

Once the thermal decomposition properties of a particular material have been characterized in the laboratory, the preliminary decision can be made as to whether high-temperature incineration is a viable disposal route for that particular material. If no adverse characteristics are detected during the laboratory experiments then, with due caution, the material can be subjected to larger-scale thermal decomposition studies. However, if the laboratory data indicate difficulties or problem areas, then incineration is probably not a viable disposal method for that particular substance.

As an example, chlorinated hydrocarbons are indeed valuable industrial chemicals; however, they are also known for their chronic and sometimes acute toxicity. Many of the compounds on the recent priority pollutant list are members of the chlorinated hydrocarbon family. High-temperature incineration is being considered for the disposal of many of these chlorinated hydrocarbons. From previous thermal decomposition experiments with chlorinated hydrocarbons and chlorocarbons, it was determined that detailed thermal decomposition data were necessary before conducting large-scale thermal disposal operations. Specifically, it was concluded that although the parent molecule may be dealt with at certain thermal exposures, other secondary or intermediate reaction products may be produced that are more toxic than the parent substance. Consequently, there is an urgent need to determine the full thermal destruction data for toxic organic materials before progressing to the larger-scale disposal units.

Laboratory-scale thermal decomposition studies of various organic materials are being performed at the University of Dayton Research Institute. These experiments are being conducted using recently developed second generation thermal decomposition instrumentation. The present instrumentation is referred to as a thermal decomposition analytical system (TDAS). This system incorporates a versatile in-line thermal decomposition unit with sophisticated analytical instrumentation capable of analyzing the various decomposition products.

The objective of this report is to describe, in detail, the various aspects associated with the design of the TDAS. This

second generation system has been designed specifically to provide precise and accurate thermal decomposition data for a wide variety of organic samples. The TDAS has also been designed to provide this information safely and in a short period of time.

SECTION 2

CONCLUSIONS

A versatile thermal decomposition analytical system (TDAS) has been designed, assembled, and tested. With this laboratory system, the thermal decomposition behavior of toxic organic substances and a wide assortment of other organic compounds can be experimentally determined. The effects of the major thermal decomposition variables (i.e., exposure temperature, composition of atmosphere, mean residence time and residence time distribution, and reactor internal pressure) can be individually investigated with the TDAS.

A number of specific design features have been incorporated into this comprehensive system, with the following results:

- Because of the closed continuous design concept of this system, toxic samples can be safely tested.
- A sample can be subjected to a very precise thermal exposure in the TDAS. At selected reactor temperatures ranging from 200° to 1150°C, the maximum temperature variation is less than ±2°C.
- This system is capable of subjecting a sample to a precise mean residence time ranging from 0.25 to 5.0 seconds. In addition, this system provides a narrow Gaussian residence time distribution.
- With the flexibility designed into the TDAS, thermal decomposition studies can be conducted using pure organic substances or organic mixtures, and only small quantities of sample are needed (micrograms). Samples can be either gases, liquids, or solids. In addition, these samples can be subjected to thermal decomposition studies in any of a wide variety of atmospheres.
- Comprehensive analyses of the thermal decomposition products are performed through the use of gas chromatography/mass spectrometry (GCMS) analytical instrumentation.
- The TDAS can provide fundamental thermal decomposition data economically and on a quick response basis.

SECTION 3

RECOMMENDATIONS

The thermal decomposition properties of organic substances can be determined with the use of a specially designed thermal decomposition analytical system (TDAS). It is therefore recommended that this laboratory system be utilized for establishing the thermal decomposition behavior of individual toxic organic substances and multicomponent industrial organic wastes. Such fundamental thermal decomposition data would be instrumental in determining the thermal requirements necessary for environmentally acceptable disposal of hazardous materials.

SECTION 4

SYSTEM PRECURSORS

The incineration of toxic organic wastes is profoundly different from the typical incineration of municipal refuse. The temperatures required for adequate thermal decomposition of hazardous organic materials are much higher than those employed in other types of incineration. These incineration temperatures must be sufficient to decompose not only the parent organic molecule, but also the various intermediate thermal reaction products (11,12).

The residence time of molecules at these elevated temperatures must be sufficient to produce complete thermal decompositions. Therefore, to insure that organic compounds experience sufficient temperature and residence time, high-temperature afterburners are usually incorporated in the process stream. The design and selection of materials for these high-temperature afterburners has received a considerable amount of study, and work is ongoing in this area (13,14).

Recommended guidelines have been prepared for selecting the exposure temperature, residence time, and excess oxygen needed for the incineration of hazardous organic waste materials (15). Most of the data compiled thus far have been associated with the decomposition of the parent molecule. Detailed data pertaining to the various products formed during the thermal decomposition are practically nonexistent.

Instrumental chemical analysis techniques have been employed for many years in the monitoring of effluents from thermal reactors and various thermal analysis instruments. Some of these effluent monitoring techniques (15-22) rely upon periodic GC separations and quantitations of the emerging products. Other methods of monitoring effluents employ different forms of analytical instrumentation (23-26). Gas chromatography (GC) has been used extensively for monitoring combustion devices (27), and also for monitoring the effluents from microreactor devices that have been incorporated into the GC flow path (28).

Thermal reactors with in-line effluent sensing instrumentation have been used in basic reaction kinetic experiments (29, 30). The coupling of thermal analysis instrumentation with GC has been used extensively in working with nonvolatile organic

materials such as plastics and polymers. The term pyrolysis gas chromatography (PGC) has been applied to this coupled instrumentation technique, and it is used routinely for the analysis and characterization of organic polymeric substances (31-35).

A gas chromatograph is an extremely versatile and sensitive analytical instrument. If due consideration (36) is given to the transport of sample between adjacent analytical components (see Figure 1), it is then possible to assemble analytical systems that by their nature can provide a vast amount of information. There are many benefits associated with the analytical system approach. Briefly, precise information can be obtained rapidly from analytical systems that cannot be gathered from isolated instrumental analysis techniques.

From previous experiences with systems (37,38) that used GC in conjunction with thermal analysis instrumentation, a system was developed that involved a high-temperature quartz tube reactor and a GC. Schematics of this discontinuous system are shown in Figure 2, and a photograph of the assembled thermal decomposition equipment is presented in Figure 3. With this system, a sample was first gradually vaporized in a continuously flowing carrier gas and then passed through a narrow-bore, high temperature quartz tube. Upon emergence from the controlled high-temperature exposure, the various condensable effluent products were captured by an adsorptive trap. This trap was then inserted into the modified chromatograph, where the products were thermally desorbed and subsequently analyzed by programmed temperature GC (39-42).

A number of environmentally important compounds have been examined for their thermal decomposition properties with the above relatively simple discontinuous system: DDT, Mirex, Kepone, hexachlorobenzene, PCBs, hexachlorocyclopentadiene, and PBBs. Other workers (43-44) have employed similar instrumentation to determine the thermal decomposition properties of some volatile compounds of high environmental interest such as benzene, vinyl chloride, and acrolein.

The determination of thermal decomposition properties in the laboratory can be accomplished with very small amounts of sample; in addition, the various parameters affecting the thermal decomposition can be closely controlled. How well these laboratory data extrapolate to field scale units remains to be seen. However, in one particular case (the Kepone Incineration Test Program at Toledo, Ohio), close agreement was found between laboratory thermal decomposition data and that obtained from a special pilot-scale test facility (45).

Although the relatively simple discontinuous system as shown in Figure 2 provided some much needed information in a relatively short period of time, it was already apparent that

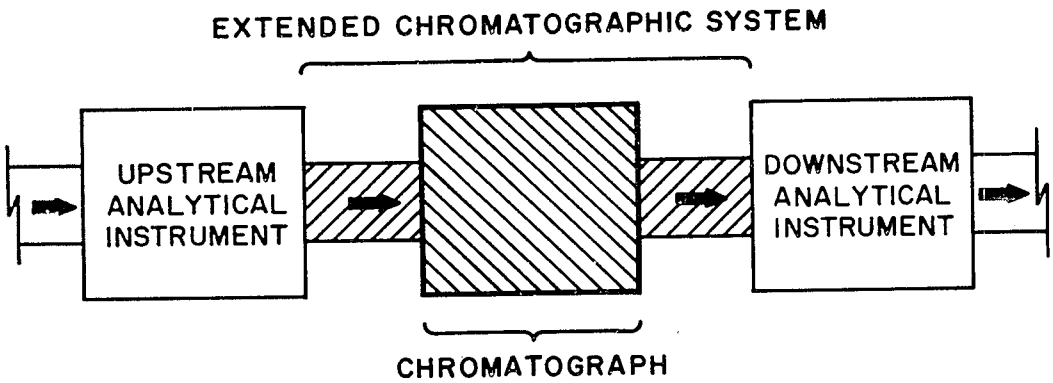

Figure 1. Transport between adjacent analytical components.

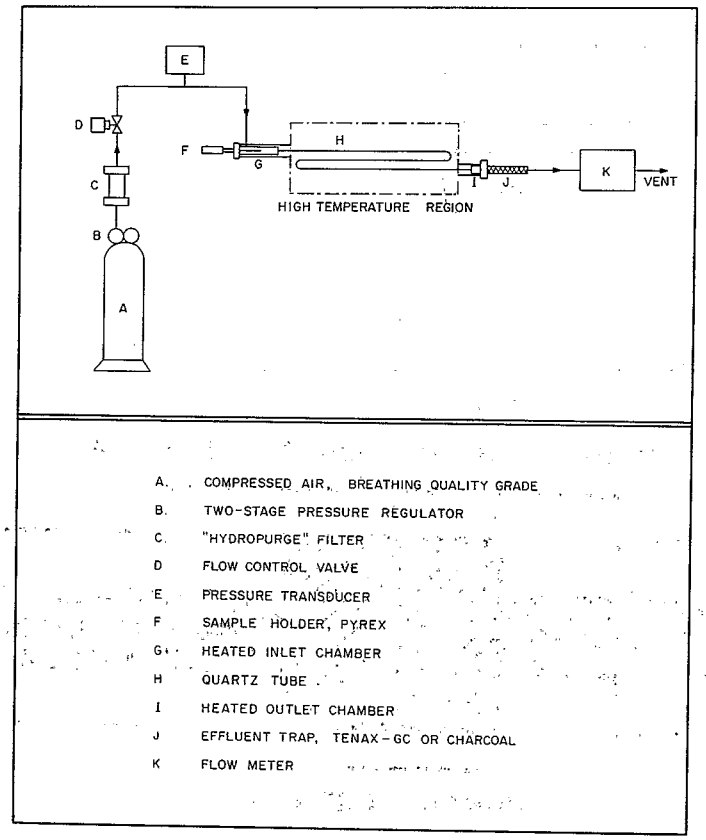

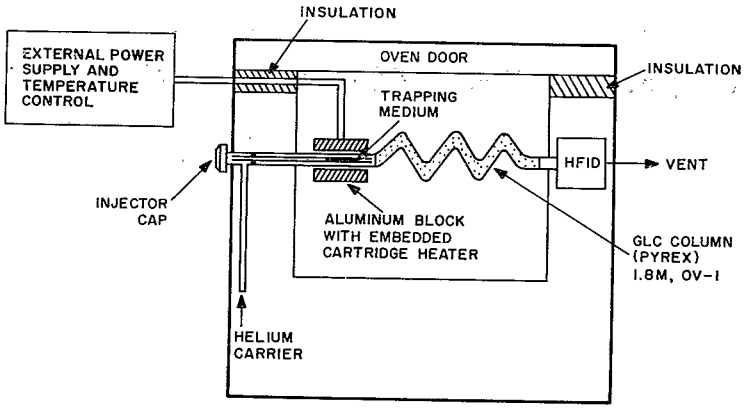

Figure 2. Schematics of the first generation discontinuous system.

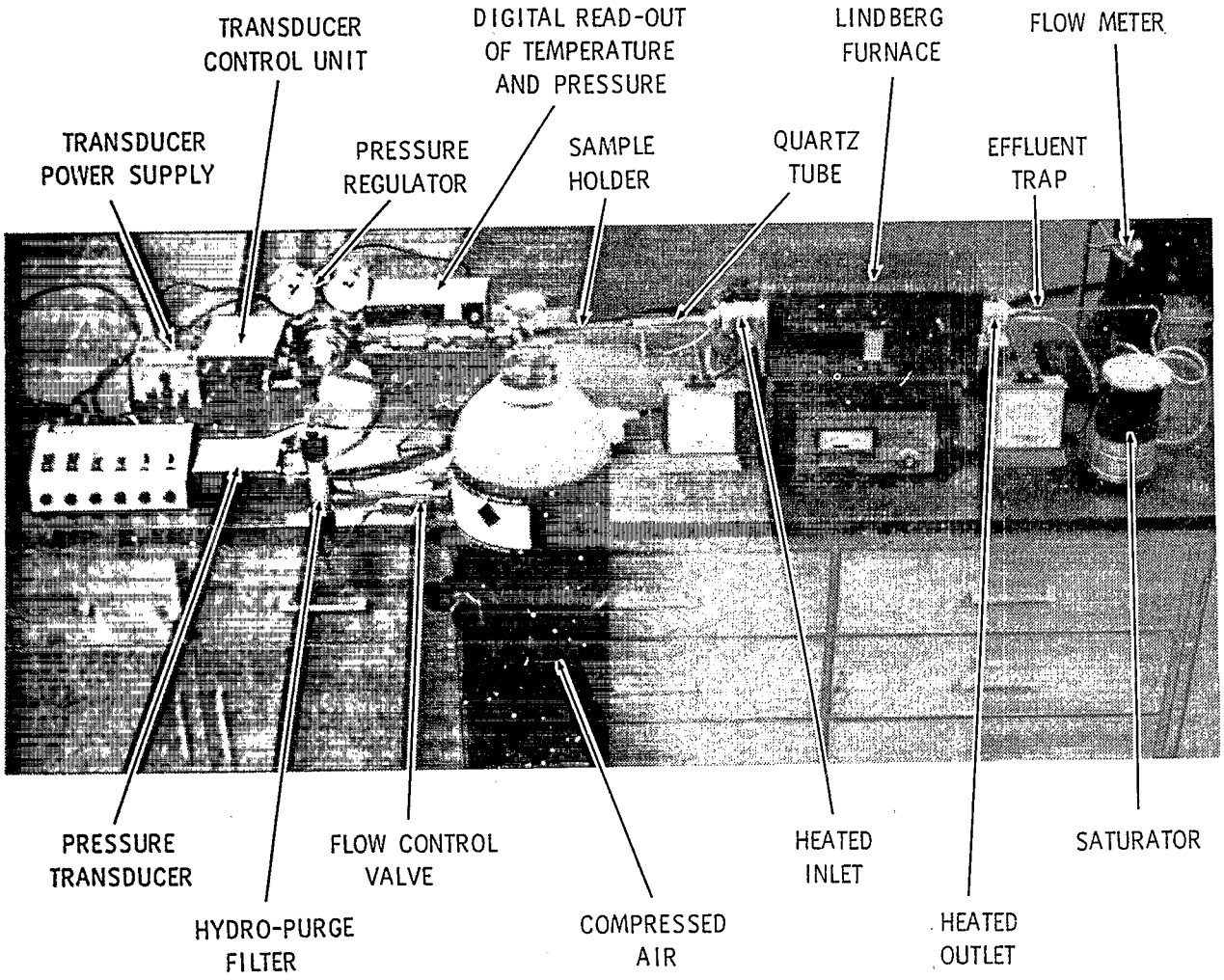

Figure 3. First generation thermal equipment.

this thermal concept could be vastly improved to provide a highly versatile in-line closed system capable of dealing with a wide range of thermal decomposition problems. An expanded system with increased versatility is definitely needed to handle a wider range of toxic organic samples and to accommodate the very complex mixtures of thermal decomposition products. The large number of products formed at intermediate temperatures and the inability to sufficiently separate and identify these products necessitated the use of more sophisticated analytical instrumentation. Also, the advantages presented by an in-line closed system would be such that gases, liquids, solids, mixtures thereof, and even nonvolatile organics could be tested. At the same time, it was realized that a more sophisticated reactor could be designed and fabricated. This device could be fully instrumented and thereby provide very accurate thermal decomposition data along with the corresponding detailed chemical analysis of the effluent products.

GC is an extremely valuable technique for separating and quantitating organic compounds that can be volatilized. However, it has a weakness when it comes to qualitative analysis or identification of the various constituents of a complicated organic mixture (46). This shortcoming of GC has been all but overcome by the combined instrumental analysis technique of GCMS. This powerful instrumental combination is ideally suited for the analysis of organic pollutants (47-49). Also, coupled GCMS seems to be compatible with an upstream in-line thermal reactor.

With respect to the thermal reactor, it is important that the mean residence time and the residence time distribution be accurately known. This is one of the distinct advantages of determining a material's thermal decomposition properties while in the laboratory. For example, in the much larger pilot- and field-scale units, a wide variety of residence time distributions might be encountered, as typified by the residence time profiles shown in Figure 4. For experiments conducted in the laboratory, a narrow bore flow path can be used that produces residence distributions as shown in Figure 4(f). Thus if the residence distribution is known, one can avoid the situation in which some molecules rapidly pass through the high-temperature zone, and other similar molecules experience a sustained exposure.

After considering these concepts and desired improvements, we decided that a suitable thermal decomposition system could be designed and assembled that would have a wide range of versatility. Such a system would be capable of handling and testing various toxic organic waste materials--both relatively pure substances and very complicated organic mixtures. Also, broader ranges of exposure temperature and mean residence time were anticipated for this system. Likewise, with appropriate instrumentation, this system should be capable of conducting tests at different reactor pressures. In addition, this system

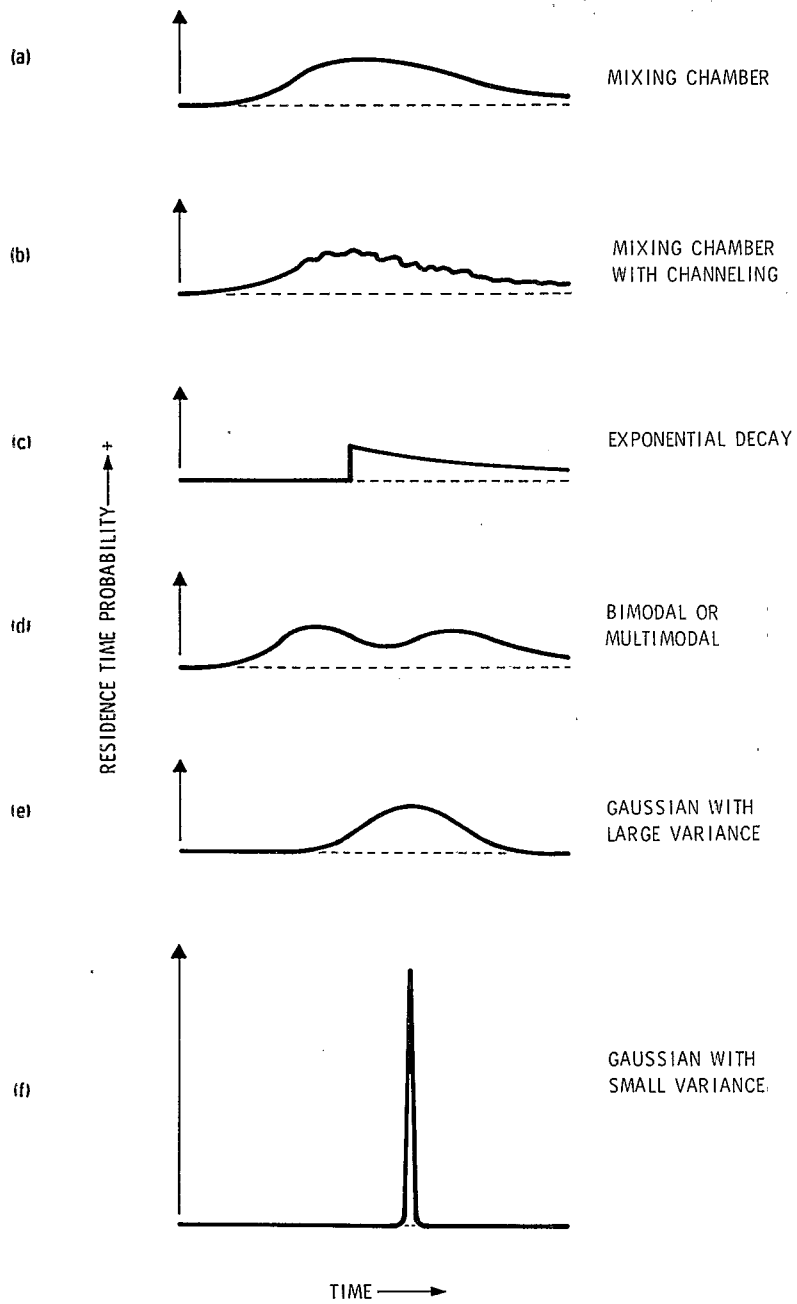

Figure 4. Variety of residence time distributions.

should be capable of conducting thermal decomposition tests in a variety of flowing atmospheres -- for example, air, nitrogen, helium, and mixtures thereof.

SECTION 5

CONCEPT AND BASIC DESIGN OF TDAS

The rationale behind the design concept of the TDAS has not changed basically from that of the earlier discontinuous system (39,40). The sample is still inserted into the system and then gradually vaporized in a flowing carrier gas. The vaporized compounds are subsequently subjected to a controlled, high-temperature exposure. The components that emerge from the high-temperature environment are then collected and subjected to instrumental chemical analysis. This same thermal analysis format has been employed with respect to the TDAS, but each operation within the system is much more sophisticated, thereby producing greatly increased experimental versatility. Each of these procedural operations will be discussed at length later in the report.

The major design changes over the earlier system are centered around the design of the reactor, the closed continuous system concept, and also the vastly increased analytical capability that is now provided by an in-line gas chromatograph/mass spectrometer/dedicated computer (GCMS-COMP). Numerous refinements have also been designed into the TDAS, and these are detailed in Sections 6 and 7.

Many design objectives were associated with the development of the TDAS. This system should be capable of conducting precise thermal decomposition tests. More precisely, it should be capable of experimentally determining the effects of the five prominent thermal decomposition variables--exposure temperature, gaseous atmosphere, pressure, mean residence time, and residence time distribution. In addition, the TDAS should be able to accommodate almost any type of organic material. Also, it should be capable of analyzing all of the thermal decomposition effluent products. This closed continuous system should be capable of dealing with toxic materials. Also, the TDAS should be capable of generating data on a quick response basis.

Figure 5 shows a block diagram of the TDAS, and Figure 6 is a simplified schematic of the assembled TDAS components. Studies can be conducted with the TDAS using almost any compressed gas as the carrier and thermal decomposition atmosphere. Indeed, pyrolytic studies can be performed using inert gases, and oxidative studies can be conducted using air or any other

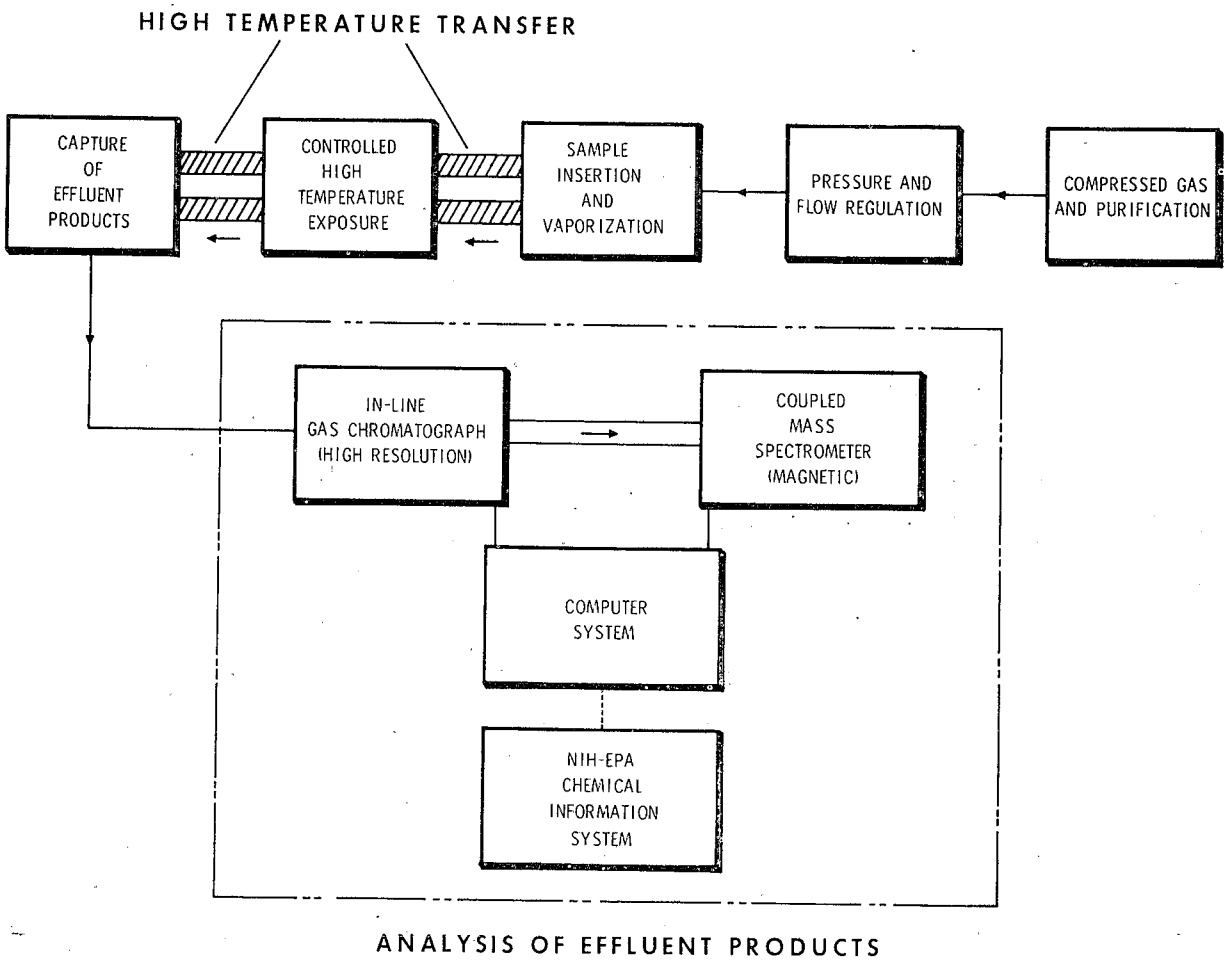

Figure 5. Block diagram of TDAS.

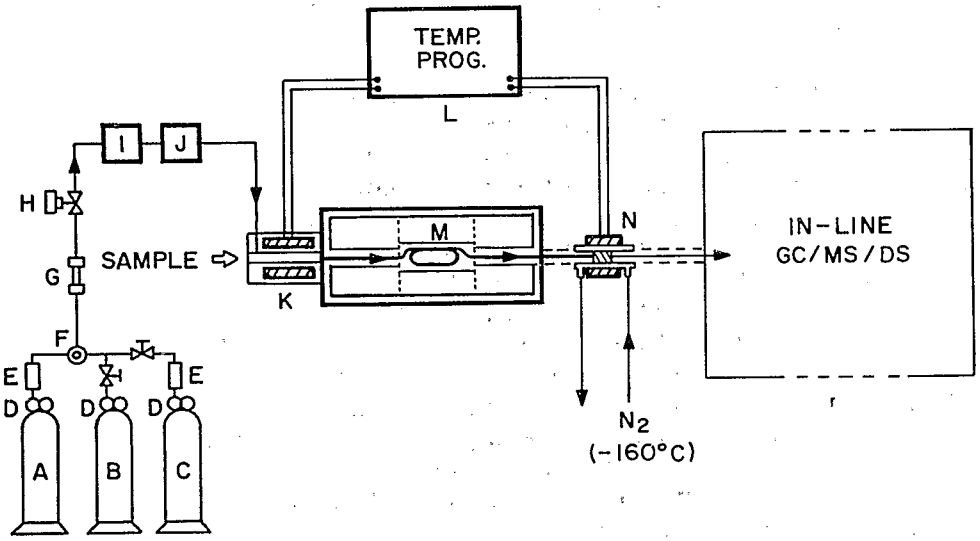

A. HELIUM GAS
B. COMPRESSED AIR
C. INERT CARRIER
D. PRESSURE REGULATOR
E. OXYGEN SCRUBBER
F. DIRECTIONAL VALVE
G. FILTER
H. FLOW CONTROL VALVE
I. FLOW TRANSDUCER
J. PRESSURE TRANSDUCER
K. INSERTION CHAMBER
L. TEMPERATURE PROGRAMMER
M. REACTOR IN FURNACE
N. PRODUCT COLLECTION TRAP

Figure 6. Simplified schematic of TDAS.

oxygen-containing carrier. Accurate measurements of pressure and flow can be readily obtained with the TDAS. The internal pressure in the reactor and mass flow rate (thus mean residence time) can be continuously monitored by in-stream instrumentation.

In the earlier work with the discontinuous system, only low-volatility organic samples could be tested. The TDAS has been designed for measuring the thermal decomposition properties of a wide range of organic samples--gases, liquids, solids, and even polymers. Complicated organic mixtures can also be tested with the TDAS by using the process of slow vaporization of the sample. After vaporization, the gas phase molecules are subjected to precise high-temperature conditions (these range between 200° and 1150°C and are held with ±2°C) in a fused quartz tube reactor. The emerging products are then rpaidly swept into a cryogenic, adsorbent in-line trap where the condensable products are captured at temperatures down to minus 110°C. The collected effluent products are subsequently thermally desorbed from the trap and then subjected to GC analysis using high-resolution glass, open tubular columns. The separated compounds are then subjected to detailed analysis by mass spectrometry (MS). The thermal decomposition test parameters and the chemical analysis data are then retained, and a complete analysis of the thermal decomposition process is carried out.

Although the TDAS is a complicated system with many interacting components, the operation of this system and the conducting of thermal decomposition tests can be accomplished with relative ease (that is, after suitable familiarization and experience). Most of the crucial instrumentation for conducting experiments with the TDAS have been mounted in an instrumentation console, and most of the test functions can be continuously monitored on this console.

An artist's rendering of the assembled TDAS is presented in Figure 7. This equipment is located in a temperature and humidity controlled laboratory that was specifically designed for conducting sensitive chemical analyses.

The basic procedure for testing a particular sample* begins with selection of the thermal decomposition atmosphere or carrier gas. Next, the mode of sample insertion must be selected. Then the actual exposure temperature is chosen, and each of the furnace zones are set to this temperature. The internal pressure under which the test is to be conducted can now be established by adjusting the gas flow restrictors situated downstream of the reactor. The next parameter to be established is the mean

*All samples subjected to analysis by the TDAS would be screened beforehand using other chromatographic instruments to verify that the sample would indeed be conducive to a TDAS examination.

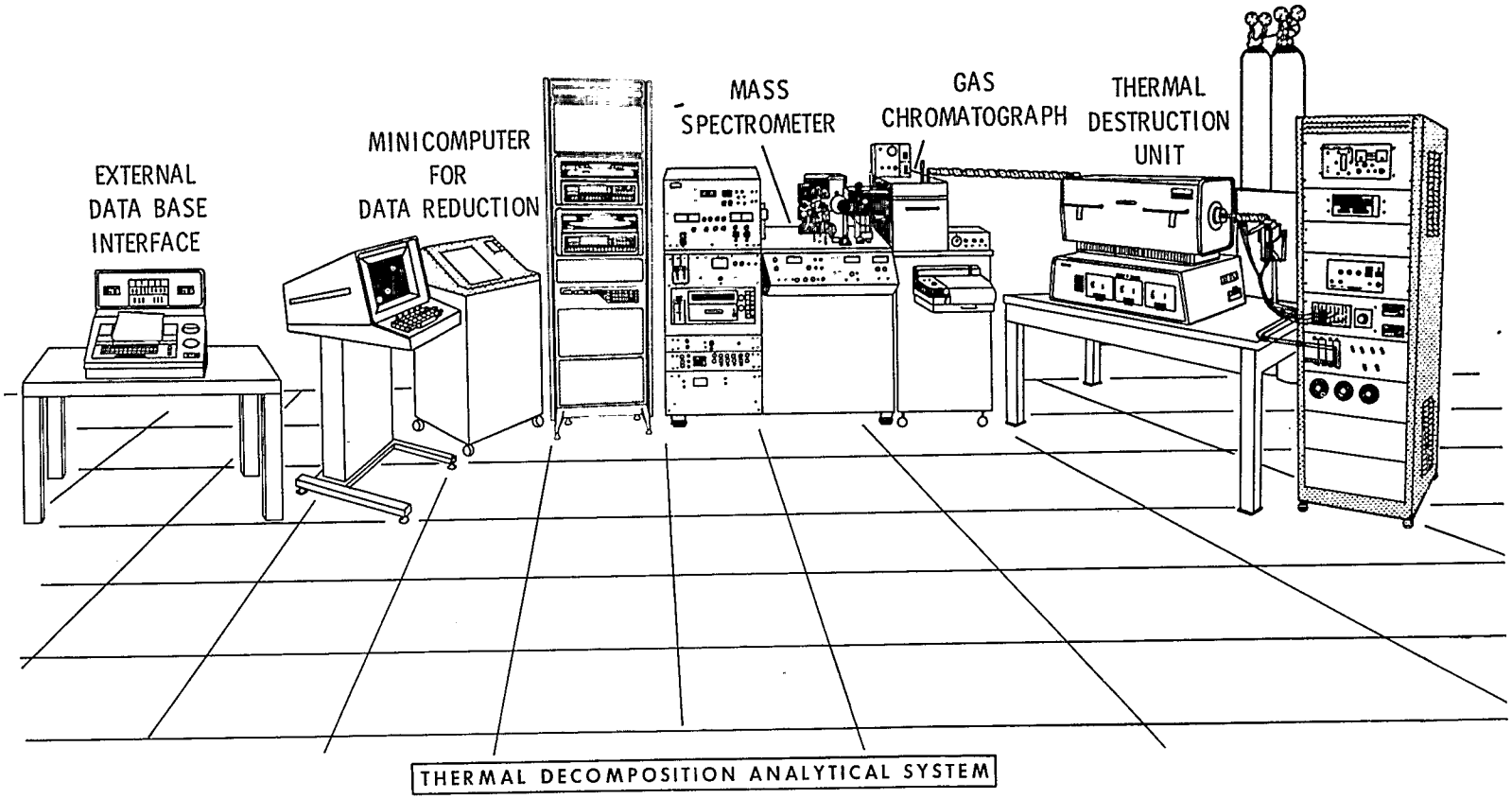

Figure 7. Artist's rendering of assembled TDAS.

residence time. Once the other variables have been stabilized and measured, it is a simple matter of calculating the desired carrier flow and dialing off that value with the adjustable flow control.

After establishing the thermal decomposition test parameters, the next step in the procedure is to cool down the effluent collection trap so that the condensable products can be captured in the adsorptive cryogenic trap. The remaining steps are relatively routine. The sample must then be admitted, the products collected, and after switching to helium carrier gas, the captured products must be subjected to in-line analysis by GCMS-COMP.

The above test procedures would yield one set of data points in the thermal decomposition procedure. Any one of the above variables could now be changed for the next thermal decomposition test, and so on, until the thermal decomposition properties of the sample are adequately characterized.

Extensive design details covering the various TDAS component parts and assemblies are presented in the following sections.

SECTION 6

THERMAL DECOMPOSITION UNIT

The TDAS is a continuous system that can be viewed as three in-line instrumental stations or units. The first unit in the system is designated as the thermal decomposition unit (TDU). Block diagrams of the TDU are shown in Figure 8. Specifically, this unit consists of the various gas supplies, an instrumentation control console, the sample insertion chamber along with the high-temperature reactor, the effluent collection trap, and the various associated transfer lines. All of these components will be discussed later in this section.

The primary function of the TDU is to subject gas phase molecules to well-defined thermal exposures and to collect the various emerging chemical compounds. The remaining stations of the TDAS will subsequently separate and analyze these collected compounds.

The schematic shown in Figure 8(a) can be redrawn as in Figure 8(b) to depict the physical relationships within the gas flow path of the TDU. From this sketch, it is seen that the pressures, temperatures, and volumes can be related according to the ideal gas law as follows:

$$\frac{V_2 p_2}{\bar{T}_2} = \frac{V_o p_o}{T_o} \tag{1}$$

where V is volume, p is pressure, T is temperature, and $\bar{T}$ is temperature averaged over the length of the reactor. The subscript 2 denotes the quartz tube interior, and the subscript o represents the ambient outlet conditions.

If the impedance or resistance to gas flow presented by the downstream transfer lines R_ℓ, the packing within the trap R_t, and the restrictor R_r, is such that

$$(R_\ell + R_t + R_r) \gg R_q \tag{2}$$

where R_q represents the resistance to gas flow of the quartz tube reactor assembly, then the differential pressure P_d can be

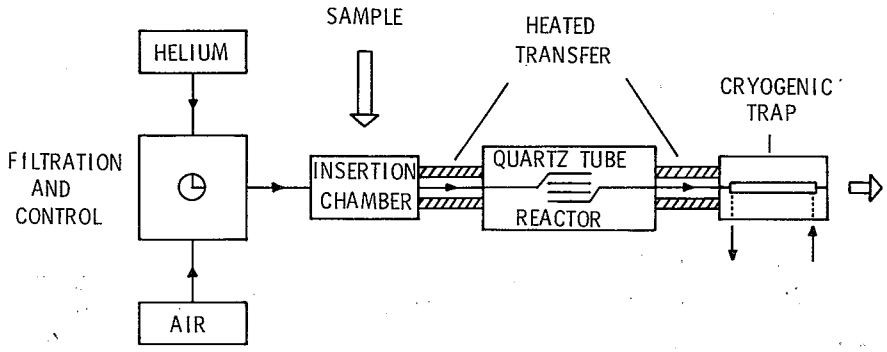

a) BASIC SCHEMATIC

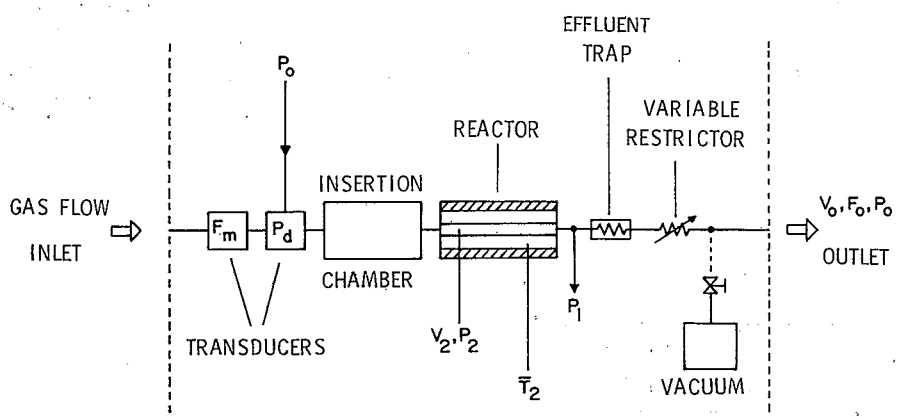

b) SCHEMATIC REDRAWN TO SHOW PHYSICAL RELATIONSHIPS WITHIN THE GAS FLOW PATH

Figure 8. Diagrams of the TDU.

expressed as

$$p_d = p_2 - p_o = p_1 - p_o \tag{3}$$

Now, volume flow F can be written as

$$F = \frac{V}{t} \tag{4}$$

where t is time, and equation 1 can be rewritten as

$$\frac{V_2 p_2}{\overline{T}_2} = \frac{F_o t p_o}{T_o} \tag{5}$$

or

$$\frac{\pi r^2 L p_2}{\overline{T}_2} = \frac{F_o t p_o}{T_o} \tag{6}$$

where r and L are the tube radius and length, respectively. Therefore, it is seen that time, or, in this case, residence time, can be written simply as

$$\overline{t}_r = \left(\frac{\pi r^2 L}{F_o}\right)\left(\frac{T_o}{\overline{T}_2}\right)\left(1 + \frac{p_d}{p_o}\right) \tag{7}$$

where $\overline{t}_r$ represents the calculated mean residence time of a substance in the quartz tube interior.

The equipment used to measure these parameters will be discussed at length later in this section. Also, an error analysis associated with these measurement variables is presented as part of the appendices.

One of the distinct advantages in conducting thermal decomposition experiments using the laboratory scale TDAS is that each molecule is subjected to essentially the same thermal exposure. To illustrate, consider the transport of like molecules through the high-temperature reactor. First, the individual molecules experience random entry into the gas flow over a relatively long period of time. However, as the pressure, temperature, and linear gas velocity within the reactor are constant, the individual molecules generate a residence time distribution as shown in Figure 9.

There are many advantages in having a Gaussian or normal residence time distribution. Linear combinations of Gaussian random variables lead to new random variables that are also Gaussian. Such simplicity is not the case for most other

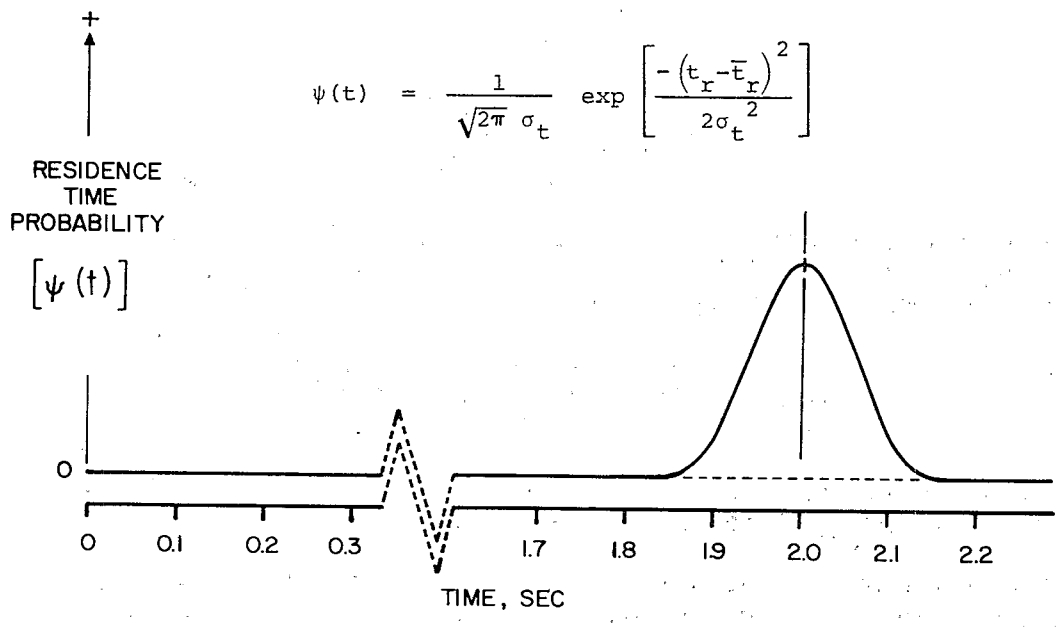

$$\psi(t) = \frac{1}{\sqrt{2\pi}\,\sigma_t} \exp\left[\frac{-\left(t_r-\bar{t}_r\right)^2}{2\sigma_t^{\,2}}\right]$$

Figure 9. TDAS residence time distribution.

distribution functions. This is but one of the desirable features of working with the narrow Gaussian function as opposed to some of the skewed and distorted distribution profiles depicted earlier in Figure 4.

Before the sample handling in the TDU is described, it is interesting to note from Figure 8 that both the mass flow transducer and the pressure transducer are upstream, yet in-line with the reactor and product collection trap. Therefore, with the use of these in-line sensing devices, thermal decomposition experiments can be conducted at subatmospheric, atmospheric, or elevated pressure.

SAMPLE HANDLING AND INSERTION

The sample insertion section of the TDAS was designed to be as versatile as possible. This fabricated sample insertion assembly is rigidly mounted on a machined aluminum support located between the TDU instrumentation console and the high-temperature reactor furnace. A photograph of this assembly is presented in Figure 10. The actual sample reception chamber consists of fused quartz tubing surrounded by an isolated aluminum block that can be readily heated and temperature programmed.

The exit end of the sample reception chamber empties into 1.0 mm ID quartz tubing that is connected to the inlet of the quartz tube reactor assembly. An outer jacket of quartz tubing surrounds this small bore transfer tube, so that by using a counter flow of heat transfer air, a uniform temperature distribution is obtained for the transport of the gas sample to the reactor assembly.

There are numerous modes for inserting samples into the TDAS, and because of the built-in flexibility, almost any type of organic sample can be examined. Some of these sample handling modes are listed in Table 1. A sketch of the glass or quartz rod probe is shown in Figure 11, and the special packed tube probe is depicted in Figure 12. A photograph of the different sample handling devices is shown in Figure 13.

The one major requirement with respect to sample handling with the TDAS is that substances leaving the sample insertion chamber must be in the gas phase. Precautions must be taken to prevent particulate material from migrating into the heated transfer lines and the high-temperature quartz tube assembly.

TDAS samples are either volatilized or thermally degraded in the sample insertion chamber. Volatilization is accomplished by controlled heating of the insertion chamber with a special temperature programmer. If sample thermal degradation is required, it can be accomplished using the probe sample holders

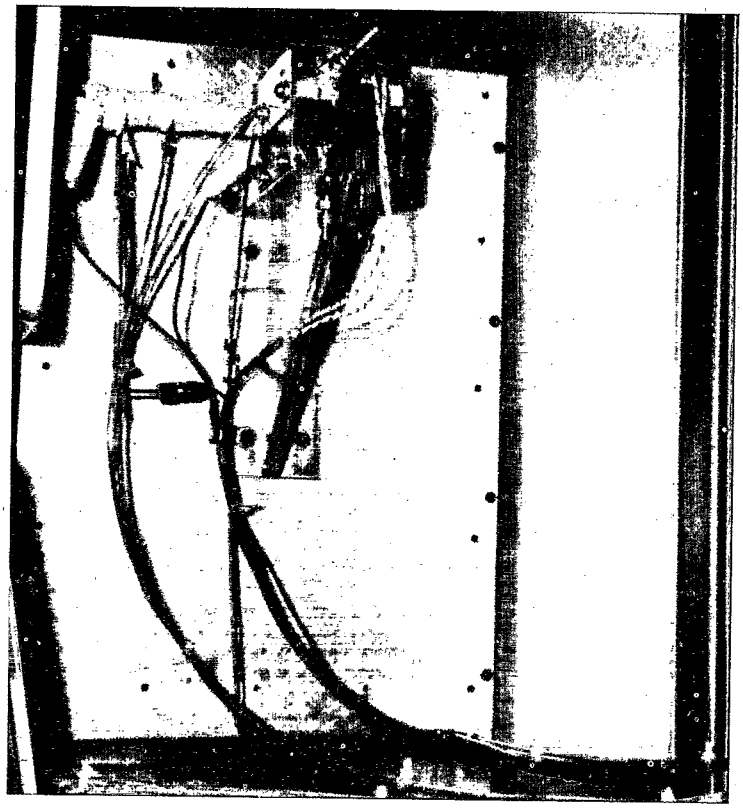

Figure 10. Sample insertion assembly.

TABLE 1. SAMPLE HANDLING MODES

Types of organic samples	Mode of insertion into TDAS
Gases	• Gas sampling valve • Gas-tight syringe
Liquids (low and high volatility substances)	• Syringe • Ampoule • Quartz rod probe
Solids (molecular weights less than 800)	• Platinum ribbon probe • Quartz rod probe • Packed tube probe
Non-volatiles or polymeric organics	• Platinum ribbon probe • Packed tube probe

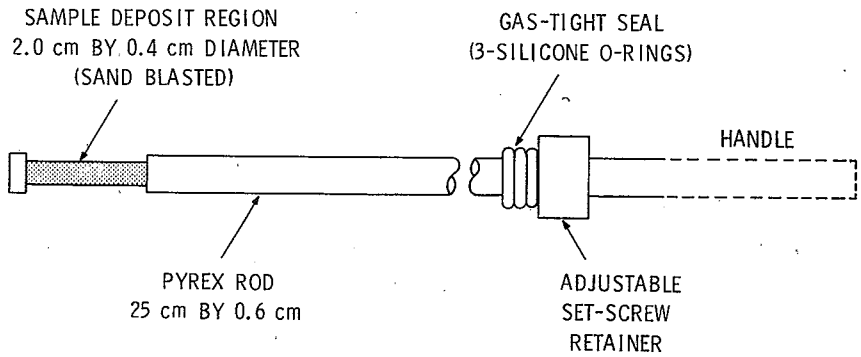

Figure 11. Glass rod probe.

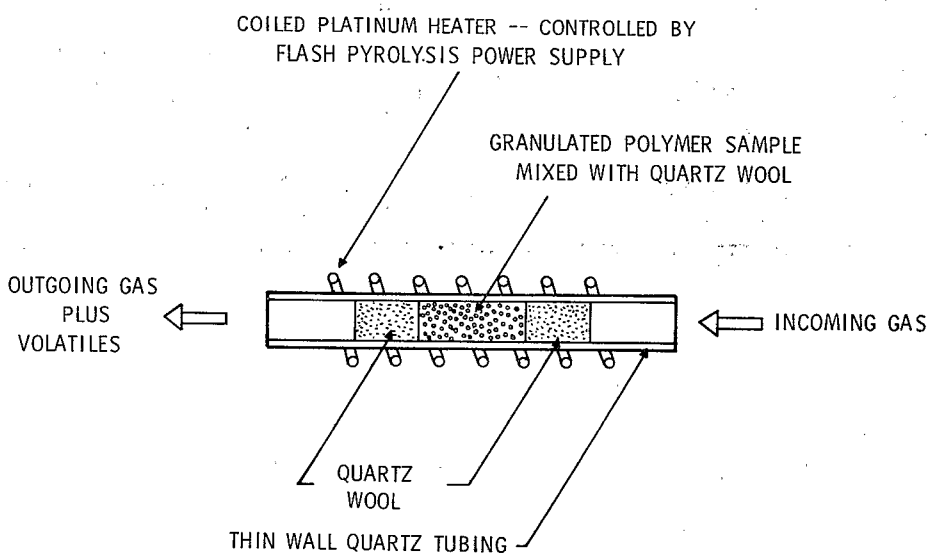

Figure 12. Packed tube probe.

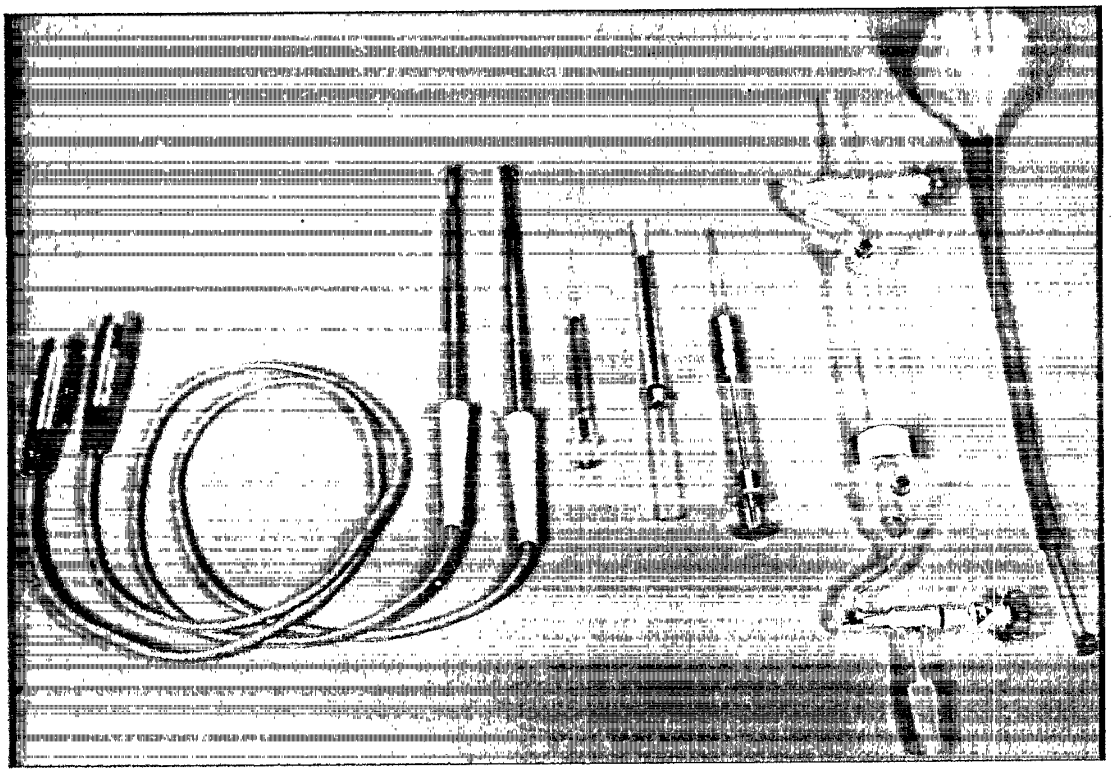

Figure 13. Sample handling devices.

and a versatile pyrolysis unit. These two programmable thermal controllers will be described later when discussing the TDU instrumentation.

The sample insertion section of the TDAS has been designed so that a Plexiglass glove box can be installed that will completely encompass the sample entry region. If needed, samples could actually be prepared in the isolated environment of the glove box and then inserted into the TDAS.

TRANSPORT OF SAMPLE AND EFFLUENT PRODUCTS

Three basic criteria must be met for proper transport of gas phase samples. First, the transport tubing material must not interact with any of the chemical substances that constitute the flowing media. Second, it is important that a constant flow of sweeping gas be maintained throughout every portion of the transport line. Third, the gas transfer must be maintained at elevated temperatures that are compatible with the flowing media. Each of these criteria require some elaboration relative to the transport of sample and products in the TDAS.

Wherever possible, fused quartz was used as the tubing material for sample transport in the TDAS. However, certain portions of this continuous system required metal to metal connections, and the decision was made to use glass-lined stainless steel tubing (from Scientific Glass Engineering) at these locations. Other possible tubing materials were nickel 200 and stainless steel. Indeed, these latter materials are physically more rugged, but the glass-lined SS tubing was selected primarily because of its increased inertness. Other types of materials are also encountered in the transport path downstream of the reactor. Stainless steel, Teflon, and polyimide surfaces are found in such components as Swagelok unions, the switching valve interior, and tubing ferrules.

The second basic requirement for good transport of sample involves the continual gas sweeping of the transfer tubing. It is desirable that the transport gas flow be maintained at relatively high linear velocities (that is, greater than 20 cm sec^{-1}). Thus the inside diameter (ID) of the transport tube should be relatively small, e.g., less than 1.0 mm ID. Unswept recesses in a gas flow path can present major transport problems. Consequently, the use of various tube fittings should be minimized. Several unions were necessary in this system; however, to minimize difficulties at these junctions, the ends of the tubing material were faced off with a grinder before assembly.

A common problem in transporting gases arises when a gas stream must be split into two or more branches. In the TDAS,

this splitting was accomplished with the use of tee connectors that had been filled with quartz wool (Figure 14). With the placement of quartz wool at the point of branching, considerable gas phase mixing is induced. This mixing essentially avoids such difficulties as molecular weight fractionation and non-linear splitting.

The selection of transport temperature and the maintenance of uniform temperatures along the transport path, constitutes the third criteria for proper transfer of sample. The selected transport temperature must be high enough to avoid any serious condensation and possible adsorption effects. However, it must be low enough that additional gas phase reactions do not occur during transport. Localized cold or hot regions must be avoided.

The transfer tubing used in the TDAS was not directly heated but was actually jacketed with much larger diameter glass or quartz tubing. The outer tube was first instrumented with thermocouples located at key positions along the tube. The thermocouples were attached to the outer tube with the use of glass adhesive tape (No. 27 from 3M Co.). After electrically insulating the various conductors along the transport line with woven glass tape (Ware Apparatus Co.), the tubular assembly was wrapped with high-temperature heating tape (Electrothermal flexible tape). The heating tape was then wrapped with another layer of woven glass tape. A photograph of an assembled transport line is shown in Figure 15. Table 2 also shows the various thermocouple locations and their corresponding maximum temperatures for gas transport in the TDAS.

During the course of conducting experiments with the TDAS, certain vital components in the transport path are intentionally cooled to very low temperatures. This localized cooling is necessary (50,51) for capturing the products emerging from the TDAS. Details concerning this low temperature procedure will be discussed later in this section.

QUARTZ TUBE REACTOR

The design and performance of the high-temperature reactor is vitally important to the entire TDAS. Consequently, considerable attention has been centered upon this component. As stated earlier, the important thermal decomposition variables (i.e., gas phase environment, mean residence time and distribution profile, exposure temperature, and pressure) apply directly to the interior of the reactor.

In the earlier thermal decomposition studies conducted with the first generation unit, a narrow-bore folded quartz tube was used (Figure 16). This particular quartz tube reactor was of heavy wall construction and occupied most of the internal volume

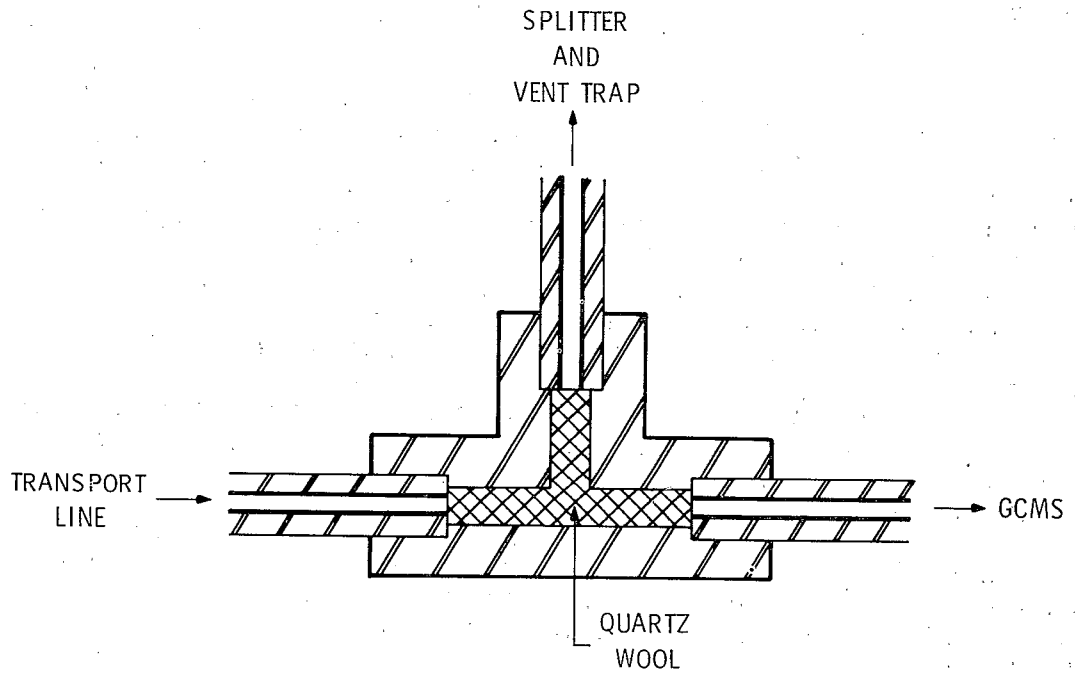

Figure 14. Transport tubing tee connector.

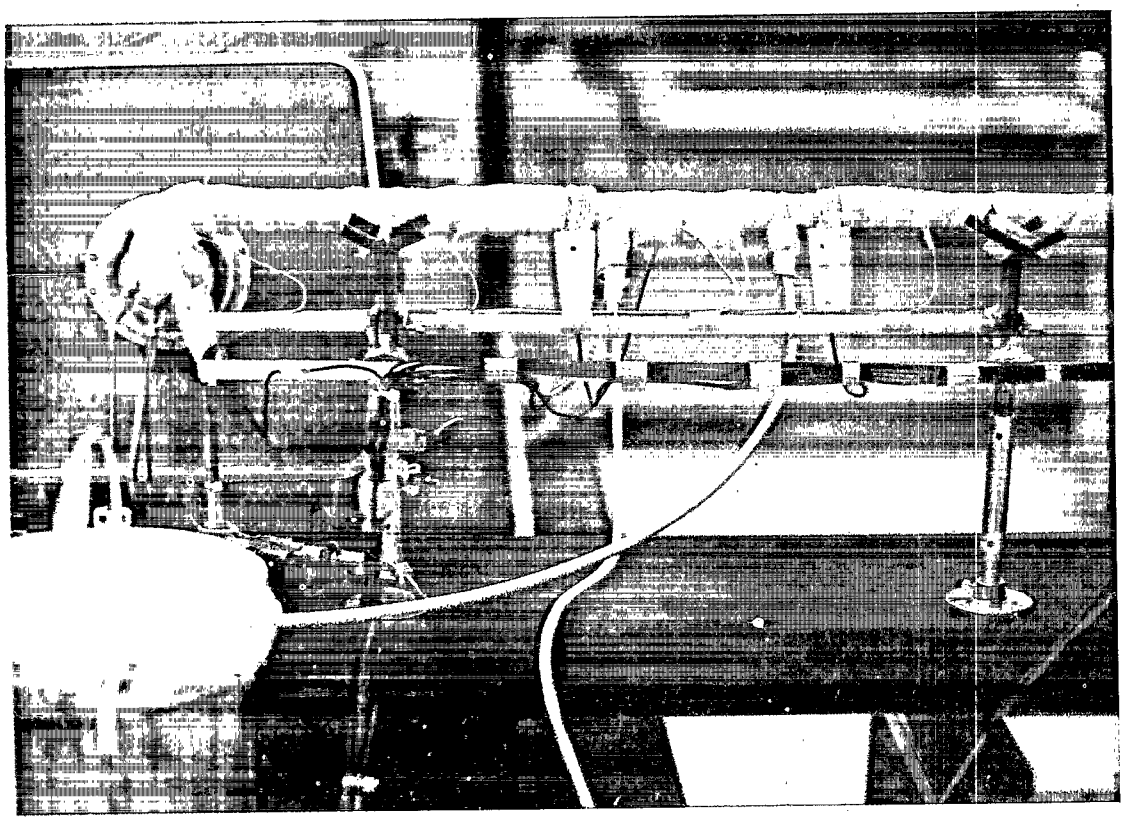

Figure 15. Heated transport lines.

TABLE 2. TDU TEMPERATURES

Temperature selector position	Thermocouple location	Maximum temperature (°C)
1	Room temperature (tc in connector)	30
2	Insertion block	300
3	Interior of pre-reactor tube	300
4	Mid point of inlet heat transfer cavity	400
5	Reactor end region of inlet cavity	350
6	Reactor end region of outlet cavity	350
7	Mid point of outlet heat transfer cavity	400
8	Junction of glass-lined and quart tubing	350
9	Transfer tube between valve and GC	300
10	Glass-lined tubing upstream of collection trap	300
11	Effluent collection trap	300
12	Glass-lined tubing downstream of collection trap	300
13	Junction of glass-lined tubing and valve inlet	250
14	Switching valve	240
15	GC oven interior	300

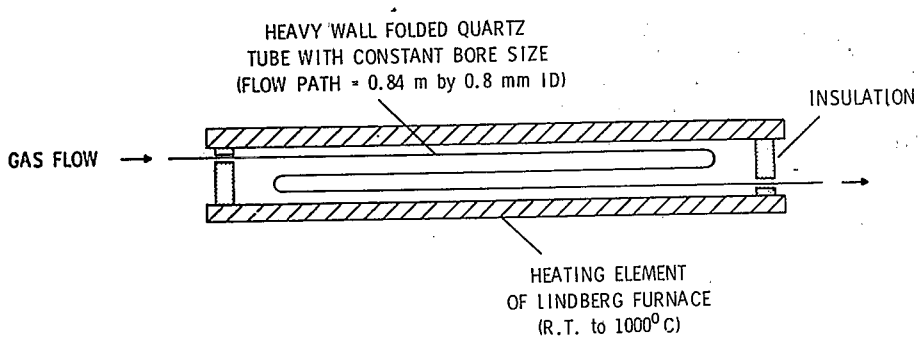

Figure 16. First generation reactor configuration.

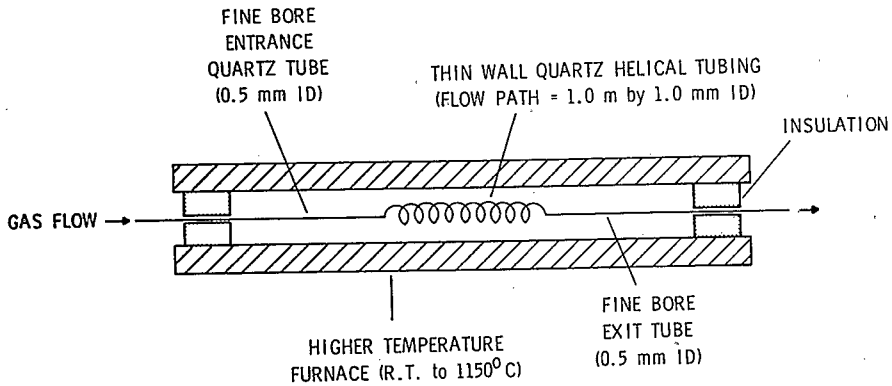

Figure 17. Proposed second generation reactor.

of its high-temperature furnace. Many tests were conducted with this reactor, and it experienced considerable use at temperatures up to 1000°C. Even so, a number of design refinements were considered for the second generation quartz tube reactor. Better control of exposure temperature throughout the gas flow path was desired, and the minimization of end effects would be beneficial. Also, the ability to conduct thermal decomposition tests at somewhat higher temperatures was considered most advantageous. Therefore, the initial conceptual design for the second generation quartz tube reactor was as shown in Figure 17. Again, the major portion of the proposed new reactor was a narrow-bore flow path of considerable length. (It is this design concept that is of paramount importance in obtaining narrow residence time distributions of Gaussian profile.)

A variety of studies have been conducted on laminar fluid flow through narrow-bore flow paths (52-57). Methods for determining gas diffusion coefficients have been developed using the precise control of dispersion afforded by the narrow flow path (58,59). Thermal decomposition testing using this narrow-bore flow path concept requires a high-temperature tubing material, and fused quartz (also referred to as fused silica and vitreous silica) seems to be the best material presently available for high temperature use (60,61). The proposed quartz tube reactor shown in Figure 17 uses very fine bore entrance and exit tubes to transport the gas rapidly into and out of the central portion of the reactor. Later in this section even further refinement of this transport concept is discussed.

Unfortunately, fabrication difficulties are encountered in preparing tightly coiled quartz tubing. Specifically, when requests were sent to various quartz fabricators, the common reply was that they could not provide helical quartz tubing with a precise circular cross section flow path. It was our understanding that when quartz tubing is tightly coiled, the circular cross section bore distorts into an ovalized cross section and even takes the shape of a "D" with the flat side being on the inner diameter of the helix. As a result of the apparent fabrication difficulties, and before contemplating other geometric configurations for the reactor, it was decided to assess the possibility of bending narrow bore quartz tubing without changing the circular cross section of the tubing bore.

Maintenance of the circular cross section flow path is essential because it affects the ability to describe the effects of secondary flow on the residence time distribution. Secondary flow occurs whenever a fluid is passed through a tube that exhibits a significant amount of axial curvature. Figure 18(a) shows the typical streamlines associated with secondary flow, and Figure 18(b) depicts the corresponding radial mixing pattern. Secondary flow has been observed and studied for decades (62-67). Dean (62) studied the effects of secondary flow as early as 1927.

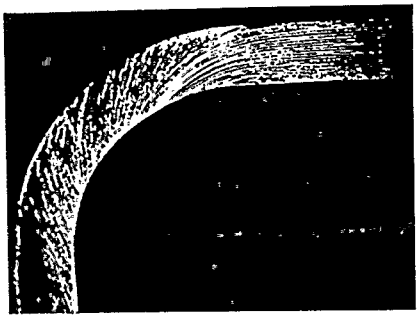

(a) STREAMLINES

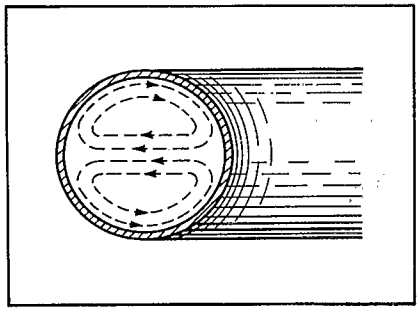

(b) RADIAL MIXING

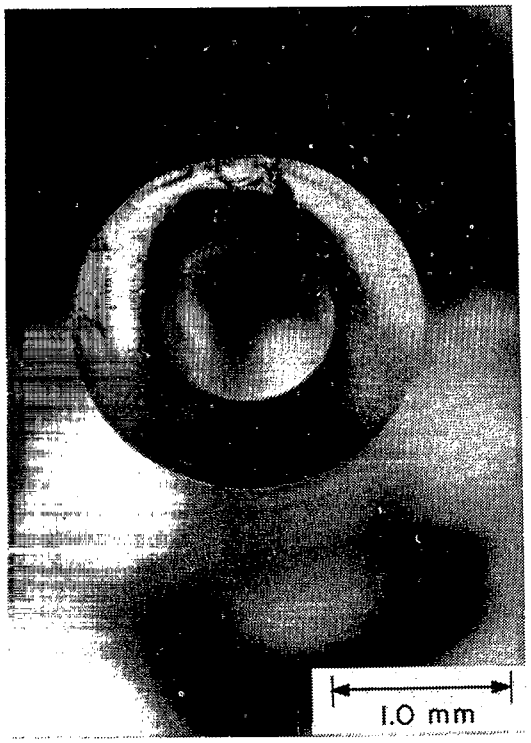

(c) CURVED QUARTZ TUBE OF CIRCULAR CROSS SECTION

Figure 18. Secondary flow and circular cross section flow path.

Also, pressure losses (68) were associated with secondary flow in bent tubes as early as 1937. To characterize accurately the residence time contribution in a tube that exhibits some degree of secondary flow, it is imperative that the flow path be of circular cross section. The description of secondary flow in an elliptical, ovalized, or noncircular flow path is practically an impossible task.

Therefore, upon giving this fabrication problem to the University scientific glass blower, thin-wall, 1.0 mm ID quartz tubing was eventually obtained that retained its circular cross section when bent through a 180° arc at a radius of 2.1 cm. Figure 18(c) shows a photograph of a typical cross section of curved tubing. Indeed, there is no visible ovalization of the tubing bore. Circular cross section was maintained by locally heating the tubing on a mandrel and allowing the quartz to bend by its own weight.

The ability to maintain the circular cross section flow path in a curved tube permitted the eventual design of a compact folded tube reactor. The actual configuration and dimensions of this quartz tube reactor will be presented later, along with a detailed description of the gas flow behavior.

With the ovalization difficulty overcome, it was then possible to design a complete quartz tube reactor assembly that could be fitted into a high-temperature tubular furnace. The furnace selected for heating this quartz assembly was a Lindberg Model 54357, a three-zone furnace of hinged construction that was designed for continuous operation at temperatures up to 1200°C. This furnace has its own control console (Model 58744-A) which separately regulates the temperatures of each of the three zones. Only the middle portion of the furnace's central zone is used to heat the high-temperature reactor, although during operation the entire length of the tubular furnace is held under isothermal conditions. Figure 19 shows a sectional view of the furnace interior along with the locations of the thermocouples used for controlling temperatures within the three separate zones.

The assembled quartzware, which was eventually positioned in the high-temperature furnace, is detailed in Figure 20. This quartzware, and all of the other glassware employed in the TDAS, was fabricated in the University Glass Shop by a scientific glassblower. Even though the assembled quartzware is delicate, it has experienced considerable use without problems at extreme temperatures.

A better understanding of the actual behavior of the entire quartz tube assembly can be obtained by close inspection of the schematic shown in Figure 21. In this figure, three separate gas flow paths are depicted. The main flow is the carrier

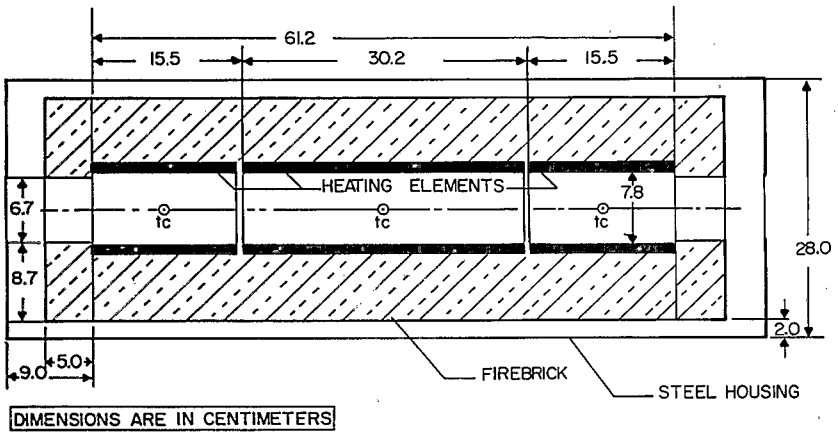

Figure 19. Sectional view of furnace interior.

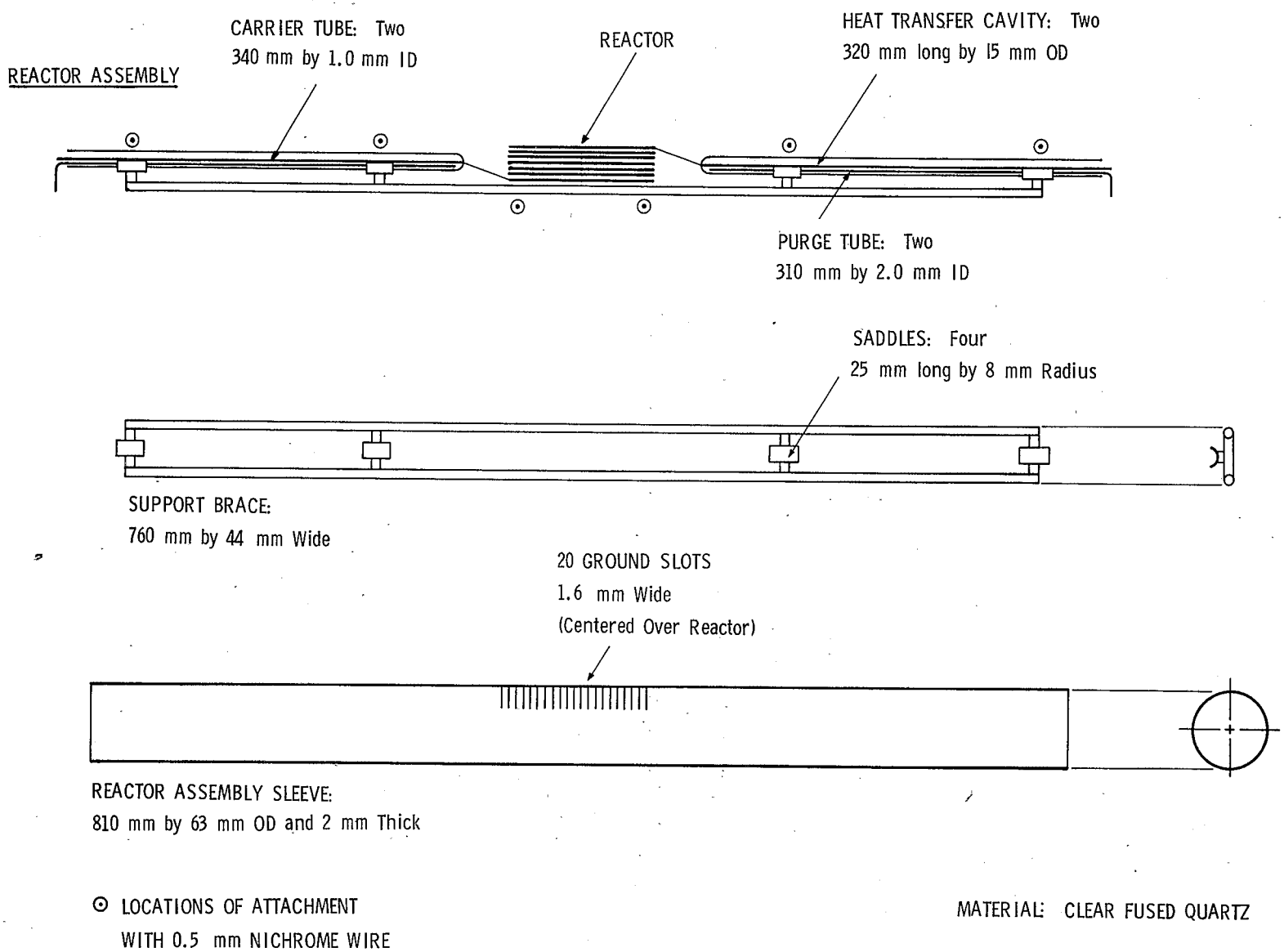

Figure 20. Quartz tube reactor components.

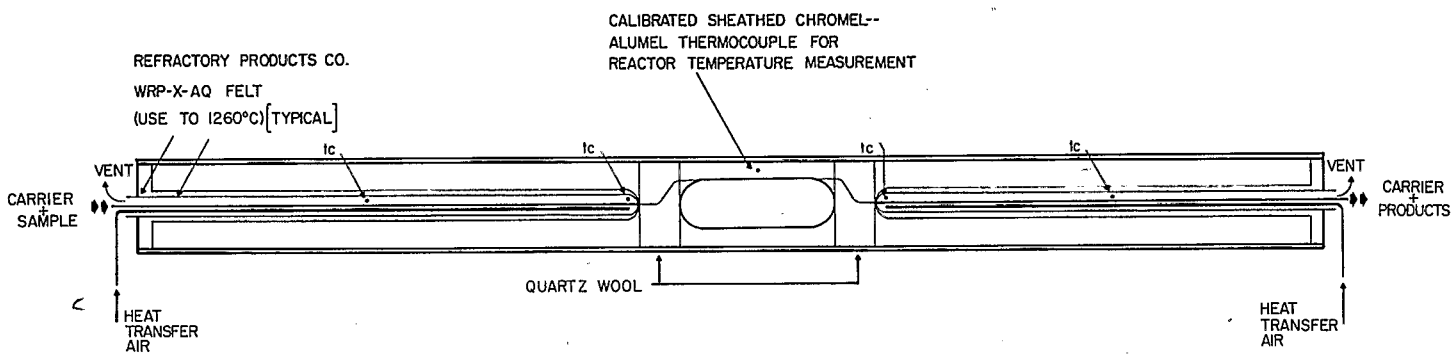

Figure 21. Assembled quartzware.

stream through the transfer tubing, into the reactor, and out the exit transfer tubing. This gas flow path carries the vaporized sample molecules into the reactor, where they are subjected to the controlled high-temperature conditions and then passed downstream where the various products are collected and eventually subjected to analysis. The other two gas flow paths consist of adjustable flows of heat transfer air that cool the entrance and exit chambers of the quartz tube assembly. Thus the main gas flow into the reactor is maintained at lower nondestructive temperatures right up to the point of entry into the high temperature reactor. As soon as the sample or product molecules leave the reactor, the gas temperature is abruptly decreased to the same nondestruction transport level (approximately 275°C). The gas then flows on to the collection trap at approximately the same temperature. Figure 22 shows the quartzware assembly centrally located in the three-zone furnace.

The reactor was constructed from quartz tubing obtained from Heraeus-Amersil, Inc., and their smooth-wall tubing was found to possess uniform wall thickness and bore diameter over the entire tubing length. The tubing diameter measurements, as shown in Figure 23, were obtained by carefully filling the particular tubing section with mercury and then removing the mercury and obtaining its respective weight with the use of an analytical balance. This mercury displacement technique was very similar to that described by Barr and Anhorn (69).

A narrow-bore, multiple-fold quartz tube reactor of race track configuration (Figure 23) was selected for several reasons. First, with the relatively short overall length of the main portion of the reactor and with utilization of the multiple-fold tube design, any existing longitudinal temperature gradient within the furnace would be effectively averaged out over seven cycles, thereby assuring that sample molecules encounter essentially isothermal conditions during their controlled traverse through the reactor. Second, these flow path dimensions would permit mean residence time studies of between 0.25 and 5.0 seconds, which was a TDAS design objective. In addition, as there are no protrusions into the flow path, and as the tubing diameter transitions are very gradual, eddy currents would be negligible. With this size reactor, gas phase thermal decomposition studies would be conducted in the laminar flow region at Reynolds numbers that are orders of magnitude below the onset of turbulence. Calculated Reynolds number extremes for this quartz tube reactor range from 0.7 to 140. Furthermore, there would be a very low pressure drop across this reactor even at the very high linear gas velocities. Also, in view of the narrowness of the gas flow path, back diffusion in the reactor would be nonexistent.

In the TDAS design, gas phase molecules are subjected to a narrow residence distribution while maintaining, within the

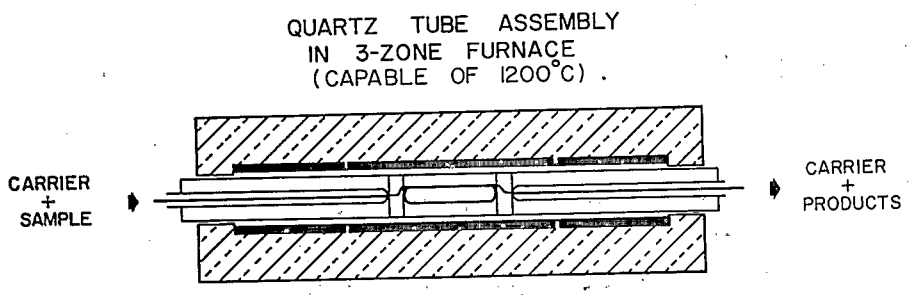

Figure 22. Quartzware assembly in three-zone furnace.

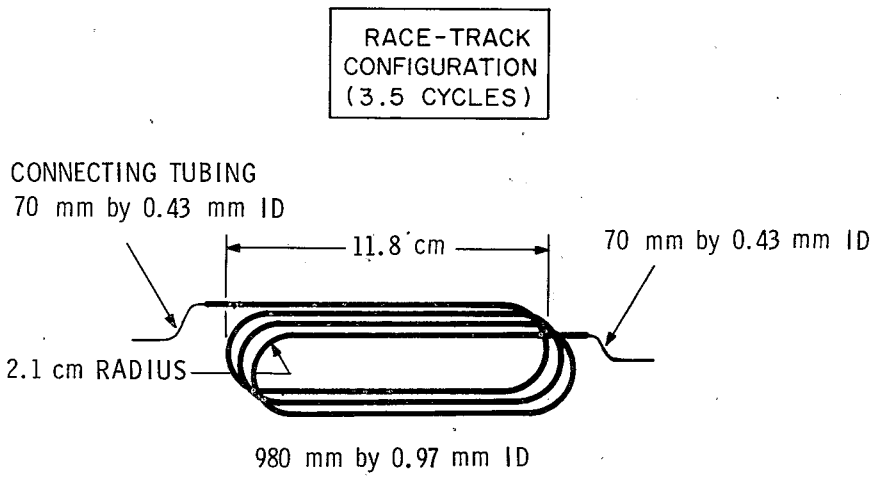

Figure 23. Detail of quartz tube reactor.

reactor, an acceptable ratio of gas volume to surface area. The design of this quartz tube reactor permits a detailed description of gas flow behavior within the reactor. (Such a detailed analysis is presented in Appendix A.)

As derived earlier in Section 6, the mean residence time for gas phase molecules in the above reactor is

$$\bar{t}_r = \left(\frac{\pi r^2 L}{\bar{F}_o}\right)\left(\frac{T_o}{\bar{T}_2}\right)\left(1 + \frac{p_d}{p_o}\right) \tag{7}$$

and the standard deviation of the residence time distribution is

$$\sigma_t = \left[\frac{2D_g(L_c + L_s)}{(\bar{v})^3} + \frac{\omega r_o^2 L_c}{24\ \bar{v}\ D_g} + \frac{r_o^2 L_s}{24\ \bar{v}\ D_g}\right]^{\frac{1}{2}} \tag{8}$$

as obtained from the derivation presented in Appendix A (see list of symbols for the designations of the various terms). An error analysis pertaining to the mean residence time determination for this reactor has also been conducted (see Appendix B).

Additional details concerning the high-temperature gas flow into and out of the quartz tube reactor are illustrated in Figure 24. Basically, this design permits negligible flow path end effects and entrance length distortions. The steady state heat transfer effects for this reactor were studied in Appendix C, and a very rapid temperature transition time was found for molecules passing through the quartz tube reactor. Specifically, Figure 25 shows the incoming gas reaching the elevated temperature in less than 5 milliseconds. This essentially square-wave profile of temperature versus time is accomplished through the use of the low-temperature heat transfer principle, whereby the incoming gas is maintained at transport temperatures right up to the point of entry into the high-temperature region. Then by employing fine bore connecting tubes, the linear gas velocity is increased by a factor of five at the entrance and exit portions of the high-temperature reactor.

This high-temperature quartz tube reactor is capable of withstanding intense temperatures for long periods of time. However, it can be easily damaged by some corrosive gases. For example, the scanning electron microscope photographs shown in Figure 26 were obtained from various sections of quartz tubing that were intentionally exposed to corrosive and destructive gaseous environments. From this figure, it is observed that the smooth quartz surface can be drastically changed by corrosive agents. Consequently, care must be exercised with respect to determining what samples are to be subjected to analysis by the

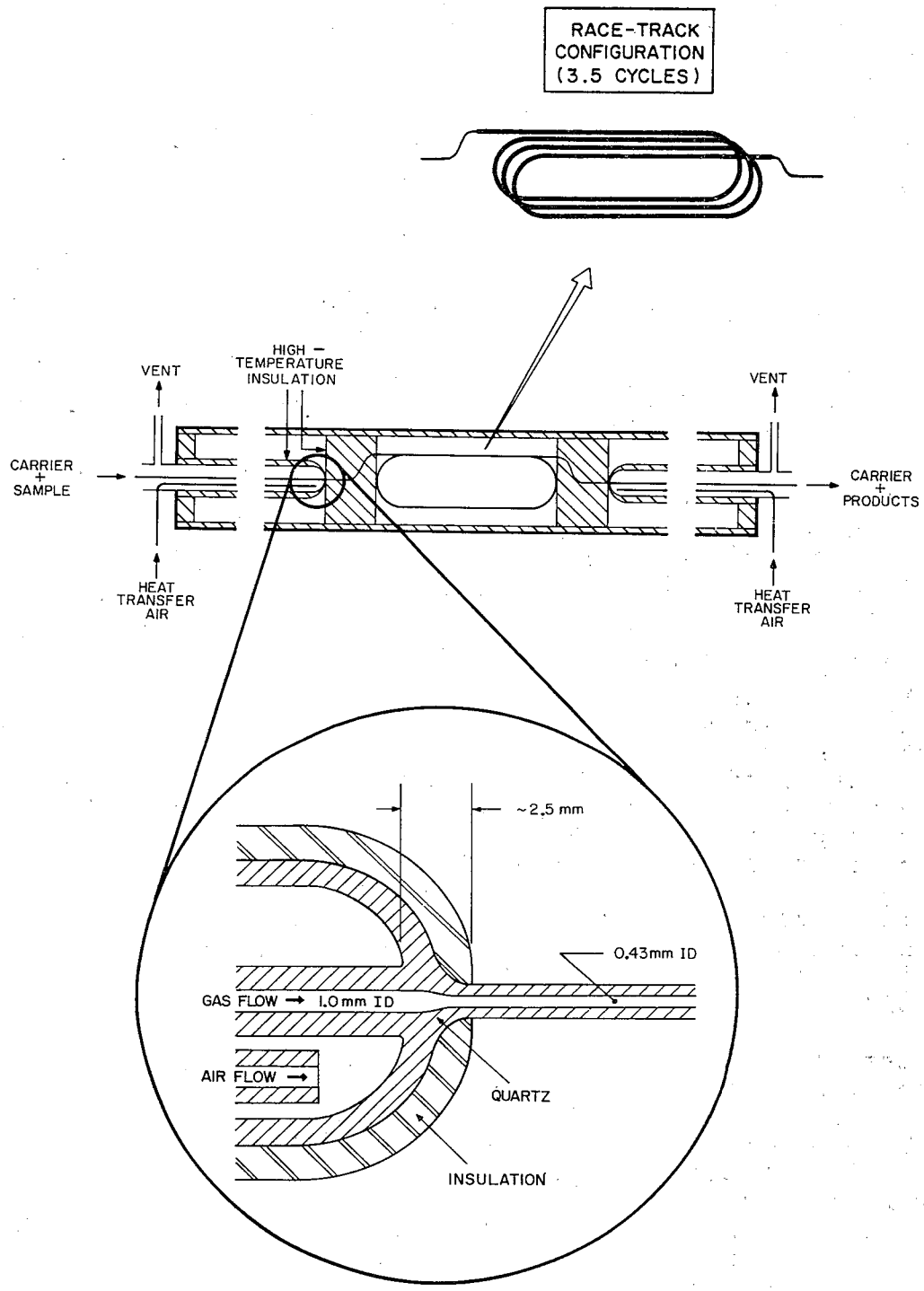

Figure 24. Additional details of reactor assembly.

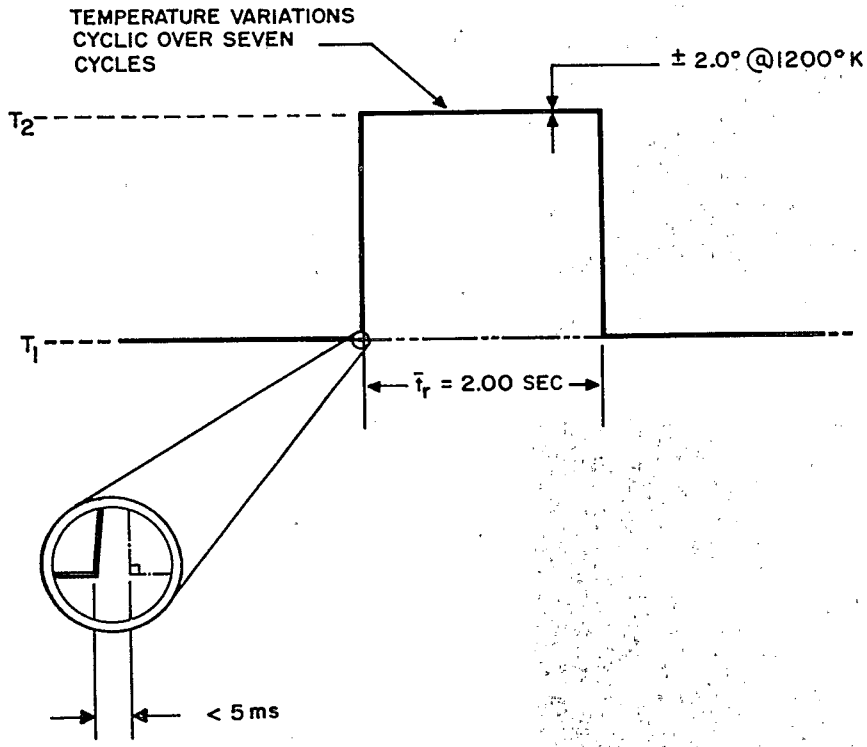

Figure 25. Square wave profile of gas phase temperature versus time.

CLEAN QUARTZ SURFACE
(10,000X)

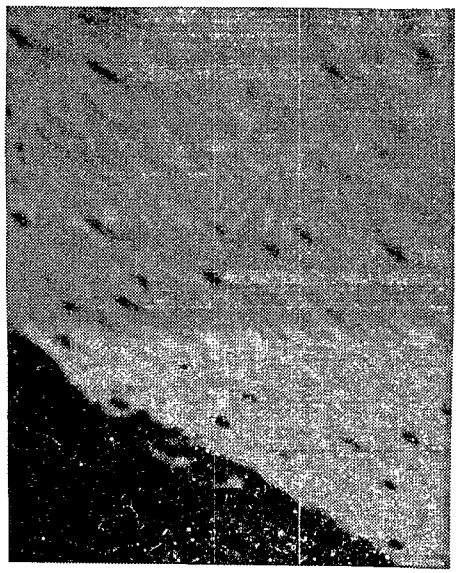

QUARTZ SURFACE AFTER ATTACK
BY HF AT HIGH TEMPERATURE
(10,000X)

QUARTZ SURFACE AFTER EXPOSED
TO NF_4HF_2 AT 400°C FOR 4 HOURS
(3,000X)

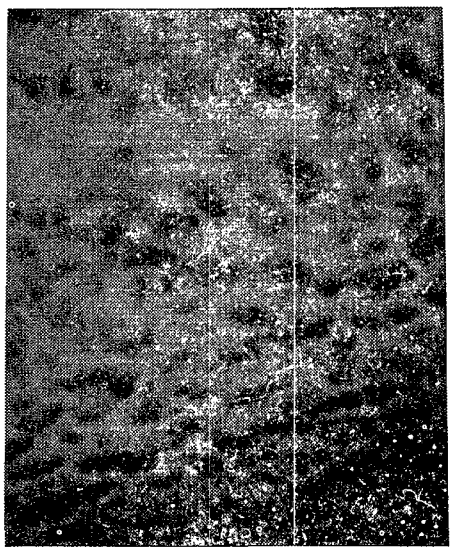

QUARTZ SURFACE AFTER EXPOSED
TO NF_4HF_2 AT 400°C FOR 4 HOURS
(10,000X)

Figure 26. Scanning electron microscope photographs of quartz surfaces.

TDAS. If indeed the surface of the quartz tube is attacked, and increased surface area and adsorptive behavior result, then the precise residence time control no longer applies. A certain amount of sample screening is necessary before an unknown sample can be subjected to thermal decomposition analysis by the TDAS.

COLLECTION OF EFFLUENT PRODUCTS

As the gas phase sample and its various decomposition products emerge from the high-temperature reactor, they are swept downstream through the heated transfer line and into the effluent product collection trap. This product collection trap is an important component in the TDAS and requires considerable discussion.

As stated in Section 4, the product collection trap must possess a slight resistance to gas flow, as should the smaller bore transfer tubes. However, the primary function of the product collection trap is to quantitatively capture the unreacted sample and the various products of thermal decomposition that emerge from the high-temperature reactor.

The utilization of collection traps at cryogenic temperatures has been in practice for many years in the field of gas chromatography (70-74). Indeed, the benefits of low-temperature trapping of samples are well known. However, there are also numerous problems associated with low-temperature condensing traps. One of the major difficulties is that of the condensing out of very large quantities of water along with the various organic compounds of interest.

Many procedures have been developed for thermally desorbing collection traps, including cryogenic sample collections (75-79). Some of these techniques can liberate the captured sample in a very short period of time. It can then be passed downstream into either a chromatograph or some other analytical instrument.

One of the most useful and intriguing sample trapping methods was devised by Kaiser (80-83). He employed the properties of an adsorbent trapping media along with cryogenic trapping for the collection of sample. He then used thermal desorption for liberating the trapped contents. Basically, Kaiser employed the concept of a reversible countercurrent heat exchanger for capturing and liberating substances while in an in-line system. This trapping technique has seen a considerable amount of use in both in-line and discontinuous sampling systems.

The selection of trapping media is very important, and there are many different trapping materials commercially available. Some of the commercially available trapping media used primarily for collecting organic compounds are as follows: carbon

molecular sieves, graphitized carbon black, Ambersorb adsorbents, XAD resins, chromosorb polymer series, Porapak polymer series, Tenax GC, activated charcoal, and polyurethane foam. Studies have been conducted concerning the physico-chemical behavior and trapping properties for many of the adsorbent trapping media (84-89). There are numerous applications to which these various trapping materials have been applied (90-100). Also, to increase trapping versatility, some of these trapping media have been placed in series arrangements and then used in the same trapping device.

The adsorbent trapping material that was eventually selected for use in the TDAS was Tenax GC. There were many reasons for selecting this particular porous polymer. Tenax GC can withstand high temperatures before appreciable thermal degradation occurs. High molecular weight materials can be trapped and readily liberated by thermal desorption from this particular adsorbent. Also, water in the gas flow path does not adversely affect the behavior of this adsorbent to any great extent (101). Tenax GC does have some disadvantages relative to some of the other trapping materials, but for the intended uses in the TDAS, it seemed to be the best material presently available for in-line cryogenic trapping of organic products.

Tenax GC was introduced in 1969 and was initially intended for use as a gas chromatographic column packing. However, it was quickly recognized that it could also be used most beneficially as an adsorbent trapping material. Tenax GC is a porous polymer based on 2,6-diphenylparaphenylene oxide and is reported to have an upper temperature limit in the vicinity of 450°C (102). Even so, for sensitive analytical work where a minimum of degradation or bleed can be tolerated, its upper temperature limit is significantly below this value. Many workers routinely condition Tenax GC traps at 325°C in a flowing inert gas.

In the past five years, the use of Tenax GC as a trapping medium has seen wide use. It has been used to capture and analyze organic compounds in environmental samples (103,104), volatile polar organics found in water (105), organic components present in human breath (106), pesticides, polychlorinated biphenyls and polynuclear aromatics found in surface and drinking waters (107,108), the gas phase of cigarette smoke (109), organics in marine biota (110), and the exhaust of jet engines (111).

If a Tenax GC trap is swept with a high velocity gas stream while at high temperatures, high molecular weight substances can be quantitatively liberated from the adsorbent particles (12,112). Accordingly, this high velocity sweeping procedure has been incorporated into the subsequent design of the in-line trap used in the TDAS.

A schematic of the effluent collection trap used in the TDAS is shown in Figure 27. This design is modeled after the trapping concept as introduced by Kaiser. However, rather than using a bidirectional flow of nitrogen, the gas flow through the jacket is discontinued during the thermal desorption mode. To liberate the sample from the in-line trap, the temperature of the aluminum heating block that surrounds the trap tubing is linearly increased to an eventual desorption temperature of 280°C. Note in Figure 27 that the trap contents are designated simply as in-line trapping media. The reason for this is that for most of the work done with the TDAS, an adsorbent porous polymer trapping medium is used (specifically, an 80/100 mesh Tenax GC trap as shown in Figure 28). The remainder of the sample collections are obtained using a trap containing phosphoric-acid-treated glass wool or chemically bonded packings at cryogenic temperatures.

Very recently a problem concerning irreversible adsorption of certain types of organic molecules by various porous polymers has received considerable attention by analysts and environmental scientists. Therefore, to avoid any difficulties with the very low levels of residual adsorptivity, the Tenax GC trap is employed for the thermal decomposition studies in which the concentrations that go onto the trap are relatively large and the interest concerning low-level trace components is relatively minor. When the objective is to determine the trace level remnants of the unreacted parent sample after exposure to very high temperatures, a glass wool trap or a chemically bonded packing trap is used along with cryogenic trapping temperatures.

TDU INSTRUMENTATION

Most of the measurements pertaining to the thermal decomposition unit have been instrumented, and the various control and measurement devices* have been incorporated into an instrumentation console. A photograph of this instrumentation console is presented in Figure 29, along with the descriptive designations of the modules that measure or control the various operations performed by the TDU. These modules are mounted in a Cabtron Series C modular electronic cabinet.

The temperature programming function for both the sample insertion process and the desorption of the collection trap is accomplished with the use of a Theall Engineering TP-2000 temperature programmer. This device is capable of generating linear temperature programs from minus 100°C to plus 700°C. A switch has been installed in this module so that power can be

*calibration data are presented in Appendix D.

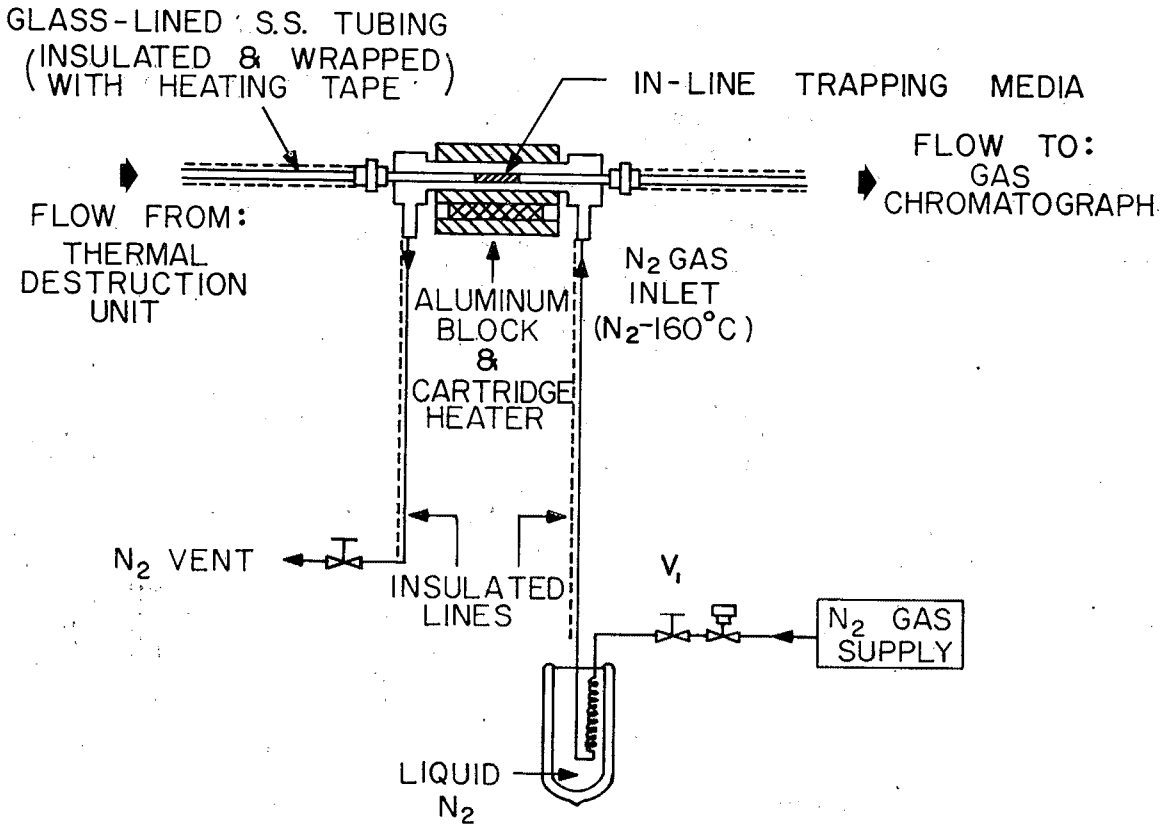

Trapping Mode:	Valve V_1 is open and trap temperature approaches - 160°C.
Desorb Mode:	Valve V_1 is closed and trap is subjected to a temperature program of -160° to +300°C at a pre-selected programming rate.

Figure 27. Schematic of collection trap assembly.

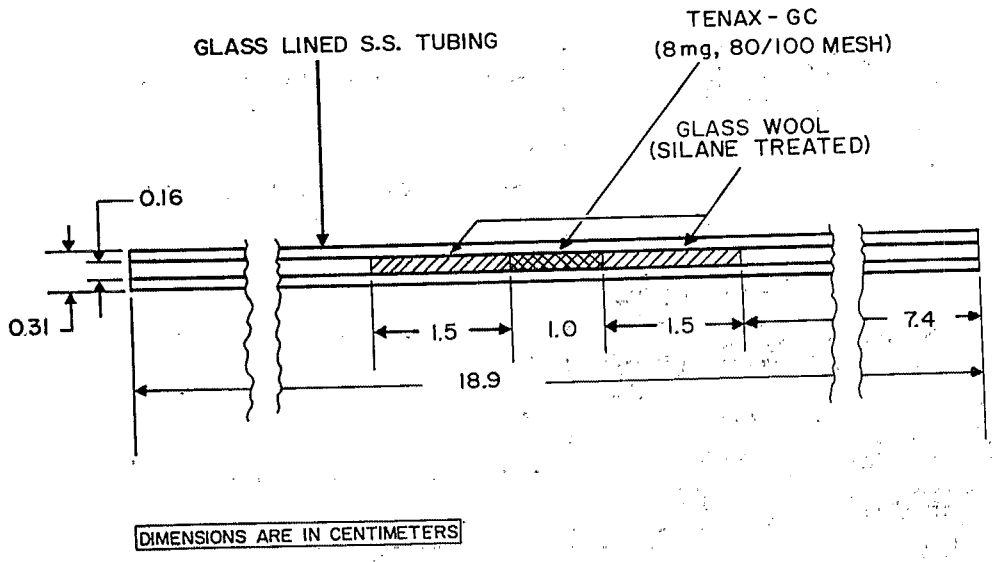

Figure 28. Adsorption trap insert.

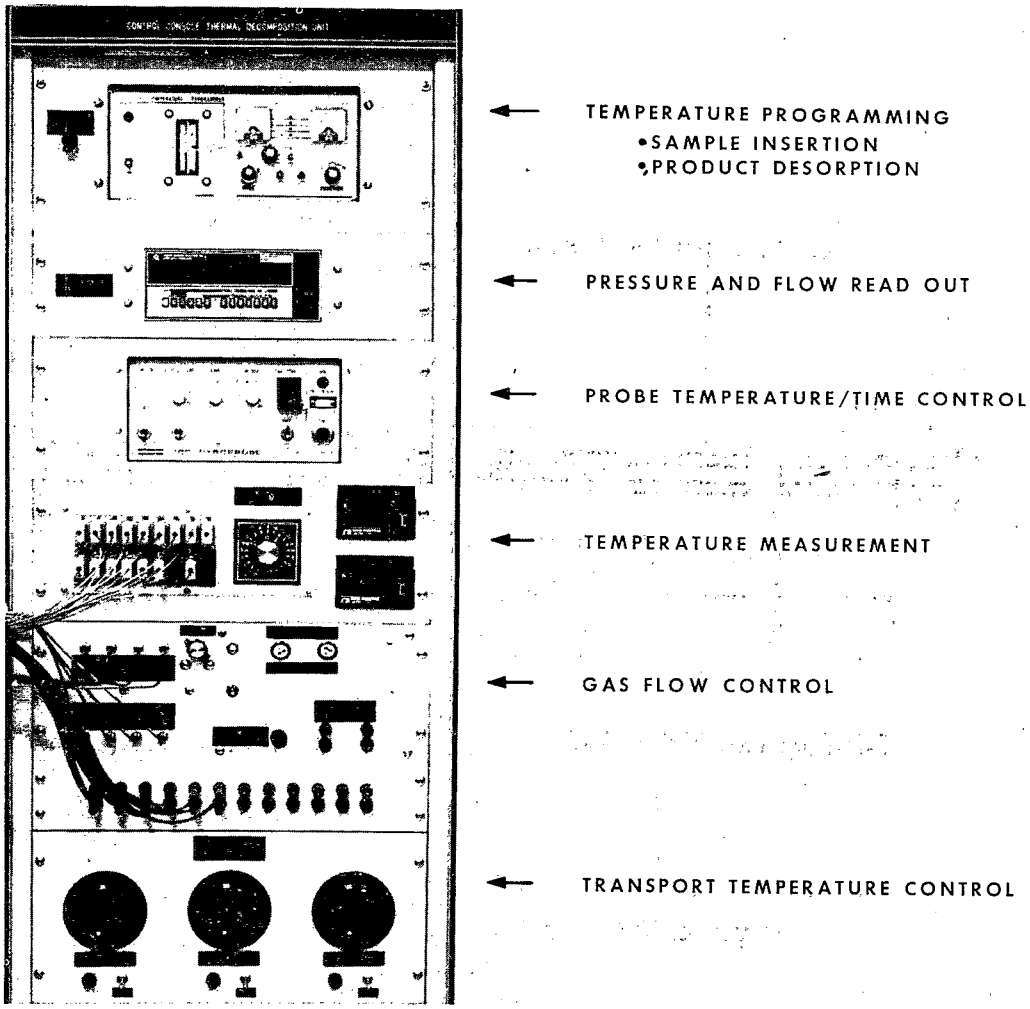

Figure 29. TDU Console and instrumention modules.

applied to either the sample insertion chamber or the product collection trap.

The pressure and flow readout module consists essentially of a Hewlett-Packard 3465A digital multimeter. The signal output from the mass flow transducer is in the range of volts DC, whereas the output from the differential pressure transducer is read out in millivolts DC.

Certain low volatility samples can be inserted into the TDU with the use of an electrically heated probe. A modified Chemical Data Systems Pyroprobe 100 solids pyrolyzer is used to perform this sample insertion and subsequent volatilization. A number of sample insertion techniques have been developed using this type of programmed heated probe. This pyrolyzer can also be used to study nonvolatile materials such as polymers.

The temperature measurement module consists of 18 electrically shielded thermocouple inputs, a thermocouple selector switch (Omega MTG-OSW3-18), and two digital temperature indicators (Omega 175-KCl and Omega 250-KCl-05). The average temperature of the quartz tube reactor is continually monitored by the Omega 250-KCl-05 instrument.

The gas flow control module contains the gas input connections, a carrier gas filter (Applied Science Laboratory's Hydro-Purge), a gas switching valve (Carle Instruments' 5511), needle valves that control the flow of heat transfer air in the high-temperature reactor assembly, the variable flow controller (Porter Instruments' VCD 1000) that controls the actual gas flow to the reactor, a switch for the solenoid valve that controls the nitrogen gas flow in the cryogenic trapping unit, and the flow and pressure transducers along with their associated electronics.

Because of its direct interaction with the high-temperature reactor, the gas flow control module is a very crucial component. A photograph of the interior of this isolated module is presented in Figure 30. (Notice the positioning of the mass flow and differential pressure sensing elements relative to the thermometer and the mounted circular level.)

The principle behind the operation of the mass flow meter is well established (113,114). Although there is a number of different methods for measuring in-line gas flow (115), this particular flow measurement device has performed quite well in laboratory studies where accurate measurements of in-line gas flow were required (116). A schematic showing the principle of operation of the transducer and the simplified associated electronic circuitry is shown in Figure 31. The mass flow transducer is position sensitive. Therefore, a circular level was mounted on the same flat base that supports the mass flow

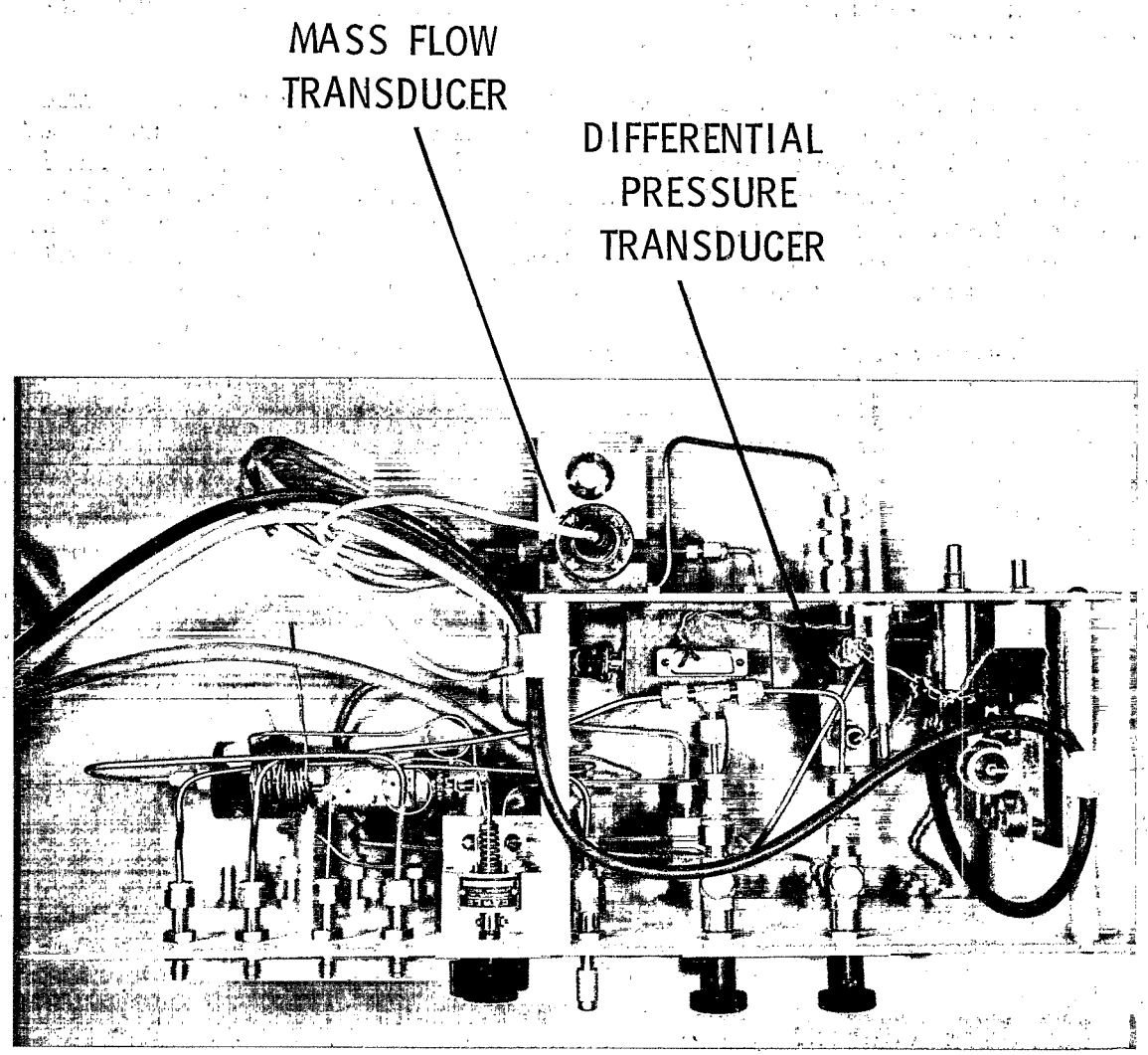

Figure 30. Interior of gas flow control module.

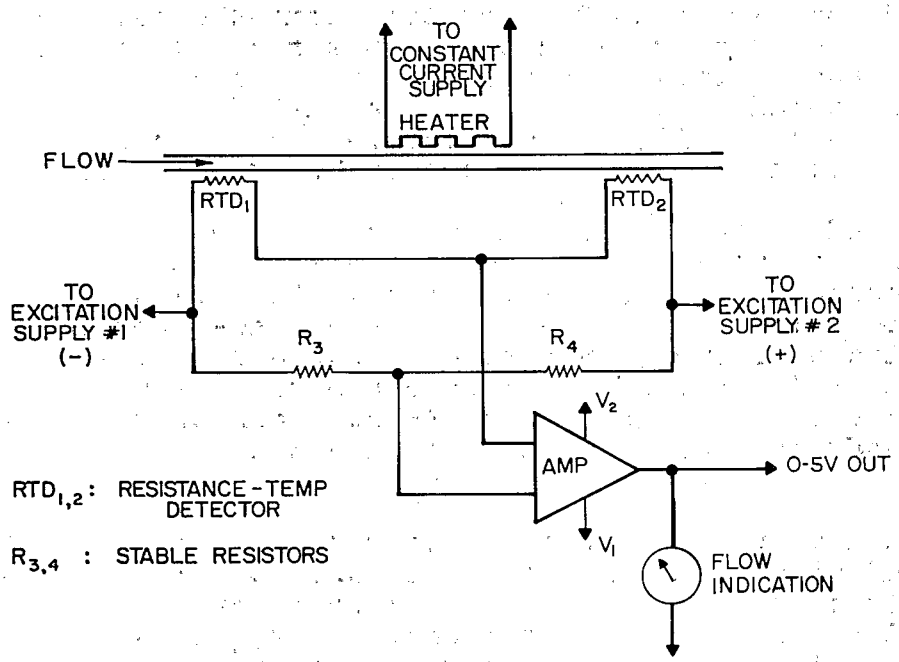

Figure 31. Fundamenetal schematic of mass flow transducer.

sensing element, thus providing the means of establishing the required perpendicularity of the device.

The differential pressure transducer used in this module is somewhat similar to the device used in our earlier work with the first generation system. However, a number of circuitry revisions have been made that resulted in improved signal stability. A schematic drawing of the transducer used in this module is shown in Figure 32.

Both of these transducers have a fixed working range. The mass flow transducer is calibrated to handle flows of air up to 50 cm^3 min^{-1}, and the differential pressure transducer is designed for use up to 2.0 absolute atmospheres. Each of these sensitive components has a built-in safety factor that allows them to handle somewhat higher gas flows and pressures. However, the recommended upper values are as stated above. If TDAS work is anticipated at flows and pressure beyond these limits, different transducers would have to be substituted.

Two additional measurements are routinely made in the course of conducting a test with the TDAS. One of these measurements is ambient temperature. This temperature measurement is made with a mercury-in-glass thermometer, which is located as shown previously in Figure 30. The other important measurement is that of barometric pressure, and this measurement is taken using a Sargent-Welch S-4565 vernier rack barometer, which reads the height of the mercury column to the nearest 0.1 mm.

The transport temperature control module consists of a number of different variacs, adjustable power supplies, temperature controllers, and assorted fuses and switches, which are used for heating the transport lines, gas switching valve chamber, and the GC inlet block. These power supplies have adjustable outputs, and the temperatures of the various heated components are routinely measured using the temperature measurement module. The power lines for the various heaters are sufficiently separated from the shielded thermocouples and the temperature measurement module.

There are several advantages to housing these instrumentation modules in one compact console. First, it is particularly advantageous in conducting detailed experiments with the TDAS to have at one location the controls and readouts of the various test parameters. In addition, by employing the versatile modular concept for the TDU instrumentation, future modifications to the TDAS can be readily accommodated.

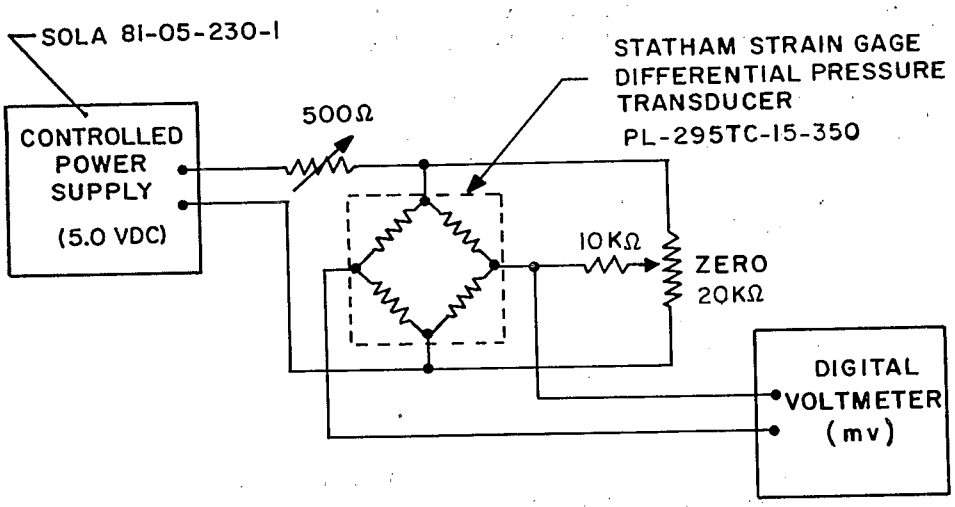

Figure 32. Pressure transducer schematic.

SECTION 7

CHROMATOGRAPHIC SEPARATION AND ANALYSIS

The TDAS concept relies strongly on the analysis of the chemical compounds that emerge from the high-temperature reactor. This analysis establishes the extent of thermal decomposition of the parent substance and at the same time provides information on the various thermal reaction products.

The seven stages of a typical instrumental chemical analysis are as follows:

1. Collection
2. Storage
3. Extraction
4. Concentration
5. Isolation
6. Identification
7. Quantification

Now the primary function of the GC located in the TDAS is to separate the constituents of the various complicated chemical mixtures. In addition, this GC unit is also responsible for stages 4 and 7 of the above analysis scheme.

The GC installation within the TDAS is shown schematically in Figure 33. The glass open tubular column (see Appendix E) and the bypass tubing are located in the interior of a modified Pye 104 gas chromatograph (Figure 34). This particular instrument is part of the LKB-2091 GCMS-COMP system. A high-temperature gas switching valve has been attached to the side of this GC, and the interior of the heated valve chamber is maintained at a constant elevated temperature.

Water and volatile acids can present difficulties to most glass open tubular columns. Therefore, a sample bypass feature has been incorporated into this installation so that harmful low molecular weight species bypass the open tubular column (OTC) and pass on to the mass spectrometer (MS), where they can be continually monitored. This bypass mode can also be used for MS analysis of the low molecular weight products. The columns that have been prepared and used in the TDAS can accept small quantities of water without adversely affecting the performance

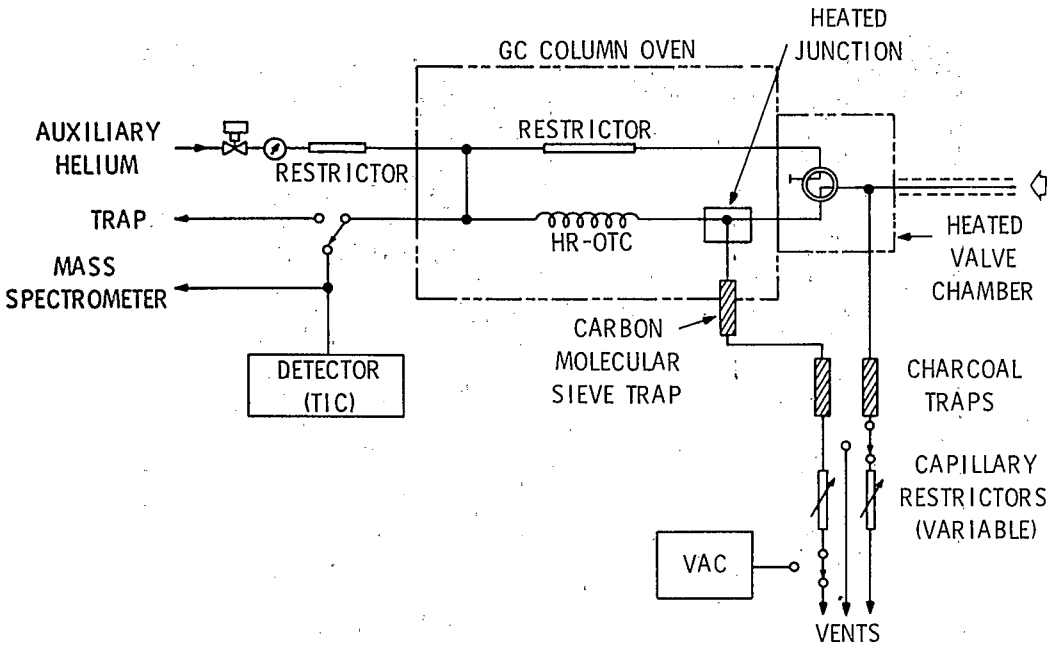

Figure 33. Schematic of GC column installation.

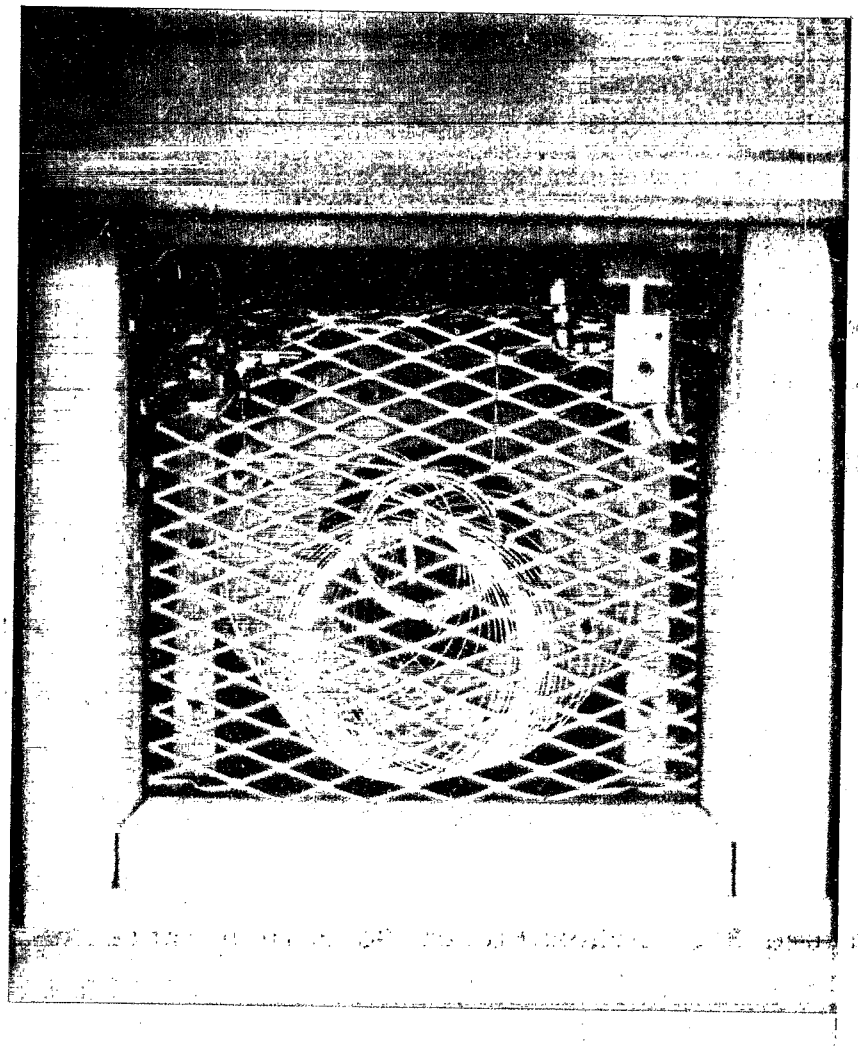

Figure 34. Glass OTC installation in modified Pye 104.

of the column. Even so, if possible, it is desirable to keep oxygen, water, and various harmful substances from entering the glass capillary.

As mentioned earlier, another vital function of the TDAS chromatographic column is to trap the condensable products that are liberated from the effluent collection trap during the thermal desorption process. A chromatographic column can indeed be an excellent trap, and if held at room temperature, it can quantitatively capture most substances having a molecular weight of 100 or greater. If the column oven is maintained at sub-ambient temperatures with the use of auxiliary coolant (e.g., dry ice, etc.), much lower molecular weight species can be successfully trapped (117-119). This thermal focusing process (see Appendix F) is a crucial step in the sample handling with the TDAS. Also, for the analysis of products from the TDAS, programmed temperature GC is essential.

The TDAS depends on high-resolution separation of the various chemical compounds. Therefore, this necessitates the use of glass capillary GC columns.

The gas-liquid chromatographic separation of volatile organic compounds was first accomplished in 1951 (120), and OTC's (121-124) were introduced in 1958. The latter continue to receive the attention of many researchers. The various mechanisms that influence chromatographic separation have been placed on a firm technical foundation (125), and today it is not uncommon to find a sample containing more than a hundred different compounds being adequately separated for qualitative and quantitative analysis. Research work with glass OTC's is relatively recent, although glass capillaries were introduced as early as 1960. Much of the recent interest in glass OTC's has come about through increased attention being devoted to surface chemistry and physical compatibility with the various stationary liquid phases. A bibliography has been prepared (126) concerning some of the more recent developments in this field of open tubular gas chromatographic columns. Also, a text on glass OTC's has recently been published (127).

The various columns used in the TDAS, and those used in the other supporting GC's, are fabricated in our laboratory. Appendix E describes the procedures used for preparing these OTC's. Our OTC preparation procedures have been influenced collectively by the works of many researchers (128-137) in the field of capillary columns. The columns that are used in the TDAS are first subjected to a performance examination in a separate GC instrument. Figures 35, 36, and 37 show chromatograms obtained by such columns. Figure 35 indicates the separating efficiency for a series of normal alkanes; Figure 36 indicates the tremendous complexity of some samples (e.g., a distillation fraction of crude oil), and Figure 37 shows the

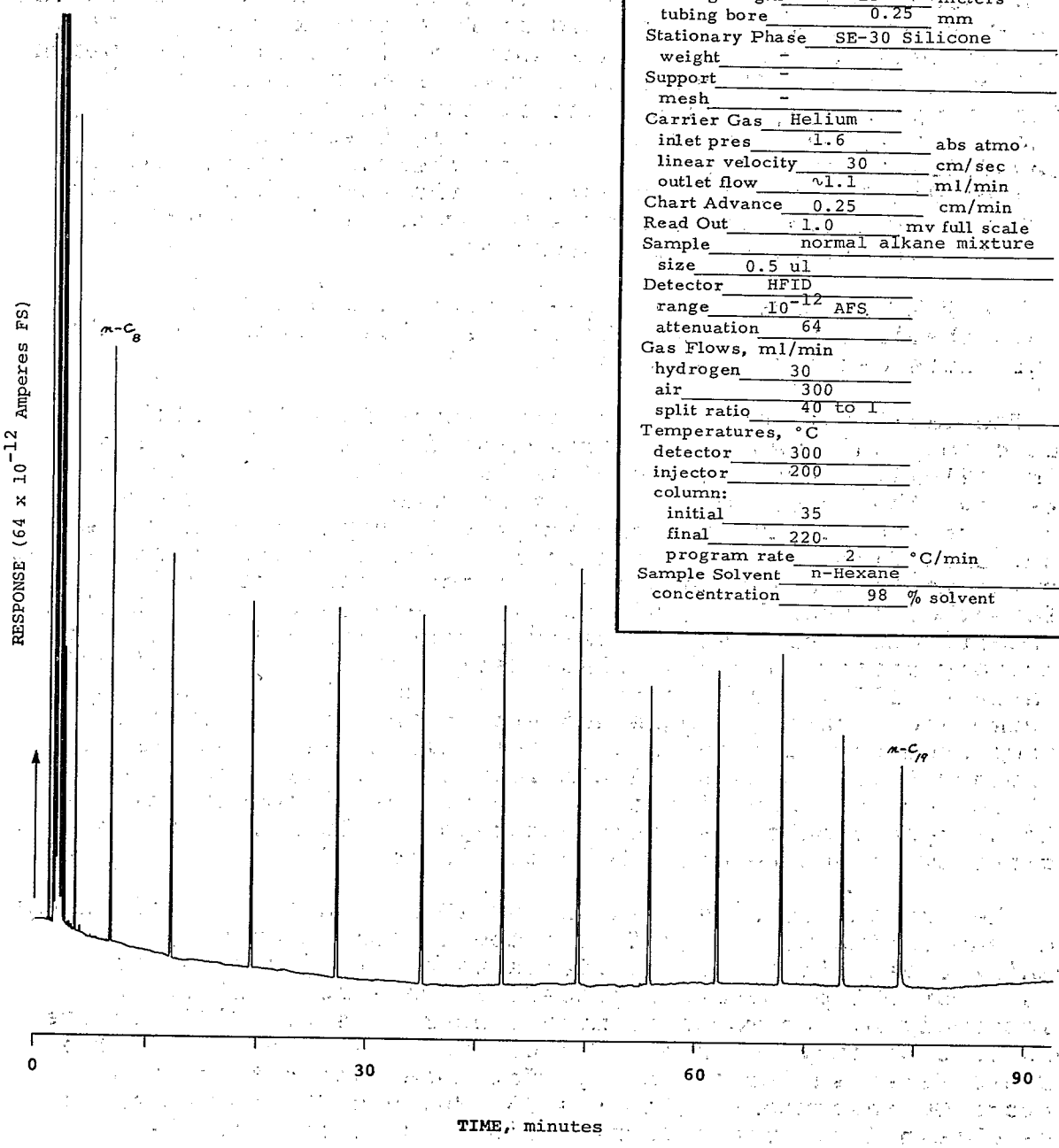

GAS CHROMATOGRAPHIC CONDITIONS

Instrument: Varian 1860-1
Analyst: W. Rubey
Date: 5-23-79
Column:
- tubing material: Pyrex
- tubing length: 15 meters
- tubing bore: 0.25 mm

Stationary Phase: SE-30 Silicone
- weight: -

Support: -
- mesh: -

Carrier Gas: Helium
- inlet pres: 1.6 abs atmo
- linear velocity: 30 cm/sec
- outlet flow: ~1.1 ml/min

Chart Advance: 0.25 cm/min
Read Out: 1.0 mv full scale
Sample: normal alkane mixture
- size: 0.5 ul

Detector: HFID
- range: 10^{-12} AFS
- attenuation: 64

Gas Flows, ml/min
- hydrogen: 30
- air: 300
- split ratio: 40 to 1

Temperatures, °C
- detector: 300
- injector: 200
- column:
  - initial: 35
  - final: 220
  - program rate: 2 °C/min

Sample Solvent: n-Hexane
- concentration: 98 % solvent

Figure 35. Glass OTC separation of normal alkanes.

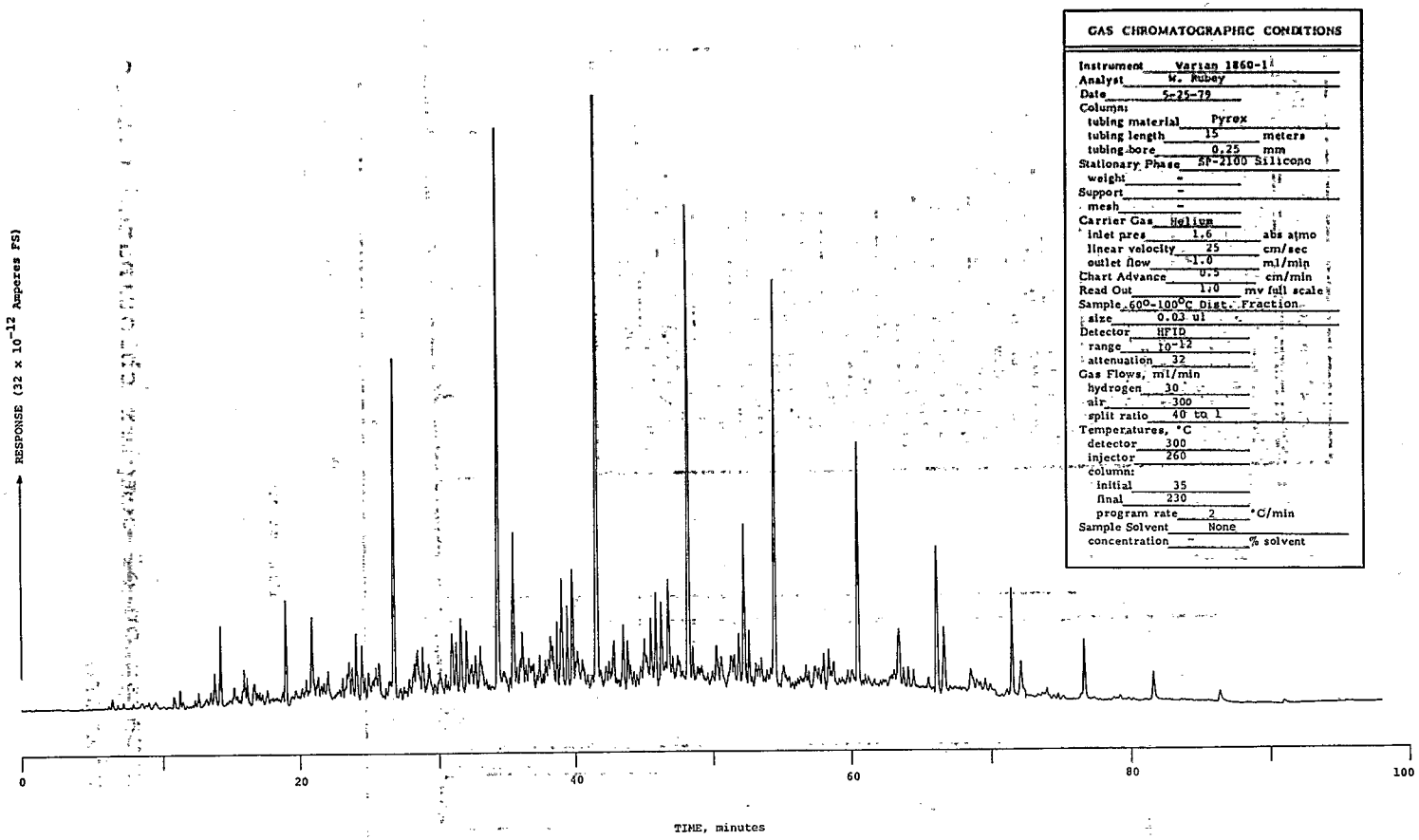

Figure 36. Chromatographic separation of a complex mixture.

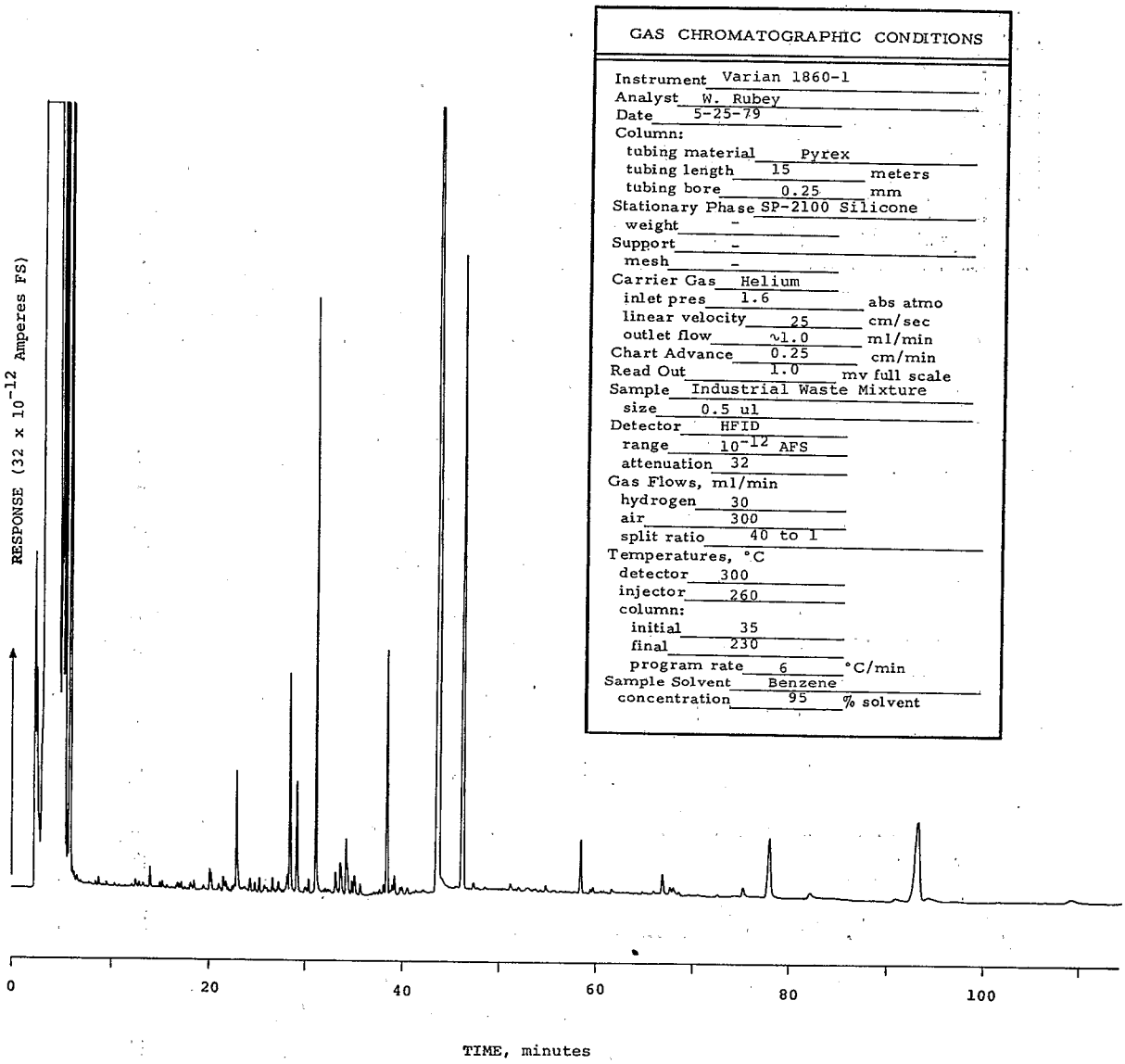

Figure 37. Separation of complex chlorinated hydrocarbon mixture.

separating capability for a very complex mixture of chlorinated hydrocarbons and other organic compounds.

The columns that are presently used in the TDAS are relatively thin film OTC's in that the stationary phase film thickness is on the order of 0.1 microns. This produces a relatively low stationary phase bleed level and also permits low temperature elution of relatively heavy compounds (138). The one disadvantage is that these thin film OTCs have low sample capacity. The columns that are usually used in the TDAS are from 10 to 20 meters long. However, the columns that are used in the other GC's which support the TDAS operation, are much longer; consequently, higher efficiency separations can be obtained with these instruments. Presently, the separation capability within the TDAS is adequate for the samples currently being tested. In the future, other types of OTC's will also be incorporated in the TDAS. These will contain chemically bonded stationary phases (139,140) and other types of high-temperature substrates.

The gas flow to and from a gas chromatograph must be especially free of extraneous organic contaminants. Otherwise the chromatographic separation and subsequent analysis are adversely influenced by these contaminants (141). Also, the geometry of the flow path should be free of mixing chambers and unswept regions (142). In a system as complicated as the TDAS, there are a number of potential sources for organic contamination. However, by using thermally stable materials throughout the gas flow path, the level of bleed contaminants can be minimized.

With the TDAS, there is an additional trapping procedure that can be invoked when it is desirable to conduct an analysis with a very low background level. Specifically, this is accomplished by cooling the cryogenic adsorptive trap immediately after the collected products have been thermally desorbed from the trap. In short, by cooling the in-line trap to subambient temperatures, any residual compounds that would normally be migrating during the time period of the GC analysis would now be captured by this cryogenic trap. These contaminants are therefore not continuously migrating through the GC column during the programmed temperature GC analysis. Any condensable contaminants that are admitted to the column before or during the thermal desorption of the product collection trap are subsequently captured by the thermal focusing feature of the GC column before the start of the programmed temperature GC analysis. And of course, these condensable contaminants would eventually be chromatographed as typical solutes.

In the TDAS, the GC effluent is passed into an electron impact source mass spectrometer, which is described briefly in Section 8. The influence of the GCMS coupling on the

performance of the OTC can be negligible, providing the gas transport between the two instruments is fully understood (143-145). In reality, the MS probably has far less influence on the behavior of the chromatographic column than the column has on the MS (e.g., column bleeding, etc.)

The ability to separate complex volatile mixtures is at a relatively advanced technological state. Even so, recent developments indicate that this already high resolving capability will probably be advanced even further (146-149). Therefore, if situations arise in the future in which greater resolution is needed in the TDAS, it would appear that such could be readily accomplished.

SECTION 8

MASS SPECTROMETER WITH DEDICATED MINICOMPUTER AND ASSOCIATED DATA REDUCTION EQUIPMENT

In the TDAS, the identification of the various thermal decomposition products is accomplished through the use of an in-line MS. As shown earlier in Figures 5 and 7, the MS is an integral and vitally important component of the TDAS. The particular MS instrument incorporated into the TDAS is an LKB 2091 GCMS. A photograph of this instrument along the upstream TDU is shown in Figure 38.

A combined GCMS is a very powerful analytical tool (46, 150, 151) and is especially applicable for analyzing complex mixtures of organic compounds. The LKB 2091 is a single focusing MS equipped with a 90° sector magnetic analyzer. The MS assembly consists of one unit, housing both analyzer and controls. There are individual high-capacity vacuum systems for the analyzer tube, the source, and the inlet systems. This instrument employs the Ryhage two-stage molecular separator (152), which is capable of operation at temperatures up to 350°C.

The MS incorporated into the TDAS uses an electron impact source, and this instrument has a mass range of 0 to 2000 at 1.17 kV acceleration voltage. In the GC mode, the resolution of the mass spectra is better than 700 at 3.5 kV acceleration voltage, and at an ionization potential of 70 eV. This MS can be automatically scanned at different rates over the full spectrum range or parts thereof. Parabolic scanning rates range from 1 to 240 seconds for a full-scale scan.

There are two detectors in the LKB 2091 GCMS. A total ion current detector is used for generating a chromatographic signal that represents the ionized effluent at the exit of the ion source. The output from this detector is displayed on a potentiometric recorder. The other detector is an electron multiplier that is positioned at the outlet of the magnetic analyzer tube. The output of the electron multiplier-preamplifier can be displayed on a UV-recording oscillograph, or data can be fed to the data reduction system. This instrument has its own mass marker (LKB 2091-110), which has an accuracy of ±0.3 amu at 3.5 kV acceleration voltage. This MS is also equipped with a direct inlet system (LKB 2091-210)

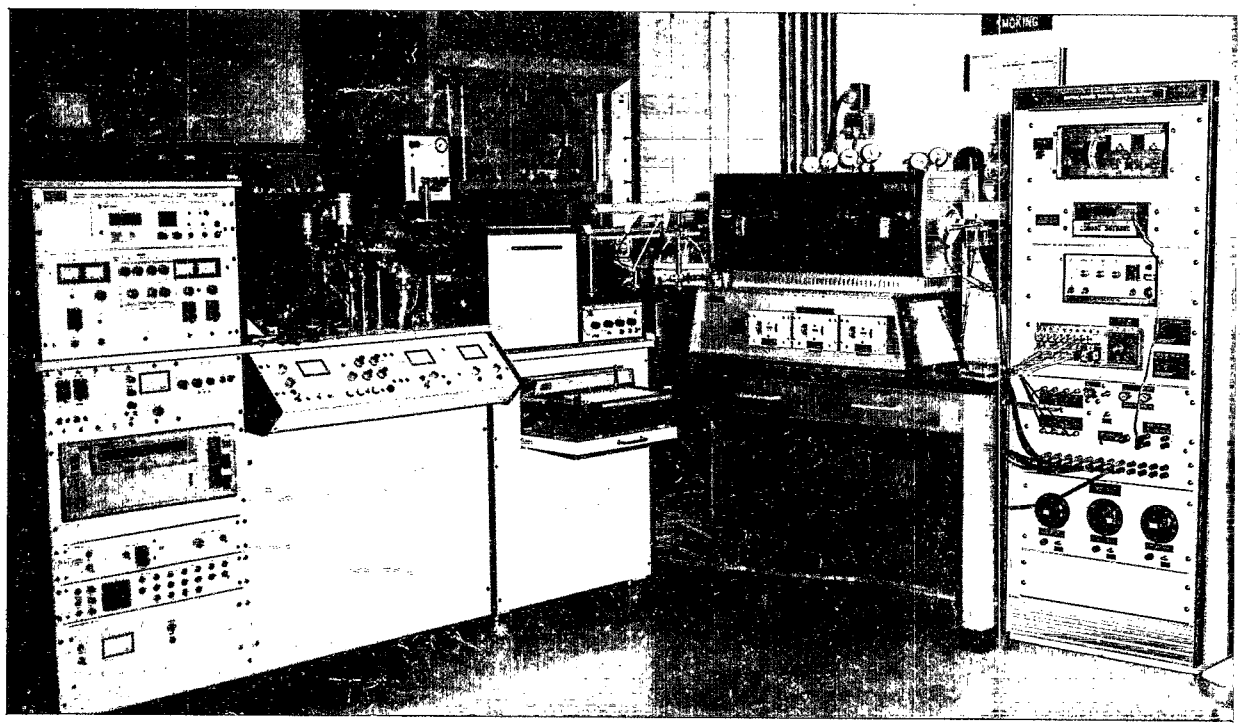

Figure 38. LKB 2091 GCMS and TDU.

whereby a sample can be admitted to the spectrometer through the use of a special probe.

The data reduction equipment that supports the GCMS is an LKB 2130 data system. A photograph of this equipment is shown in Figure 39. The data system consists of a Digital Electronics Corporation PDP 11/04 Minicomputer. The graphics terminal is a Tektronix 4012, and the line printer/plotter is a Versatec 800. Included with the data system is the LKB applications software package and the LKB 2130-220 library.

In addition to the above data handling components, another terminal has been incorporated into the TDAS. This additional terminal is a Texas Instruments 733 ASR, which uses dual cassettes. This terminal functions as an external data base interface through which searches can be conducted of the EPA-NIH Chemical Information System (153, 154) mass spectral library. A photograph of this mass spectra searching terminal is shown in Figure 40.

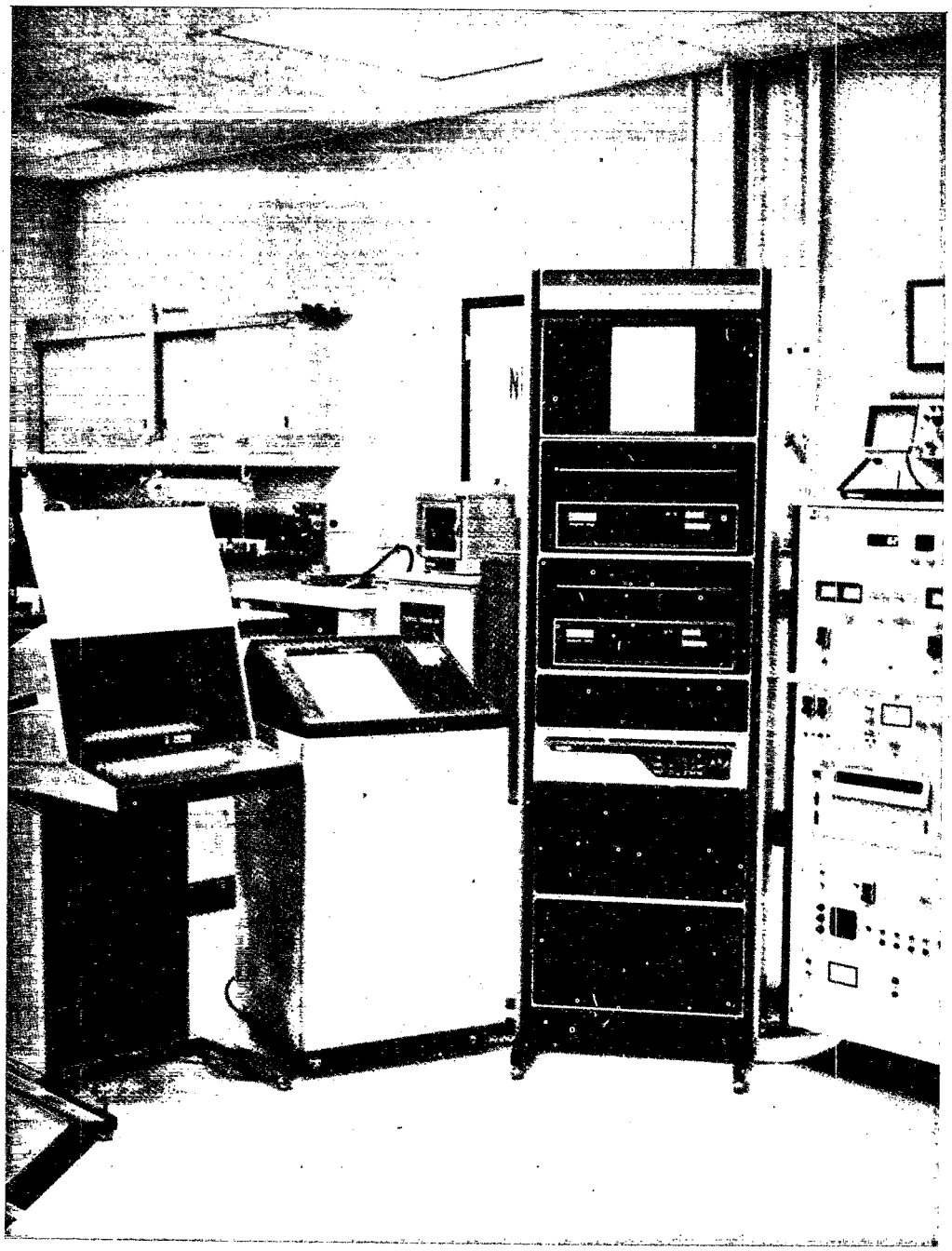

Figure 39. Minicomputer for data reduction.

Figure 40. Mass spectra searching terminal.

SECTION 9

UTILIZATION OF THE TDAS IN THERMAL DECOMPOSITION STUDIES

The TDAS has been designed with the objective of conducting precise thermal decomposition experiments in the laboratory. This system is capable of investigating a wide variety of organic materials and experimentally examining the effects of the major thermal decomposition variables. The TDAS can handle relatively pure substances and also very complex samples (e.g., multi-component industrial organic wastes).

The most important immediate use of the TDAS is in determining the thermal decomposition behavior of toxic organic substances. This is a very sensitive problem area in which information is urgently needed with respect to the tremendous variety of toxic organic materials.

With the flexibility built into the TDAS, many types of thermal decomposition experiments can be conducted. Essentially, the various types of information that are obtained from TDAS experiments can be grouped into four categories:

1. Establishment of the thermal decomposition profile of a substance.

2. Determination of residence time effects and associated kinetic behavior.

3. Investigation of different gaseous atmospheres, pressure effects, and other related thermal decomposition variables.

4. Collection of data for prediction of thermal decomposition behavior.

The thermal decomposition profile of a substance is obtained by subjecting a known quantity of the material to a controlled thermal exposure. Analyses are then conducted to determine the amount of the unreacted parent substance and also to identify and quantitate the various thermal decomposition products. By subjecting a sample to a series of thermal exposures covering a broad experimental range, the thermal

decomposition behavior of that substance can be established. Although the thermal decomposition behavior of the parent substance is of major importance, the detection and identification of various thermally stable decomposition products is also of vital concern (12). There are many instances where an organic substance decomposes and forms other chemical species of equal or greater toxicity (155). The major objective in obtaining a thermal decomposition profile is to determine the thermal exposure conditions that are necessary to produce essentially complete destruction of the parent substance and its various products. This profile also shows the thermal regions where toxic products are formed (12,156). Such thermal decomposition data are of considerable value in providing guidance for large-scale thermal disposal operations. The thermal decomposition profile of a substance can form the basis for establishing its safe incineration conditions (15,45). This same type of TDAS experiment can be conducted with very complex industrial wastes, only here the objective is simply to determine at what thermal conditions no toxic substances are emerging in the effluent.

The effect of residence time on the extent of thermal decomposition can be readily measured with the TDAS. This system can also be used for a variety of reaction kinetic studies, as the reactor incorporated into the TDU is ideally suited for determining residence time and kinetic effects (12, 41). Some excellent data have been obtained for lower molecular weight organic substances using a similar laboratory reactor (43,44).

The third group of experiments encompasses studies in which the thermal decomposition behavior of a substance is evaluated while it is in different gaseous environments. Also, studies can be conducted where the macroscopic reaction pressure is varied to determine the effect of pressure on the thermal reaction.

The fourth experimental area in which the TDAS can have broad application is in the prediction of the thermal decomposition behavior of different organic molecules. This is a promising experimental area of considerable potential. From laboratory data generated thus far (12,41,43), there seems to be a good possibility that eventually thermal decomposition behavior can be predicted (at least in part) by simply knowing the molecular structure of a substance (157). It is anticipated that by conducting special TDAS experiments aimed at collecting thermal decomposition data on different chemical families or bond structures, some level of predictability will emerge for organic compounds of similar structure. The ability to predict the thermal decomposition behavior of a waste substance strictly by knowing its molecular structure would be of considerable practical value.

REFERENCES

1. Paulson, E. G. How to Get Rid of Toxic Organics. Chem. Eng./Deskbook Issue, Oct. 1977, p. 21.

2. Bell, B. A., Welday, J., and Gilley, W. Alternate Methods for the Disposal of the Pesticide Kepone. Paper presented at the Third Annual Conference on Treatment and Disposal of Industrial Wastewaters and Residues. April 1978, Houston, TX.

3. Kennedy, M. V., Stojanovic, B. J., and Shuman, F. L., Jr. Chemical and Thermal Aspects of Pesticide Disposal. J. Environ. Qual., 1:63, 1972.

4. Bailin, L. J., Hertzler, B. L., and Oberacker, D. A. Development of Microwave Plasma Detoxification Process for Hazardous Wastes-Part 1. Environ. Sci. Tech., 12:673, 1978.

5. Oberacker, D. A., and Lees, S. Microwave Plasma Detoxification of Hazardous and Toxic Materials. NERC Topic, Oct. 1977.

6. Molten Salt Decomposes Pesticide Wastes. Chem. and Eng. News, Sept. 1977, p. 44.

7. Wastler, T. A., Offutt, C. K., Fitzsimmons, C. K., and Des Rosiers, P. E. Disposal of Organochlorine Wastes by Incineration at Sea. EPA-430/9-75-014, U.S. Environmental Protection Agency, Washington, DC, 1975.

8. Paige, S. F., Baboolal, L. B., Fisher, H. J., Scheyer, K. H., Shaug, A. M., Tan, R. L., and Thorne, C. F. Environmental Assessment: At-Sea and Land-Based Incineration of Organochlorine Wastes. EPA-600/2-78-087, U.S. Environmental Protection Agency, Research Triangle Park, NC, 1978.

9. Shih, C. C., Tobias, R. F., Clausen, J. F., and Johnson, R. J. Thermal Degradation of Military Standard Pesticide Formulations. Contract No. DADA 17-73-C-3132, U.S. Department of the Army, Washington, DC, 1975.

10. Waste Disposal by Burning at Sea. Chem. Week, April 11, 1979, p. 44.

11. Benbow, A. W., and Cullis, C. F. The Formation of Toxic Products During the Combustion of Halogen-Containing Polymers. European Polym. J. 11:723, 1975.

12. Duvall, D. S., and Rubey, W. A. Laboratory Evaluation of High Temperature Destruction of Kepone and Related Pesticides. EPA-600/2-76-299, U.S. Environmental Protection Agency, Cincinnati, OH, 1976.

13. Rolke, R. W., Hawthorne, R. D., Garbett, C. R., Slater, E. R., Phillips, T. T., and Towell, G. D. Afterburner System Study. EPA-R2-72-062, U.S. Environmental Protection Agency, Research Triangle Park, NC, 1972.

14. Barrett, R. E. Environmental Assessment of Afterburner Combustion Systems. In: Proceedings of the Second Stationary Source Combustion Symposium, p. 107. Vol. III. EPA-600/7-77-073c, U.S. Environmental Protection Agency, Research Triangle Park, NC, 1977.

15. Hazardous Waste: Proposed Guidelines and Regulations and Proposal on Identification and Listing. Federal Register, 43, Dec. 1978.

16. Girard, L., and Harkness, A. C. Method for Analyzing the Effluent from a Microreactor. J. of G.C. 5:516, 1967.

17. Keulemans, A. I. M., and Perry, S. G. Identification of Hydrocarbons by Thermal Cracking. In: Gas Chromatography 1962. Van Swaay, M., ed. Butterworth, London, 1962, p. 356.

18. Kokes, R. J., Tobin, H., Jr., and Emmett, P. H. New Microcatalytic-Chromatographic Technique for Studying Catalytic Reactions. J. Am. Chem. Soc. 77: 5860, 1955.

19. Munday, C. W., and Primavesi, G. R. A Modular Gas-Chromatography System for Analyzing Exit Streams from Reactors. Analyst 88:551, 1963.

20. Chiu, J. Polymer Characterization by Coupled Thermogravimetry-Gas Chromatography. Anal. Chem. 40:1516, 1968.

21. Chang, T., and Mead, T. E. Tandem Thermogravimetric Analyzer-Gas Chromatograph-High Resolution Mass Spectrometer System. Anal. Chem. 43:534, 1971.

22. Shen, J. In-Situ Sampling System for Thermal Volatilization Analysis of Nonvolatile Materials by Gas Chromatography-Mass Spectrometry. Anal. Chem. 49:886, 1977.

23. Johnson, D. R., and Smith, J. W. Bureau of Mines Apparatus for Thermal Analysis: Simultaneous DTA-TG-EGA for Oil Shale and Solid Fuels. Report of Investigations 7429, U.S. Department of Interior, Bureau of Mines, Washington, DC, 1970.

24. Lodding, W., ed. Gas Effluent Analysis. Marcel Dekker, Inc., New York, NY, 1967.

25. Ayres, W. M., and Bens, E. W. Differential Thermal Studies with Simultaneous Gas Evolution Profiles. Anal. Chem. 33:568, 1967.

26. Wendlandt, W. W. A New Apparatus for Simultaneous Differential Thermal Analysis and Gas Evolution Analysis. Anal. Chem. Acta 27:309, 1962.

27. Norem, S. D. A Combustion Device for Use in Conjunction with Chromatographic Columns. In: Proceedings of First ISA Symposium on Gas Chromatography. Academic Press, New York, NY, 1958, p. 191.

28. Steingaszner, P. Microreaction Gas Chromatographic Techniques. In: Ancillary Techniques of Gas Chromatography, Ettre, L. S., and McFadden, W. H., eds. Wiley-Interscience, New York, NY, 1969, p. 11.

29. Kwart, H., Sarner, S. F., and Olson, J. H. Homogeneous Gas-Phase Thermolysis Kinetics. An Improved Flow Technique for Direct Study of Rate Processes in the Gas Phase. J. Phys. Chem. 73:4056, 1969.

30. McCarter, R. J. Apparatus for Rate Studies of Vapor Producing Reactions. In: Proceedings of a Symposium on the Current Status of a Thermal Analysis. National Bureau of Standards, Washington, DC, April, 1970.

31. Iglauer, N., and Bentley, F. F. Pyrolysis GLC for the Rapid Identification of Organic Polymers. J. Chrom. Sci. 12:23, 1974.

32. Derby, J. V., and Freedman, R. W. Vapor-Phase Pyrolysis and GC Analysis of Fire-Retardant Materials Containing PVC. Amer. Lab. May 1974.

33. Cramers, C. Pyrolysis Gas Chromatography of Volatile Hydrocarbons. In: Gas Chromatography 1968. Elsevier Pub., Amsterdam, Netherlands, 1969, p. 395.

34. Uden, P. C., Henderson, D. E., and Lloyd, R. J. Comprehensive Interfaced Pyrolysis Gas Chromatographic Peak Identification System. J. Chromatog. 126:225, 1976.

35. Uden, P. C., Henderson, D. E., and Lloyd, R. J. An Interfaced Vapor Phase Instrumental System for Thermal Analysis and Pyrolysis. In: Proceedings of the Third International Symposium on Analytical Pyrolysis, Amsterdam, Elsevier Scientific, Amsterdam, Netherlands, Sept. 1976.

36. Rubey, W. A. The Measurement of Concentration Zone Profile in Elution Chromatography. Technical Report, UDRI-TR-70-45 University of Dayton Research Institute, Dayton, OH, Dec. 1970.

37. Rubey, W. A. Design of a System for Simultaneous Thermogravimetric-Gas Chromatographic Analysis of Stabilized Polyacrylonitrile Fiber. Technical Report, UDRI-TR-71-28 University of Dayton Research Institute, Dayton, OH, Sept. 1971.

38. Rubey, W. A., and Duvall, D. S. Description of Apparatus for Conducting Isothermal Aging-Evolved Gas Analysis Tests with High Temperature Polymers. Technical Report, UDRI-TR-75-01, University of Dayton Research Institute, Dayton, OH, Jan. 1975.

39. Duvall, D. S., Rubey, W. A., and Carnes, R. A. High Temperature Destruction of Kepone and Related Pesticides. Report presented at 173rd American Chemical Society National Meeting, New Orleans, LA, March 1977.

40. Carnes, R. A., Duvall, D. S., and Rubey, W. A. A Laboratory Approach to Thermal Degradation of Organic Compounds. In: Proceedings of 70th Annual Meeting of Air Pollution Control Association, Toronto, Ontario, June 1977.

41. Duvall, D. S., and Rubey, W. A. Laboratory Evaluation of High-Temperature Destruction of Polychlorinated Biphenyls and Related Compounds. EPA-600/2-77-228, U.S. Environmental Protection Agency, Cincinnati, OH, Dec. 1977.

42. Duvall, D. S., Rubey, W. A., and Mescher, J. A. Laboratory Characterization of the Thermal Decomposition of Hazardous Wastes. In: Proceedings of SWRI-EPA Conference on Disposal of Hazardous Wastes, EPA-600/9-78-016, U.S. Environmental Protection Agency, Cincinnati, OH, 1978.

43. Lee, K., Jahnes, H. J., and Macauley, D. C. Thermal Oxidation Kinetics of Selected Organic Compounds. In: Proceedings of 71st Annual Meeting of the Air Pollution Control Association, Houston, TX, June 1978.

44. Lee, K., Hansen, J. L., and Macauley, D. S. Predictive Model of the Time-Temperature Requirements for Thermal Destruction of Dilute Organic Vapors. In: Proceedings of 72nd Annual Meeting of Air Pollution Control Association, Cincinnati, OH, June 1979.

45. Bell, B. A., and Whitmore, F. C. Kepone Incineration Test Program. EPA-600/2-78-108, U.S. Environmental Protection Agency, Cincinnati, OH, 1978.

46. Leathard, D. A., and Shurlock, B. C. Identification Techniques in Gas Chromatography. Wiley-Interscience, New York, NY, 1970.

47. McFadden, W. H. Introduction of Gas-Chromatographic Samples to a Mass Spectrometer. Sep. Sci. 1:736, 1966.

48. Giger, W., Reinhard, M., Schaffner, C., and Zurcher, F. Analyses of Organic Constituents in Water by High-Resolution Gas Chromatography in Combination with Specific Detection and Computer-Assisted Mass Spectrometry. In: Identification and Analyses of Organic Pollutants in Water. Keith, L. H., ed. Ann Arbor Press, Ann Arbor, MI, 1977, p. 433.

49. Gudzinowicz, B. J., Gudzinowicz, M. J., and Martin, H. F. Fundamentals of Integrated GC-MS. Marcel Dekker, New York, NY, 1976.

50. Kirkland, J. J. Residue Analysis by Gas Chromatography. Paper presented at ACS Analytical Summer Symposium, Houston, TX, June, 1960.

51. Harris, W. E., and Habgood, H. W., Programmed Temperature Gas Chromatography. Wiley, New York, NY, 1966.

52. Westhaver, J. W. Theory of Open-Tube Distillation Columns. Ind. Eng. Chem., Jan. 1942, p. 126.

53. Westhaver, J. W. Concentration of Potassium 39 by Countercurrent Electro-migration: Some Theoretical Aspects of the Operation. J. Res. NBS 38:169, 1947.

54. Taylor, G. Dispersion of Soluble Matter in Solvent Flowing Slowly Through a Tube. Proc. Roy. Soc. A 219:186, 1953.

55. Aris, R. On the Dispersion of a Solute in a Fluid Flowing Through a Tube. Proc. Roy. Soc. A 235:67, 1956.

56. Golay, M.J.E. Theory of Chromatography in Open and Coated Tubular Columns with Round and Rectangular Cross-Sections. In: Gas Chromatography 1958. Desty, D. H., ed. Butterworths, London, 1958, p. 36.

57. Bode, H. Transfer Behavior of Narrow Bore Tubes under Laminar Flow. Chromatographia 3:113, 1970.

58. Giddings, J. C., and Seager, S. L. Rapid Determination of Gaseous Diffusion Coefficients by Means of Gas Chromatographic Apparatus. J. Chem. Phys. 33:1579, 1960.

59. Fuller, E. N., Ensley, K., and Giddings, J. C. Diffusion of Halogenated Hydrocarbons in Helium: The Effect of Structure on Collision Cross Sections. J. Phys. Chem. 73:3679, 1969.

60. Sutton, R., and Harris, W. E. Pyrolysis Gas Chromatography of Some Hydrocarbons. Can. J. Chem. 45:2913, 1967.

61. Carter, M. K., Moore, M., and Nadel, F. High Efficiency Oxidation Pyrolysis Tube for Analytical Determination of Trace Elements. Paper presented at 1974 Pittsburg Conference on Analytical Chemistry and Applied Spectroscopy.

62. Dean, W. R. Note on the Motion of Fluid in a Curved Pipe. Phil. Mag. S7 4:208, 1927.

63. Dean, W. R. The Stream-line Motion of Fluid in a Curved Pipe. Phil. Mag. S7 5:673, 1928.

64. Koutsky, J. A., and Adler, R. J. Minimization of Axial Dispersion by Use of Secondary Flow in Helical Tubes. Can. J. Chem. Eng. 42:239, 1964.

65. Tijssen, R. Effect of Column-Coiling on the Dispersion of Solutes in Gas Chromatography. Part I: Theory. Chromatographia 3:525, 1970.

66. Tijssen, R., and Wittebrood, R. T. Effect of Column-Coiling on the Dispersion of Solutes in Gas Chromatography. Part II: General Theory. Chromatographia 5:286, 1972.

67. Janssen, L.A.M. Axial Dispersion in Laminar Flow Through Coiled Tubes. Chem. Eng. Sci. 31:215, 1976.

68. Keulegan, G. H., and Beij, K. H. Pressure Losses for Fluid Flow in Curved Pipes. J. Res. NBS 18:89, 1937.

69. Barr, W. E., and Anhorn, V. J. Scientific and Industrial Glass Blowing and Laboratory Techniques. Instruments Publishing Co., Pittsburgh, PA, 1949, p. 198.

70. Rasmussen, R. A. A Quantitative Cryogenic Sampler. Amer. Lab. July 1972, p. 19.

71. Brenner, N., and Ettre, L. S. Condensing System for Determination of Trace Impurities in Gases by Gas Chromatography. Anal. Chem. 31:1815, 1959.

72. Drozd, J., Novak, J., and Rijks, J. A. Quantitative and Qualitative Head-space Gas Analysis of PPB Amounts of Hydrocarbons in Water. J. Chromatog. 158:471, 1978.

73. Tyson, B. J., and Carle, G. C. Gas Chromatographic Separation of Water from Cryogenically Collected Air Samples-Enhanced Concentration of Trace Organic Volatiles Prior to GC-MS Analysis. Anal. Chem. 46:610, 1974.

74. Des Marais, D. J. Variable-Temperature Cryogenic Trap for the Separation of Gas Mixtures. Anal. Chem. 50:1405, 1978.

75. Aue, W. A., Vogt, C. R. H., and Younker, D. R. A Gas Chromatographic Cartridge Desorption Port. J. Chromatog. 114:184, 1975.

76. Nawar, W. W., Sawyer, F. M., Beltran, E. G., and Fagerson, I. S. An Injection System for Gas Chromatography. Anal. Chem. 32:1535, 1960.

77. Russell, J. W. Analysis of Air Pollutants Using Sampling Tubes and Gas Chromatography. Environ. Sci. Tech. 9:1175, 1975.

78. Russell, J. W., and Shadoff, L. A. The Sampling and Determination of Halocarbons in Ambient Air Using Concentration on Porous Polymer. J. Chromatog. 134:375, 1977.

79. Hopkins, B. J., and Pretorius, V. Rapid Evaporation of Condensed Gas Chromatographic Fractions. J. Chromatog. 158:465, 1978.

80. Kaiser, R. E. Temperature Gradient Chromatography: Part 1. Reversion Gas Chromatography. Chromatographia 1:199, 1968.

81. Kaiser, R. E. Ultra Trace Analysis of Volatile Substances with GC Methods in the Sub ppm and ppb Range Down to 10^{-10}%. J. Chromatog. Sci. 9:227, 1971.

82. Kaiser, R. E. Enriching Volatile Compounds by a Temperature Gradient Tube. Anal. Chem. 45:965, 1973.

83. Kaiser, R. E. Gas Chromatography in Environmental Analysis. J. Chromatog. Sci. 12:36, 1974.

84. Feairheller, W., Marn, P. J., Harris, D. H., and Harris, D. L. Technical Manual for Process Sampling Strategies for Organic Materials. EPA-600/2-76-122, U.S. Environmental Protection Agency, Research Triangle Park, NC, 1976.

85. Snyder, A. D., Hodgson, F. N., Kemmer, M. A., and McKendree, J. R. Utility of Solid Sorbents for Sampling Organic Emissions from Stationary Sources. EPA-600/2-76-201, U.S. Environmental Protection Agency, Research Triangle Park, NC, 1976.

86. Adams, J., Menzies, K., and Levins, P. Selection and Evaluation of Sorbent Resins for the Collection of Organic Compounds. EPA-600/7-77-044, U.S. Environmental Protection Agency, Research Triangle Park, NC, 1977.

87. Jones, P. W., Wilkinson, J. E., and Strup, P. E. Measurement of Polycyclic Organic Materials and Other Hazardous Organic Compounds in Stack Gases: State of the Art. EPA-600/2-77-202, U.S. Environmental Protection Agency, Research Triangle Park, NC, 1977.

88. Gallant, R. F., King, J. W., Levins, P. L., and Piecewicz, J. F. Characterization of Sorbent Resins for Use in Environmental Sampling. EPA-600/7-78-054, U.S. Environmental Protection Agency, Research Triangle Park, NC, 1978.

89. Vidal-Madjar, C., Gonnord, M. F., Benchah, F., and Guiochon, G. Performances of Various Adsorbents for the Trapping and Analysis of Organohalogenated Air Pollutants by Gas Chromatography. J. Chromatog. Sci. 16:190, 1978.

90. Bruner, F., Ciccioli, P., and Di Nardo, F. Use of Graphitized Carbon Black in Environmental Analysis. J. Chromatog. 99:661, 1974.

91. Mueller, F. X., and Miller, J. A. Determination of Organic Vapors in Industrial Atmospheres. Amer. Lab. May 1974.

92. Zlatkis, A., Kaufman, H. R., and Durbin, D. E. Carbon Molecular Sieve Columns for Trace Analysis in Gas Chromatography. J. Chromatog. Sci. 8:416, 1970.

93. Grob, K., Grob, K., Jr., and Grob, G. Organic Substances in Potable Water and its Precursor. J. Chromatog. 106:299, 1975.

94. Thomas, T. C., and Jackson, J. W. A Technique for Sampling of 2, 4-D; 2, 4, 5-T Herbicides in Air. Paper presented at 1975 Pittsburg Conference on Analytical Chemistry and Applied Spectroscopy.

95. Coburn, J. A., Valmanis, I. A., and Chau, A. S. Y. Evaluation of XAD-2 for Multiresidue Extraction of Organochlorine Pesticides and Polychlorinated Biphenyls from Natural Waters. J. AOAC 60:224, 1977.

96. Ambersorb Carbonaceous Adsorbents: Technical Notes. Unpublished data. Rohm and Haas Co., Philadelphia, PA, 1977.

97. Ciccioli, P., Bertoni, G., Brancaleoni, E., Fratarcangeli, R., and Bruner, F. Evaluation of Organic Pollutants in the Open Air and Atmospheres in Industrial Sites Using Graphitized Carbon Black Traps and Gas Chromatographic-Mass Spectrometric Analysis with Specific Detectors. J. Chromatog. 126:757, 1976.

98. Lee, K. Y., Nurok, D., and Zlatkis, A. Combined Headspace and Extraction Technique for Profile Analysis by Capillary Gas Chromatography. J. Chromatog. 158:377, 1978.

99. Lewis, R. G., Brown, A. R., and Jackson, M. D. Evaluation of Polyurethane Foam for Sampling of Pesticides, Polychlorinated Biphenyls, and Polychlorinated Naphthalenes in Ambient Air. Anal. Chem. 49:1668, 1977.

100. Averill, W., and Purcell, J.E. Concentration and Analysis of Organic Compounds from Air and Water. Paper presented at 1978 Pittsburgh Conference on Analytical Chemistry and Applied Spectroscopy.

101. Janak, J., Ruzickova, J., and Novak, J. Effect of Water Vapour in the Quantitation of Trace Components Concentrated by Frontal Gas Chromatography on Tenax-GC. J. Chromatog. 99:689, 1974.

102. Van Wijk, R. The Use of Poly-Para-2, 6-Diphenyl-Phenylene Oxide as a Porous Polymer in Gas Chromatography. J. Chromatog. Sci. 8:418, 1970.

103. Bursey, J. T., Smith, D., Bunch, J. E., Williams, R. N., Berkley, R. E., and Pellizzari, E. D. Application of Capillary GC/MS/Computer Techniques to Identification and Quantitation of Organic Components in Environmental Samples. Amer. Lab. Dec. 1977.

104. Bellar, T. A., Lichtenberg, J. J. The Determination of Volatile Organic Compounds at the μg/l Level in Water by Gas Chromatography. EPA-670/4-74-009, U.S. Environmental Protection Agency, Cincinnati, OH, 1974.

105. Kuo, P. P. K., Chian, E. S. K., DeWalle, F. B., and Kim, J. H. Gas Stripping, Sorption, and Thermal Desorption Procedures for Preconcentrating Volatile Polar Water-Soluble Organics from Water Samples for Analysis by Gas Chromatography. Anal. Chem. 49:1023, 1977.

106. Gearhart, H. L., Pierce, S. K., and Payne-Bose, D. A Sampling Technique for Organic Components in Human Breath. J. Chromatog. Sci. 15:480, 1977.

107. Leoni, V., Puccetti, G., and Grella, A. Preliminary Results on the Use of Tenax for the Extraction of Pesticides and Polynuclear Aromatic Hydrocarbons from Surface and Drinking Waters for Analytical Purposes. J. Chromatog. 106:119, 1975.

108. Leoni, V., Puccetti, G., Colombo, R. J., and D'Ovidio, A. M. The Use of Tenax for the Extraction of Pesticides and Polychlorinated Biphenyls from Water: II. Tests with Artificially Polluted and Natural Waters. J. Chromatog. 125:399, 1976.

109. Zeldes, S. G., and Horton, A. D. Trapping and Determination of Labile Compounds in the Gas Phase of Cigarette Smoke. Anal. Chem. 50:779, 1978.

110. Chesler, S. N., Gump, B. H., Hertz, H. S., May, W. E., and Wise, S. A. Determination of Trace Level Hydrocarbons in Marine Biota. Anal. Chem. 50:805, 1978.

111. Black, M. S., Rehg, W. R., Sievers, R. E., and Brooks, J. J. Gas Chromatographic Technique for Compound Class Analysis of Jet Engine Exhaust. J. Chromatog. 142:809, 1977.

112. Peterson, H., Eiceman, G. A., Field, L. R., and Sievers, R. E. Gas Chromatographic Injector Attachment for the Direct Insertion and Removal of a Porous Polymer Sorption Trap. Anal. Chem. 50:2152, 1978.

113. Katys, G. P. Continuous Measurement of Unsteady Flow. Pergamon Press, New York, NY, 1964.

114. Laub, J. H. An Electric Flow Meter. Electrical Engineer Dec. 1947, p. 1216.

115. Grey, J., and Liu, F. F. Methods of Flow Measurement, J. Amer. Rocket Soc. May-June 1953, p. 133.

116. Lochmuller, C. H., and Gordon, B. M. The Determination of Binary Gas Diffusion Coefficients Through Measurement of the Time-Based, Chromatographic Peak Variance. J. Chromatog. Sci. 16:74, 1978.

117. Baumann, F., Klaver, R. F., and Johnson, J. F. Subambient Programmed Temperature Gas Chromatography. In: Gas Chromatography, 1962, Butterworths, London, 1962, p. 152.

118. Rasmussen, R. A., Harsch, D. E., Sweany, P. H., Krasnec, J. P., and Cronn, D. R. Determination of Atmospheric Halocarbons by a Temperature-Programmed Gas Chromatographic Freezeout Concentration Method. J. Air Poll. Control Assoc. 27:579, 1977.

119. DeRuwe, H. J. J., Schulting, F. L., and Van Grondelle, J. A Simple, Inexpensive Cryogenic Unit for Subambient Gas Chromatographic Analysis. HRC and CC 1:211, 1978.

120. James, A. T., and Martin, A. J. P. Gas-Liquid Partition Chromatography: The Separation and Micro-estimation of Volatile Fatty Acids from Formic Acid to Dodecanoic Acid. Biochem. J. 50:679, 1952.

121. Golay, M. J. E. Theory and Practice of Gas Liquid Partition Chromatography with Coated Capillaries. In: Gas Chromatography. Coates, V. J., ed. Academic Press, New York, NY, 1958, p. 1.

122. Golay, M. J. E. Theory of Chromatography in Open and Coated Tubular Columns with Round and Rectangular Cross-Sections. In: Gas Chromatography 1958. Desty, D. H., ed. Butterworths, London, 1958, p. 36, p. 62.

123. Golay, M. Brief Report on Gas Chromatographic Theory. In: Proceedings of Third International Symposium on Gas Chromatography 1960. Edinburgh, Scotland, Butterworths, Washington, 1960, p. 139.

124. Golay, M. Height Equivalent to a Theoretical Plate of an Open Tubular Column Lined with a Porous Layer. Anal. Chem. 40:382, 1968.

125. Giddings, J. C. Dynamics of Chromatography: Part I - Principles and Theory. Marcel Dekker, New York, NY, 1965.

126. Rubey, W. A. Bibliography of Open Tubular Column Gas Chromatography. Technical Report, UDR-TR-79-11 University of Dayton Research Institute, Dayton, OH, Jan. 1979.

127. Jennings, W. Gas Chromatography with Glass Capillary Columns. Academic Press, New York, NY, 1978.

128. Sandra, P., and Verzele, M. Surface Treatment, Deactivation and Coating in $(GC)^2$ (Glass Capillary Gas Chromatography). Chromatographia 10:419, 1977.

129. Sandra, P., Verstappe, M., and Verzele, M. HRC and CC 1: 28, 1978.

130. Grob, K. The Glass Capillary Column in Gas Chromatography. A Tool and a Technique. Chromatographia 8:423, 1975.

131. Schomburg, G., Dielmann, R., Hussmann, H., and Weeke, F. Gas Chromatographic Analysis with Glass Capillary Columns. J. Chromatog. 122:55, 1976.

132. Novotny, M., Blomberg, L., and Bartle, K. Some Factors Affecting the Coating of Open Tubular Columns for Gas Chromatography. J. Chrom. Sci. 8:390, 1970.

133. Ettre, L., and March, E. Efficiency, Resolution and Speed of Open Tubular Columns as Compared to Packed Columns. J. Chromatog. 91:5, 1974.

134. Rijks, J., van den Berg, J., Diependaal, J. Characterization of Hydrocarbons in Complex Mixtures by Two-Dimensional Precision Gas Chromatography. J. Chromatog. 91:603, 1974.

135. Blomberg, L. Uniformity of Stationary Phase Films in Dynamically Coated Glass Capillary Columns for Gas Chromatography. Chromatographia 8:324, 1975.

136. Onuska, F., and Comba, M. Comparison of Surface Modification Techniques Used for the Preparation of Wall Coated Open Tubular Glass Capillary Columns. In: Proceedings of Second International Symposium on Glass Capillary Chromatography, Hindelang, Germany, Institute of Chromatography, Bad Durkheim, Germany, 1977, p. 283.

137. Madani, C., Chambaz, E., Rigaud, M., Durand, J., and Chebroux, P. New Method for the Preparation of Highly Stable Polysiloxane-Coated Glass Open-Tubular Capillary Columns and Application to the Analysis of Hormonal Steroids. J. Chromatog. 126:161, 1976.

138. Grob, K., Jr., and Grob, K. Are We Using the Full Range of Film Thickness in Capillary-GLC. Chromatographia 10:250, 1977.

139. Madani, C., Chambaz, E., Rigaud, M., and Bretton, J. Use of Hydrolyzed Chlorosilanes for the Preparation of High Resolution Glass Capillary Columns. Second International Symposium on Glass Capillary Chromatography, Hindelang, Germany, Institute of Chromatography, Bad Durkheim, Germany, 1977, p. 249.

140. Blomberg, L., Buijten, J., Gawdzik, J., and Wannman, T. Preparation of Thermostable, Phenyl Silicone Coated, Glass Capillary Columns for Separation of Polyaromatic Hydrocarbons. Chromatographia 11:521, 1978.

141. Purcell, J. E., Downs, H. D., and Ettre, L. S. Extraneous Peaks in Gas Chromatography: Their Source and Elimination. Chromatographia 8:605, 1975.

142. Guiochon, G. Influence of the Apparatus on the Apparent Efficiency of Columns in Gas Chromatography. J. Gas Chromatog. 2:139, 1964.

143. Sellier, N., and Guiochon, G. Influence of GC-MS Coupling on the Performances of Chromatographic Columns. J. Chromatog. Sci. 8:147, 1970.

144. Eyem, J. The Role of Wall-Coated Capillary Columns in GC-MS Techniques. Chromatographia 8:456, 1975.

145. Novotny, M. Coupling of Open Tubular Columns with a Mass Spectrometer through the Jet-Type Molecular Separator. Chromatographia 2:350, 1969.

146. Ducass, A., Gonnord, M. F., Arpino, P., and Guiochon, G. Simple Techniques for Two-Dimensional Gas Chromatography. J. Chromatog. 148:321, 1978.

147. Anderson, E. L., Moskot, M., and Bertsch, W. High Resolution Columns in Gas Chromatography. Paper presented at 174th ACS Meeting, Chicago, IL, Aug. 1977.

148. Cram, S. P. Extended Capabilities in Gas Chromatography through High Resolution Techniques. Paper presented at 1979 Pittsburgh Conference on Analytical Chemistry and Applied Spectroscopy.

149. Jennings, W. G. Food and Essential Oil Analysis with Glass Capillary Columns. Paper presented at 1979 Pittsburgh Conference on Analytical Chemistry and Applied Spectroscopy.

150. Fenselau, C. Gas Chromatography Mass Spectrometry: A Report on State of the Art. Appl. Spectrosc. 28:305, 1974.

151. Gudzinowicz, B. J., Gudzinowicz, M. J., and Martin, H. F. Integrated GC-MS Analytical Systems: Part I - Recent Technological Advances Affecting Integrated GC-MS System Utilization. Chem. Instr. 8:225, 1977.

152. Ryhage, R. Use of a Mass Spectrometer as a Detector and Analyzer for Effluents Emerging from High Temperature Gas-Liquid Chromatography Columns. Anal. Chem. 36:759, 1964.

153. Heller, S. R., McGuire, J. M., and Budde, W. L. Trace Organics by GC/MS. Environ. Sci. Tech. 9:210, 1975.

154. Milne, G. W. A., and Heller, S. R. The MSDC/EPA/NIH Mass Spectra Search System. Amer. Lab. Sept. 1976.

155. Edwards, J. B. Combustion: The Formation and Emission of Trace Species. Ann Arbor Science, Ann Arbor, MI, 1974, p. 64.

156. Carnes, R. A., Rubey, W. A., Mescher, J. A., and Duvall, D. S. The Thermal Decomposition Analytical System (TDAS): Its Development and Application. In: Proceedings of the 72nd Annual Meeting of Air Pollution Control Association, Cincinnati, OH, June, 1979.

157. Hutzinger, O., Sundstrom, G., Karasek, F. W., and Safe, S. The Chemistry of Some Potential Polyhalogenated Water Pollutants. In: Identification and Analyses of Organic Pollutants in Water. Keith, L. H., ed. Ann Arbor Press, Ann Arbor, MI, 1977, p. 15.

BIBLIOGRAPHY

Benedict, R. P. Fundamentals of Temperature, Pressure, and Flow Measurements. Wiley, New York, N.Y., 1969.

Bird, R. B., Stewart, W. E., and Lightfoot, E. N. Transport Phenomena. Wiley, New York, N.Y., 1960.

Dal Nogare, S., and Juvet, R. S., Jr. Gas-Liquid Chromatography. Wiley - Interscience, New York, N.Y., 1962.

Danials, T. Thermal Analysis. Wiley, New York, N.Y., 1973.

Deelder, R. S., Kroll, M.G.F., and Beeren, A.J.B. Post-Column Reactor Systems in Liquid Chromatography. J. Chromatog. 149:669, 1978.

Edwards, J. B. Combustion: The Formation and Emission of Trace Species. Ann Arbor Science, Ann Arbor, Mich., 1974.

Harris, W. E., and Habgood, H. W. Programmed Temperature Gas Chromatography. Wiley, New York, N.Y., 1966.

Hettmann, E. Chromatography. Van Nostrand Reinhold, New York, N.Y., 1975.

Jones, C. E. R., and Cramers, C. A. Analytical Pyrolysis. Elsevier, Amsterdam, Netherlands, 1976.

Kays, W. M. Convective Heat and Mass Transfer. McGraw-Hill, New York, N.Y., 1966.

Keith, L. H. Identification and Analysis of Organic Pollutants in Water. Ann Arbor Science, Ann Arbor, Mich., 1976.

Kennedy, M. V., ed. Disposal and Decontamination of Pesticides. ACS Symposium Series No. 73, The American Chemical Society, Washington, D.C., 1978.

Kreith, F. Principles of Heat Transfer. International Textbook Co., Scranton, Pa., 1958.

Lewis, B., and Von Elbe, G. Combustion, Flames, and Explosions of Gases. Academic Press, New York, N.Y., 1951.

Littlewood, A. B. Gas Chromatography. Academic Press, New York, N.Y., 1970.

Mickley, H. S., Sherwood, T. K., and Reed, C. E. Applied Mathematics in Chemical Engineering. McGraw-Hill, New York, N.Y., 1957.

Miller, J. M. Separation Methods in Chemical Analysis. Wiley-Interscience, New York, N.Y., 1975.

Purnell, H. Gas Chromatography. Wiley, New York, N.Y., 1962.

Reddick, H. W., and Miller, F. H. Advanced Mathematics for Engineers. Wiley, New York, N.Y., 1955.

Reid, R. C., and Sherwood, T. K. Properties of Gases and Liquids. McGraw-Hill, New York, N.Y., 1958.

Sternberg, J. C. Extracolumn Contributions to Chromatographic Band Broadening. Advances in Chromatography. Vol. 2. Marcel Dekker, New York, N.Y., 1966.

Wiedemann, H. G. Thermal Analysis. Academic Press, New York, N.Y., 1969.

Wilkinson, R. R., Kelso, G. L., and Hopkins, F. C. State-of-the-Art Report: Pesticide Disposal Research. EPA-600/2-78-13, U.S. Environmental Protection Agency, Cincinnati, Ohio, 1978.

APPENDIX A

GAS FLOW ANALYSIS: A DETAILED ANALYSIS OF GAS FLOW AND DISPERSION IN A NARROW-BORE CIRCULAR CROSS SECTION TUBE OF FOLDED CONFIGURATION

Residence time is an important parameter in thermal decomposition studies. To illustrate the importance of residence time, or more emphatically the residence time distribution, consider the two dramatically different residence time distributions that are represented in Figure A-1(a). Curve I is typical of the narrow and symmetric residence time distributions obtained using laboratory instrumentation. Curve II is typical of the residence time distributions associated with a large-scale unit having a high volume throughput and a minimum of mixing. The thermal decomposition profiles corresponding to these two different residence time distributions would be as depicted in Figure A-1(b). Notice that the thermal decomposition profile corresponding to the wide and asymmetric residence time distribution shows (1) the onset of thermal decomposition at lower temperatures than the narrow residence time distribution, and (2) a requirement of higher exposure temperatures for the same level of efficient thermal decomposition.

Theoretically, the narrower the residence time distribution, the more closely the thermal decomposition profile represents the actual thermal decomposition behavior of a given substance. Thus in the ideal thermal decomposition experiment, each of the molecules would be subjected to precisely the same residence time. Also, the value of this "line-function" residence time would be experimentally adjustable and measurable to a high degree of accuracy.

In practice, these uncompromising ideal conditions are unattainable, although accurately determined symmetric and narrow residence time distributions can be generated in laboratory-scale experiments. For large-scale work that involves large throughputs, such narrow residence time distributions are not presently feasible, even though progress is being made in this design area. Nevertheless, for purposes of comparison, interpretation, and extrapolation, it is of vital importance that the residence time distribution of a substance be known along with the other thermal decomposition test parameters.

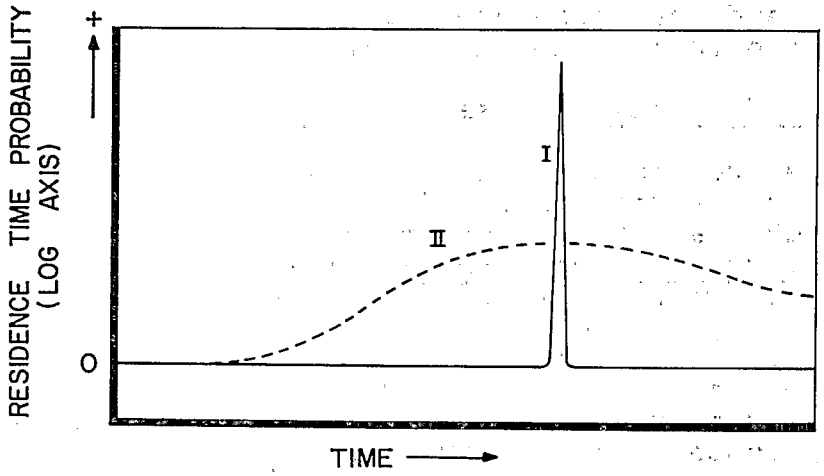

a) RESIDENCE TIME DISTRIBUTIONS

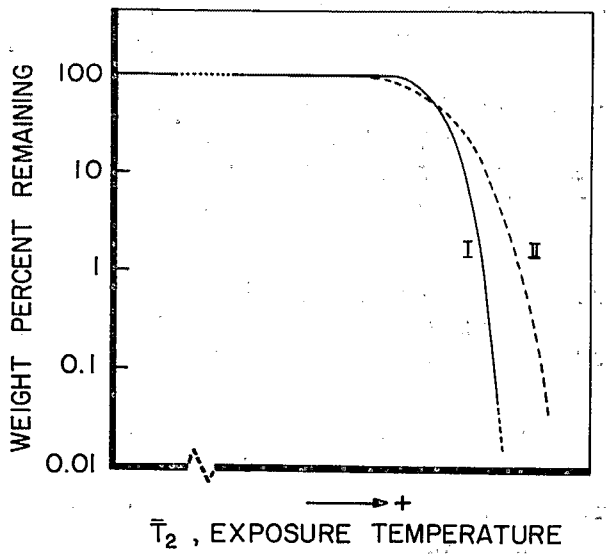

b) THERMAL DECOMPOSITION PROFILES

Figure A-1. Effect of residence time bandwidth.

In this appendix, a detailed transport analysis is presented. The objective of this analysis is to characterize the gas flow behavior and the residence time variation associated with a laboratory-scale thermal decomposition analytical system.

Straight Tube of Circular Cross Section

There are two simultaneous factors, i.e., dynamic processes, which influence the dispersion of a dilute zone of like gas molecules as they are being transported by a gaseous carrier through a straight tube of circular cross section. Fundamentally, these two factors are convection and diffusion.

The laminar flow of gases through such a tube exhibits a paraboloidal velocity profile; therefore, instantaneous axial velocity depends on radial position. Concurrently, the flowing gas will experience three dimensional diffusion according to Fick's second law.

An equation that describes the transport behavior and the concentration changes associated with these two effects can be written as

$$\frac{\partial C}{\partial t} = - v\frac{\partial C}{\partial z} + D_g\left(\frac{\partial^2 C}{\partial x^2} + \frac{\partial^2 C}{\partial y^2} + \frac{\partial^2 C}{\partial z^2}\right) \qquad \text{(A1)}$$

where C is the concentration of like molecules in the transport gas, t is time, v represents the gas axial velocity, z is axial distance, D_g is the intermolecular diffusion coefficient, and x and y represent the mutually perpendicular Cartesian coordinates.

Fluid flow through a straight tube of circular cross section can be examined by equating the applied hydrostatic force to the opposing viscous force. Then, over an axial fluid increment dz

$$A_m\, dp = (\eta\, P_s\, dz)\, \frac{dv}{dr} \qquad \text{(A2)}$$

where A_m is the cross-sectional area, η is the fluid viscosity, P_s is the surface perimeter perpendicular to the z axis, r is radial distance, and dp/dz is the negative pressure gradient.

Accordingly, for a circular cross-section flow path

$$\pi r^2 dp = (\eta\, 2\pi r\, dz)\, \frac{dv}{dr} \qquad \text{(A3)}$$

$$\frac{dv}{dr} = \left(\frac{r}{2\eta}\right) \frac{dp}{dz} \tag{A4}$$

$$\int_{o}^{v} dv = \left(\frac{1}{2\eta}\right) \frac{dp}{dz} \int_{r_o}^{r} r\, dr \tag{A5}$$

where r_o is the tube inner radius. Then,

$$v = -\left(\frac{r_o^2 - r^2}{4\eta}\right) \frac{dp}{dz} \tag{A6}$$

and the maximum velocity, V, can be written as

$$V = v\Big]_{r=o} = -\left(\frac{r_o}{4\eta}\right) \frac{dp}{dz} \tag{A7}$$

Therefore, it is seen that the axial gas velocity varies with r according to

$$v = V\left[1 - \left(\frac{r^2}{r_o^2}\right)\right] \tag{A8}$$

Next, the volumetric flow rate through the tube can be expressed as

$$F = \int_{o}^{r_o} v(2\pi r)\, dr \tag{A9}$$

and upon substituting equation A8,

$$F = 2V\pi \left[\int_{o}^{r_o} \left(r - \frac{r^3}{r_o^2}\right) dr\right] = \frac{\pi V r_o^2}{2} \tag{A10}$$

Thus the average linear gas velocity, $\bar{v}$, can be expressed as

$$\bar{v} = \frac{F}{A_m} = \frac{V}{2} \tag{A11}$$

and equation A1 can then be rewritten as

$$\frac{\partial C}{\partial t} = -2\bar{v}\left[1 - \left(\frac{r^2}{r_o^2}\right)\right]\frac{\partial C}{\partial z} + \left(\frac{\partial^2 C}{\partial x^2} + \frac{\partial^2 C}{\partial y^2} + \frac{\partial^2 C}{\partial z^2}\right) \tag{A12}$$

With the axial velocity term expressed relative to radial distance, it is likewise advantageous to rewrite the spatial diffusion term in cylindrical coordinates. Therefore, starting with the following relationships:

$$x = r\cos\theta \tag{A13}$$

$$y = r\sin\theta \tag{A14}$$

$$z = z \tag{A15}$$

$$r = \sqrt{x^2 + y^2} \tag{A16}$$

the spatial diffusion can eventually be equated according to

$$\frac{\partial^2 C}{\partial x^2} + \frac{\partial^2 C}{\partial y^2} + \frac{\partial^2 C}{\partial z^2} = \frac{\partial^2 C}{\partial r^2} + \left(\frac{1}{r}\right)\frac{\partial C}{\partial r} + \left(\frac{1}{r^2}\right)\frac{\partial^2 C}{\partial \theta^2} + \frac{\partial^2 C}{\partial z^2} \tag{A17}$$

However, for the special case involving laminar flow through a straight tube of circular cross section, it is seen that C is symmetrical about the z axis. Therefore,

$$\frac{\partial C}{\partial \theta} = \frac{\partial^2 C}{\partial \theta^2} = 0 \tag{A18}$$

thus

$$\frac{\partial^2 C}{\partial x^2} + \frac{\partial^2 C}{\partial y^2} + \frac{\partial^2 C}{\partial z^2} = \frac{\partial^2 C}{\partial r^2} + \left(\frac{1}{r}\right)\frac{\partial C}{\partial r} + \frac{\partial^2 C}{\partial z^2} \tag{A19}$$

and finally, the basic equation can be rewritten as

$$D_g \left[\frac{\partial^2 C}{\partial r^2} + \left(\frac{1}{r}\right) \frac{\partial C}{\partial r} + \frac{\partial^2 C}{\partial z^2} \right] = \frac{\partial C}{\partial t} + 2\bar{v} \left[1 - \left(\frac{r^2}{r_o^2}\right) \right] \frac{\partial C}{\partial z} \qquad \text{(A20)}$$

From equation A20, it is seen that

$$C = f(D_g, r, z, t, \bar{v}, r_o) \qquad \text{(A21)}$$

Therefore, as $\bar{v}$ represents the axial movement of the concentration centroid, and so that the axial point of reference moves with this centroid, a new coordinate, z_1, is introduced and defined as

$$z_1 = z - \bar{v}t \qquad \text{(A22)}$$

Along with this axial coordinate change, the time coordinate correspondingly must be revised. Therefore, since

$$\partial t_1 = \partial t \qquad \text{(A23)}$$

and as

$$\frac{\partial z_1}{\partial t} = -\bar{v} \qquad \text{(A24)}$$

then by adopting this new set of coordinates, z_1 and t_1, it is seen that

$$\frac{\partial C}{\partial t} = \left(\frac{\partial C}{\partial z_1}\right)\left(\frac{\partial z_1}{\partial t}\right) + \left(\frac{\partial C}{\partial t_1}\right)\left(\frac{\partial t_1}{\partial t}\right) \qquad \text{(A25)}$$

Hence,

$$\frac{\partial C}{\partial t} = \left(\frac{\partial C}{\partial z_1}\right)\left(-\bar{v}\right) + \left(\frac{\partial C}{\partial t_1}\right) \qquad \text{(A26)}$$

and equation A20 can be rewritten as

$$D_g \left[\frac{\partial^2 C}{\partial r^2} + \left(\frac{1}{r}\right) \frac{\partial C}{\partial r} + \frac{\partial^2 C}{\partial z_1^2} \right]$$

$$= \left(- \frac{\partial C}{\partial z_1}\right) \bar{v} + \frac{\partial C}{\partial t_1} + 2\bar{v}\left(1 - \frac{r^2}{r_o^2}\right) \frac{\partial C}{\partial z_1}$$

$$= \frac{\partial C}{\partial t_1} + \bar{v} \left(1 - \frac{2r^2}{r_o^2}\right) \frac{\partial C}{\partial z_1} \tag{A27}$$

If now the stipulation is made (Golay's assumption) that C never differs greatly from the average radial concentration $\bar{C}$, then

$$C = \bar{C} + \Delta C \tag{A28}$$

where

$$\bar{C} = \frac{1}{\pi r_o^2} \int_0^{r_o} C \; 2\pi r \; dr = \frac{2}{r_o^2} \int_0^{r_o} C \; r \; dr \tag{A29}$$

and

$$0 \equiv \int_0^{r_o} \Delta C \; r \; dr \tag{A30}$$

$$\Delta C << \bar{C} \tag{A31}$$

As equation A28 has been introduced and defined, equation A27 can be rewritten as

$$D_g \left[\frac{\partial^2 \bar{C}}{\partial r^2} + \frac{\partial^2 \Delta C}{\partial r^2} + \left(\frac{1}{r}\right) \frac{\partial \bar{C}}{\partial r} + \left(\frac{1}{r}\right) \frac{\partial \Delta C}{\partial r} \right.$$

$$\left. + \frac{\partial^2 \bar{C}}{\partial z_1^2} + \frac{\partial^2 \Delta C}{\partial z_1^2} \right] = \frac{\partial \bar{C}}{\partial t_1} + \frac{\partial \Delta C}{\partial t_1}$$

$$+ \left(\frac{\partial \bar{C}}{\partial z_1} + \frac{\partial \Delta C}{\partial z_1}\right) \bar{v} \left[1 - \left(\frac{2r^2}{r_o^2}\right)\right] \tag{A32}$$

and with the following assumed conditions

$$\frac{\partial^2 \overline{C}}{\partial r^2} = \frac{\partial \overline{C}}{\partial r} = 0 \tag{A33}$$

$$\frac{\partial \Delta C}{\partial t_1} \rightarrow 0 \tag{A34}$$

$$\frac{\partial^2 \overline{C}}{\partial z_1^2} >> \frac{\partial^2 \Delta C}{\partial z_1^2} \tag{A35}$$

$$\frac{\partial \overline{C}}{\partial z_1} >> \frac{\partial \Delta C}{\partial z_1} \tag{A36}$$

then, equation A32 can be rewritten as

$$D_g \left[\frac{\partial^2 \Delta C}{\partial r^2} + \left(\frac{1}{r}\right) \frac{\partial \Delta C}{\partial r} + \frac{\partial^2 \overline{C}}{\partial z_1^2} \right]$$

$$= \frac{\partial \overline{C}}{\partial t_1} + \overline{v} \left[1 - \left(\frac{2r^2}{r_o^2}\right) \right] \frac{\partial \overline{C}}{\partial z_1} \tag{A37}$$

Now, if each of the terms in equation A27 is multiplied by the operator

$$\frac{2}{r_o^2} \int_0^{r_o} r \, dr \tag{A38}$$

and simplified through the use of equations A33 to A36, along with substitution of the boundary condition

$$\left. \frac{\partial C}{\partial r} \right]_{r=r_o} = 0 \tag{A39}$$

then the following relationship is obtained:

$$D_g \frac{\partial^2 \overline{C}}{\partial z_1^2} = \frac{2\overline{v}}{r_o^2} \int_0^{r_o} \left[1 - \left(\frac{2r^2}{r_o^2}\right) \right] \frac{\partial \Delta C}{\partial z_1} r \, dr + \frac{\partial \overline{C}}{\partial t_1} \tag{A40}$$

Therefore, by subtracting equation A40 from equation A37 and taking into account the condition set forth in equation A36, then the following important equation is obtained:

$$\frac{\partial^2 \Delta C}{\partial r^2} + \left(\frac{1}{r}\right) \frac{\partial \Delta C}{\partial r} = \frac{\bar{v}}{D_g} \left[1 - \left(\frac{2r^2}{r_o^2}\right)\right] \frac{\partial \bar{C}}{\partial z_1} \tag{A41}$$

Now if

$$\frac{\partial \Delta C}{\partial r} = \phi \tag{A42}$$

and

$$\frac{\partial^2 \Delta C}{\partial r^2} = \frac{\partial \phi}{\partial r} \tag{A43}$$

then equation A41 can be rewritten as

$$\frac{\partial \phi}{\partial r} + \frac{\phi}{r} = \frac{\partial \bar{C}}{\partial z_1} \left(\frac{\bar{v}}{D_g}\right) - \frac{\partial \bar{C}}{\partial z_1} \left(\frac{\bar{v}}{D_g}\right) \frac{2r^2}{r_o^2} \tag{A44}$$

and a solution is obtained as follows:

$$r\phi = \frac{\partial \bar{C}}{\partial z_1} \left(\frac{\bar{v}}{D_g}\right) \int \left(r - \frac{2r^3}{r_o^2}\right) dr \tag{A45}$$

$$\phi = \frac{\partial \bar{C}}{\partial z_1} \left(\frac{\bar{v}}{D_g}\right) \frac{rr_o^2 - r^3}{2r_o^2} = \frac{\partial \Delta C}{\partial r} \tag{A46}$$

$$\Delta C = \frac{\partial \bar{C}}{\partial z_1} \left(\frac{\bar{v}}{D_g}\right) \frac{1}{2r_o^2} \int (rr_o^2 - r^3)\, dr \tag{A47}$$

$$\Delta C = \Delta C_o + \frac{\bar{v}r^2}{4D_g} \left(1 - \frac{r^2}{2r_o^2}\right) \frac{\partial \bar{C}}{\partial z_1} \tag{A48}$$

Upon differentiation, the ΔC_o term vanishes, and

$$\frac{\partial \Delta C}{\partial z_1} = \frac{\bar{v} r^2}{4D_g}\left(1 - \frac{r^2}{2r_o^2}\right)\frac{\partial^2 \bar{C}}{\partial z_1^2} \tag{A49}$$

Then by substitution into equation A40,

$$D_g \frac{\partial^2 \bar{C}}{\partial z_1^2} = \frac{(\bar{v})^2}{4D_g r_o^6}\left(\frac{\partial^2 \bar{C}}{\partial z_1^2}\right)\int_o^{r_o} (2r_o^4 - 5r_o^2 r^2 + 2r^4)\, r^3 dr + \frac{\partial \bar{C}}{\partial t_1} \tag{A50}$$

which eventually is rewritten as

$$\left[D_g + \frac{(\bar{v} r_o)^2}{48D_g}\right]\frac{\partial^2 \bar{C}}{\partial z_1^2} = \frac{\partial \bar{C}}{\partial t_1} \tag{A51}$$

It is now apparent that equation A51 can be expressed in the same form as Fick's second law, but with an effective diffusion coefficient defined as

$$D_e = D_g + \frac{(\bar{v} r_o)^2}{48D_g} \tag{A52}$$

If now D_e is inserted into the one dimensional diffusion equation, that is

$$D_e \frac{d^2 \bar{C}}{dz_1^2} = \frac{d\bar{C}}{dt_1} \tag{A53}$$

then consistent with appropriate initial conditions, the following is obtained as a solution:

$$\bar{C} = \bar{C}_o \exp\left(-\frac{z_1^2}{4D_e t_1}\right) \tag{A54}$$

This equation is readily recognized as a Gaussian distribution function. Also, it is seen to have a distribution variance of

$$\sigma^2 = 2D_e t_1 \tag{A55}$$

Thus for the defined uniform flow path, the behavior of the distribution variance, relative to axial distance, can be equated as

$$\frac{\partial(\sigma_z)^2}{\partial z} = 2D_e \frac{\partial t}{\partial z} = \frac{2D_e}{\bar{v}} \tag{A56}$$

and from equation A52,

$$\frac{\partial(\sigma_z)^2}{\partial z} = \frac{2D_g}{\bar{v}} + \frac{\bar{v}r_o^2}{24D_g} \tag{A57}$$

Thus equation A57 represents the longitudinal (or distance-based) variation in transport of like gas phase molecules.

If now the initial condition is

$$(\sigma_z)^2\Big]_{z=0} \rightarrow 0 \tag{A58}$$

and from equation A57

$$(\sigma_z)^2 = \int_o^{z=L} \left(\frac{2D_g}{\bar{v}}\right) dz + \int_o^{z=L} \left(\frac{\bar{v}r_o^2}{24D_g}\right) dz \tag{A59}$$

then at distance z=L, it is seen that

$$(\sigma_z)^2 = \frac{2D_g L}{\bar{v}} + \frac{\bar{v}r_o^2 L}{24D_g} \tag{A60}$$

Throughout the above examination, D_g has been assumed to be independent of concentration and only influenced by pressure and temperature. (For dilute binary mixtures, this is indeed a valid assumption.) Therefore, equation A57 also applies for the situation where like molecules are randomly entering and passing through the defined uniform flow path. However, it would be more convenient if the migration variation could be represented with a time-based independent variable. Hence it is necessary to convert the σ_z value of the Gaussian distributed population to a time-based sigma value. This is readily accomplished as

$$(\sigma_z)^2 = \left(\frac{\sigma_t F}{A_m}\right)^2 = (\sigma_t)^2 (\bar{v})^2 \tag{A61}$$

Equation A60 can now be rewritten as

$$(\sigma_t)^2 = \frac{2D_g L}{(\bar{v})^3} + \frac{r_o^2 L}{24\bar{v}D_g} \tag{A62}$$

and finally it is seen that the time-based variation in residence time is

$$\sigma_t = \sqrt{\frac{2D_g L}{(\bar{v})^3} + \frac{r_o^2 L}{24\bar{v}D_g}} \tag{A63}$$

Folded Tube of Circular Cross Section

What has been stated thus far applies strictly for laminar gas flow through a nonreactive, smooth-walled, straight tube of circular cross section. When the axis of the flow path exhibits significant curvature, then additional considerations must be included in the descriptive analysis of gas flow.

At low gas flow velocities, both convection and diffusion strongly contribute to axial dispersion in a narrow gas flow path. However, when the average linear gas velocity within a 1.0 mm ID straight tube is large ($\bar{v} > 100$ cm sec^{-1}), then the vastly dominant dispersion mechanism is associated with the convection. Longitudinal diffusion represents a negligible contribution to total dispersion at these higher gas velocities. Thus at high linear gas velocities,

$$\frac{2D_g L}{(\bar{v})^3} \rightarrow 0 \tag{A64}$$

and for the case where $\bar{v}$ is large in a straight tube, equation A63 can be written simply as

$$\sigma_t = \sqrt{\frac{r_o^2 L}{24\bar{v}D_g}} \tag{A65}$$

However, the velocity profile in a curved tube is not paraboloidal. It includes an element of flow that is perpendicular to the tube axis, and this additional element of flow is called "secondary flow" (see Section 6, and particularly Figure 18). This additional flow component can be beneficial in that at the higher gas velocities, increased radial mass transfer occurs, which thereby produces less axial dispersion.

Equation A65 applies for high velocity paraboloidal flow; however, the general variance equation for the non-paraboloidal velocity profile (which contains secondary flow) can be expressed as

$$(\sigma_t)^2 = \frac{\omega r_o^2 L}{24 \bar{v} D_g} \tag{A66}$$

where the parameter ω characterizes the actual flow profile, which in turn depends on the axial curvature, circular bore diameter, and surface roughness of the gas flow path, along with the mean axial velocity and the physical properties of the flowing gas mixture. Recent curve fitting calculations obtained from experiments with flowing liquids have empirically expressed ω in terms of the Dean number, N_{Dn}, and the Schmidt number, N_{Sc} (see the study by Deelder, R. S., Kroll, M.G.F., and Beeren, A.J.B. Post-Column Reactor Systems in Liquid Chromatography. J. Chromatog. 149:669, 1978). Specifically, for values of

$$N_{Dn} \sqrt{N_{Sc}} > 12.5 \tag{A67}$$

it is observed that

$$\omega \cong 5.6 \left(N_{Dn} \sqrt{N_{Sc}} \right)^{-0.67} \tag{A68}$$

When

$$N_{Dn} \sqrt{N_{Sc}} < 12.5 \tag{A69}$$

then ω is equal to unity.

Gas flowing through a narrow-bore tube of folded configuration (such as that shown in text Figure 23) will encounter dispersion in both the straight and curved sections of the folded tube assembly. As the circular cross section has been maintained throughout the entire length of the tube, the total

residence time variance is amenable to calculation. First, the assumption is made that for this folded tube, there are instantaneous transitions between the laminar secondary flow and the concentric laminar flow (i.e., pure paraboloidal velocity profile) and vice versa. Then by incorporating into equation A62 the variance contributed by secondary flow as expressed in equation A66, a general residence time variance equation can be obtained. Specifically, since independent Gaussian variances are additive,

$$(\sigma_t)^2 = (\sigma_t)^2_{L_c} + (\sigma_t)^2_{L_s} \tag{A70}$$

and as

$$(\sigma_t)^2_{L_c} = \left[\frac{2D_g}{(\bar{v})^3} + \frac{\omega r_o^2}{24\bar{v}D_g}\right]\sum\Delta L_c \tag{A71}$$

and

$$(\sigma_t)^2_{L_s} = \left[\frac{2D_g}{(\bar{v})^3} + \frac{r_o^2}{24\bar{v}D_g}\right]\sum\Delta L_s \tag{A72}$$

Then, the general variance equation for this tube will be as follows:

$$(\sigma_t)^2 = \frac{2D_g(L_c + L_s)}{(\bar{v})^3} + \frac{\omega r_o^2 L_c}{24\ \bar{v}\ D_g} + \frac{r_o^2 L_s}{24\ \bar{v}\ D_g} \tag{A73}$$

where L_c is the total length of curved tubing, and L_s represents the sum of the straight lengths.

Finally, to complete this analysis of gas flow, the specific data corresponding to the quartz tube reactor shown in Figure A-2 have been calculated. Table A-1 shows the range of various flow-related parameters that cover the intended mean residence time extremes of 0.20 to 5.0 seconds. These calculation values correspond to dilute levels of naphthalene in a flowing air atmosphere at a reactor internal pressure of 1.0 absolute atmospheres. With the narrow bore reactor and the relatively small curvature of the flow path, secondary flow is only a

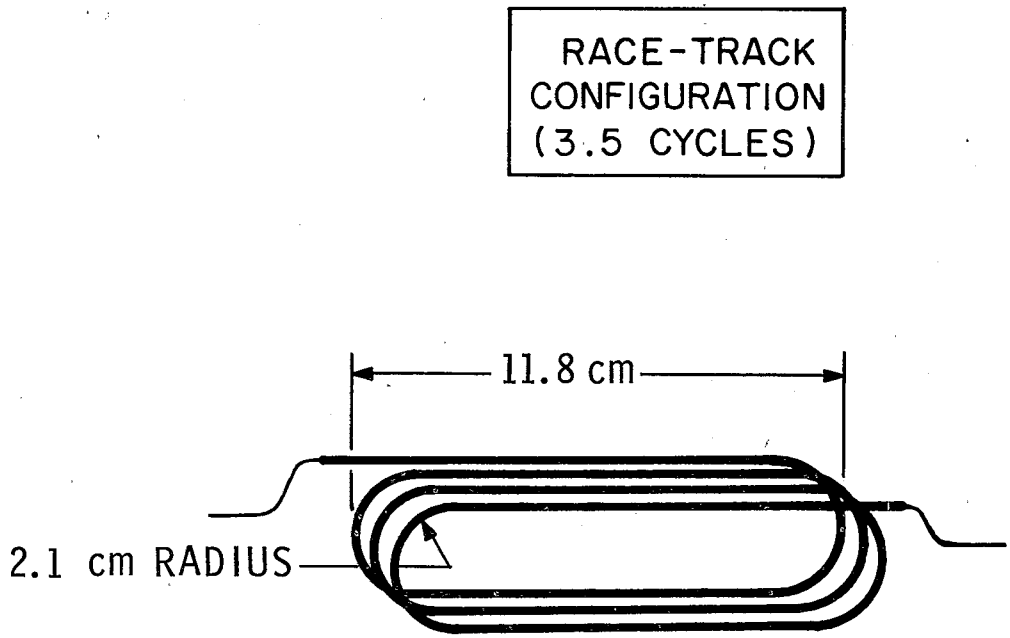

$L = 100.75$ cm

$L_s^* = 80.95$ cm

$L_c = 19.80$ cm

$V_q = 0.7445$ cm^3

$r = 0.0485$ cm

$\lambda = 43.3$

*Includes effective volume of connecting tubing

Figure A-2. Quartz tube reactor data.

TABLE A-1. CALCULATED FLUID DYNAMIC VALUES

Dimensionless term	Lower extreme $\bar{v}$ = 20 cm sec^{-1} $\bar{T}_2$ = 1423°K	Upper extreme $\bar{v}$ = 500 cm sec^{-1} $\bar{T}_2$ = 473°K
N_{Re}	0.71	134
N_{Dn}	0.108	20.3
N_{Sc}	4.28	2.97
$N_{Dn}^2 N_{Sc}$	0.050	1224
$N_{Dn}\sqrt{N_{Sc}}$	0.223	35.0

factor at the very short residence times while at the lower reactor temperatures.

The effects of temperature, molecular weight, and mean residence time on the residence time variance were investigated in a previous study (EPA-600/2-77-288, U.S. Environmental Protection Agency, Cincinnati, Ohio, 1977, p. 59). Therefore, in concluding this analysis, Figure A-3 represents the calculated relative residence time bandwidth as a function of mean residence time for the quartz tube reactor described in Figure A-2.

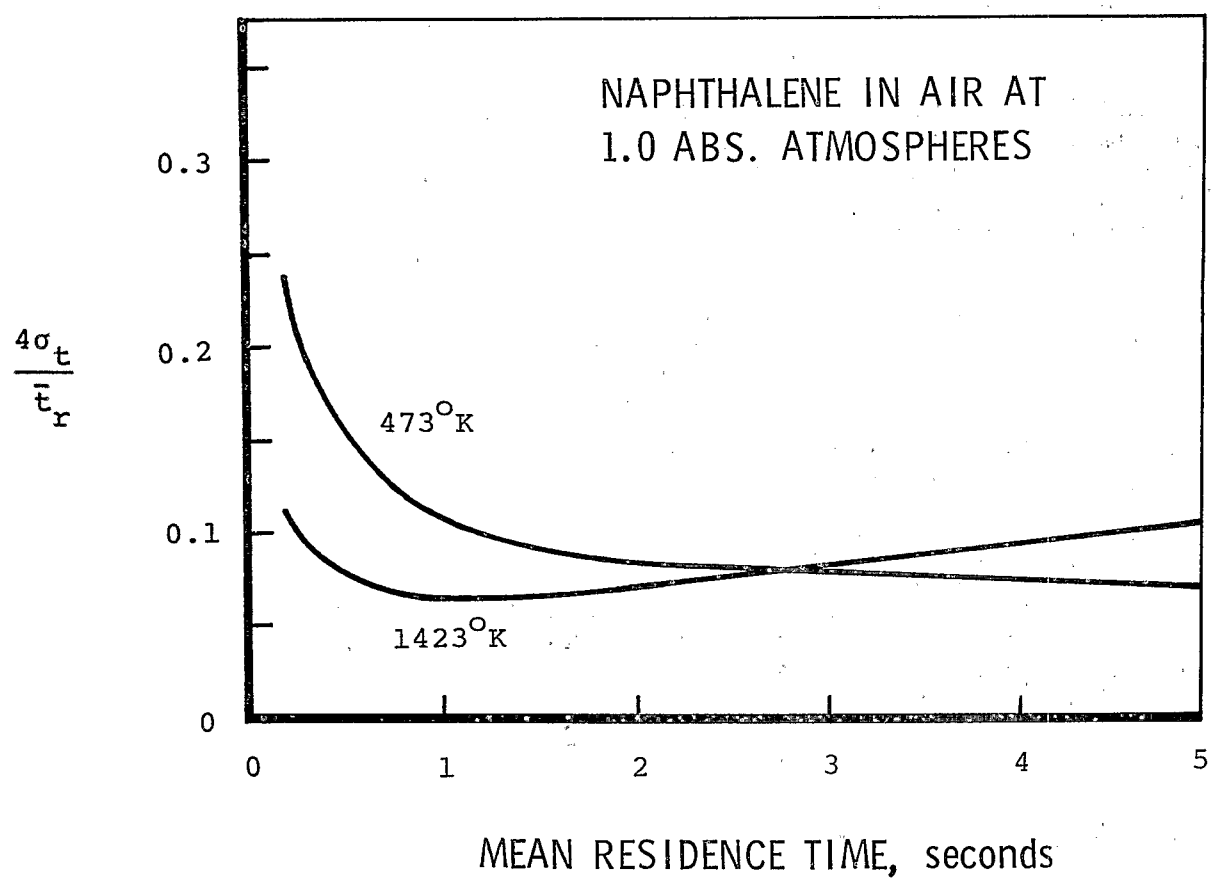

Figure A-3. Relative bandwidth as a function of mean residence time.

APPENDIX B

ERROR ANALYSIS OF MEAN RESIDENCE TIME DETERMINATION

The TDAS uses in-line instrumentation for determining the mean residence of a sample in the high-temperature reactor. Therefore, as presented in Section 6, equation 7 describes the mean residence time of a substance that has passed through the quartz tube reactor. This residence time equation

$$\bar{t}_r = \left(\frac{\pi r^2 L}{F_o}\right)\left(\frac{T_o}{\bar{T}_2}\right)\left(1 + \frac{p_d}{p_o}\right) \tag{B1}$$

contains many variables, some of which have a pronounced effect on $\bar{t}_r$ and are difficult to measure.

Upon investigation, it is found that fused quartz has a very small coefficient of expansion (approximately 0.59×10^{-6}). Therefore, for a given tube, the radius r and the length L can be assumed temperature invariant. Thus the effective volume of a specific quartz tube, i.e.

$$V_q = \pi r^2 L \tag{B2}$$

remains essentially constant.

With the refined instrumentation incorporated into the TDAS, there are now five variables that can have an effect on $\bar{t}_r$. Therefore, the maximum change in t_r, which can be attributed to an addition of errors in F_o, T_o, T_2, p_d, and p_o, can be expressed as

$$\Delta\bar{t}_r = \left|\left(\frac{\partial\bar{t}_r}{\partial F_o}\right)\Delta F_o\right| + \left|\left(\frac{\partial\bar{t}_r}{\partial T_o}\right)\Delta T_o\right| + \left|\left(\frac{\partial\bar{t}_r}{\partial\bar{T}_2}\right)\Delta\bar{T}_2\right| + \left|\left(\frac{\partial\bar{t}_r}{\partial p_d}\right)\Delta p_d\right| + \left|\left(\frac{\partial\bar{t}_r}{\partial p_o}\right)\Delta p_o\right| \tag{B3}$$

From equations B1 and B2, we find

$$\frac{\partial \bar{t}_r}{\partial F_o} = -\left(\frac{V_q T_o}{F_o^2 \bar{T}_2}\right)\left(1 + \frac{p_d}{p_o}\right) \tag{B4}$$

$$\frac{\partial \bar{t}_r}{\partial T_o} = \left(\frac{V_q}{F_o \bar{T}_2}\right)\left(1 + \frac{p_d}{p_o}\right) \tag{B5}$$

$$\frac{\partial \bar{t}_r}{\partial \bar{T}_2} = -\left(\frac{V_q T_o}{F_o \bar{T}_2^2}\right)\left(1 + \frac{p_d}{p_o}\right) \tag{B6}$$

$$\frac{\partial \bar{t}_r}{\partial p_d} = \frac{V_q T_o}{F_o \bar{T}_2 p_o} \tag{B7}$$

$$\frac{\partial \bar{t}_r}{\partial p_o} = -\frac{V_q T_o p_d}{F_o \bar{T}_2 p_o^2} \tag{B8}$$

Now the maximum errors typically associated with the selected instrumentation are

$$\Delta F_o = 1 \times 10^{-3}\ \mathrm{cm}^3\ \mathrm{sec}^{-1}$$

$$\Delta T_o = 0.2^{\circ}\mathrm{K}$$

$$\Delta \bar{T}_2 = 1^{\circ}\mathrm{K}$$

$$\Delta p_d = 2 \times 10^{-3}\ \mathrm{atm}$$

$$\Delta p_o = 1 \times 10^{-3}\ \mathrm{atm}$$

Next, an example case is presented where

$$\bar{t}_r = 1.00\ \mathrm{sec}$$

$$F_o = 0.3287\ \mathrm{cm}^3\ \mathrm{sec}^{-1}$$

$$T_o = 296^{\circ}\mathrm{K}$$

$$\bar{T}_2 = 773^{\circ}K$$

$$p_d = 0.15 \text{ atm}$$

$$p_o = 0.98 \text{ atm}$$

$$V_q = 0.7445 \text{ cm}^3$$

By substituting into equation B3 the data for this case and the typical measurement errors, the worst condition is found to be

$$\Delta\bar{t}_r = \left|\Delta\bar{t}_{r(F_o)}\right| + \left|\Delta\bar{t}_{r(T_o)}\right| + \left|\Delta\bar{t}_{r(\bar{T}_2)}\right| + \left|\Delta\bar{t}_{r(p_d)}\right| + \left|\Delta\bar{t}_{r(p_o)}\right| \tag{B9}$$

$$\Delta\bar{t}_r = 0.00304 + 0.00068 + 0.00129 + 0.00177 + 0.00014$$

Thus

$$\frac{\Delta\bar{t}_r}{\bar{t}_r} = 0.00692 \tag{B10}$$

or, the maximum relative error in $\bar{t}_r$ is approximately 0.7%.

With this in-line instrumentation and the use of calibration correction curves, accurate determinations of mean residence time can be made between the extremes of 0.25 and 5.0 seconds. Even so, most TDAS experiments will be conducted with the selected mean residence time falling between 0.5 and 2.0 seconds. Thus in this region, and with the present instrumentation, the measurement of gas flow represents the dominant source of error.

APPENDIX C

QUARTZ TUBE REACTOR HEAT TRANSFER ANALYSIS

In designing the fused quartz tube reactor for the TDAS, one of the specific objectives was to minimize the end effects (disturbances) produced by the entrance and exit regions of the reactor. This end effect minimization was accomplished to a considerable extent by employing the counterflow cooling principle as shown in Figure C-1. Using this design feature, an abrupt change in the temperature of the flowing gas is experienced as it moves from the transport region and into the high-temperature reactor.

In view of the small bore of the gas flow path, it would be very difficult to determine experimentally the exact temperature rise profile as a function of either time or distance. However, this temperature rise profile is amenable to heat transfer calculations.

The approach used for obtaining this information was to determine initially the bulk gas temperature within the fine bore connecting tube as a function of longitudinal distance. Then the effects of the longitudinal conduction within the quartz junction assembly were examined.

First, consider the steady state heat transfer condition where 550°K gas is flowing into a quartz tube that is contained in a 900°K isothermal chamber (see Figure C-1). Of primary importance is the time required for the incoming flowing gas to attain effectively the 900°K equilibrium.

A simplified version of the fine bore connecting tube is depicted in Figure C-2, and the rate of heat flow by radial conduction, q_k, into the bore of this tube can be expressed as

$$q_k = \bar{k}A \frac{dT}{dr} = \bar{k}2\pi rL \frac{dT}{dr} \qquad \text{(C1)}$$

where $\bar{k}$ is the average thermal conductivity of fused quartz, A is radial area, T is temperature, r is radial distance, z is

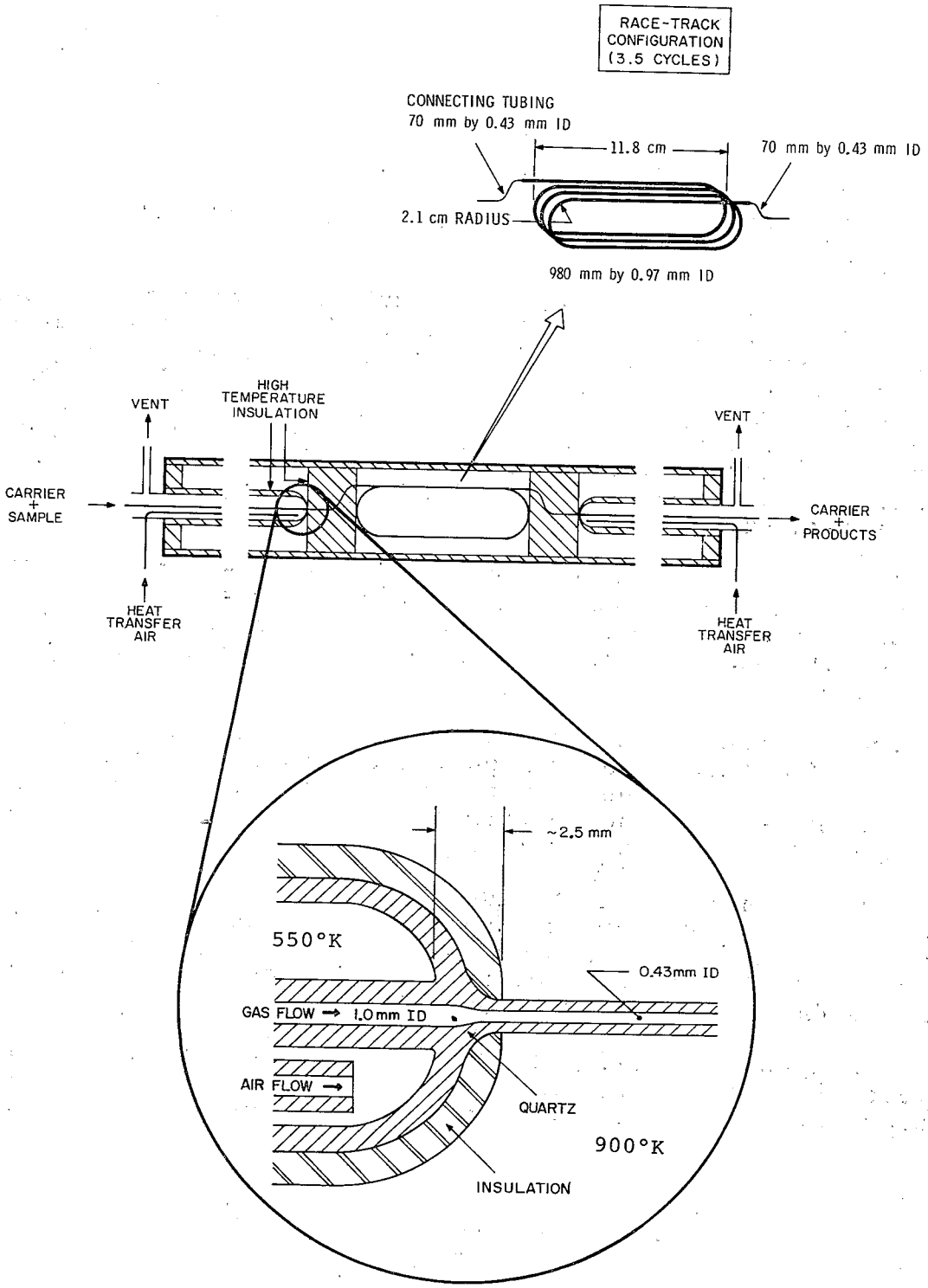

Figure C-1. Details of quartz tube reactor assembly.

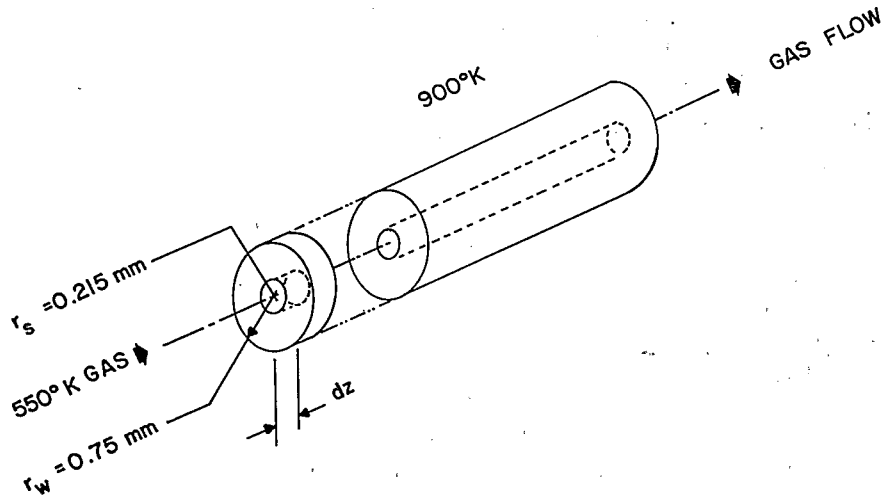

Figure C-2. Simplified version of fine bore connecting tube.

axial distance, and L is length of the tube. If conduction in the longitudinal direction is neglected, then

$$\frac{dr}{r} = \frac{\bar{k}2\pi L}{q_k} dT \tag{C2}$$

The temperatures corresponding to the boundary conditions are

$$T_w \text{ at } r = r_w \tag{C3}$$

and

$$T_s \text{ at } r = r_s \tag{C4}$$

where the subscript s denotes the tube inner surface, and subscript w represents the outer wall. Thus

$$\int_{r_s}^{r_w} \frac{dr}{r} = \frac{2\pi L\bar{k}}{q_k} \int_{T_s}^{T_w} dT \tag{C5}$$

or

$$q_k = \frac{2\pi L\bar{k}(T_w - T_s)}{\ln\left(\frac{r_w}{r_s}\right)} \tag{C6}$$

and therefore for the dz axial element depicted in Figure C-2,

$$dq_k = \frac{2\pi\bar{k}(T_w - T_s)}{\ln\left(\frac{r_w}{r_s}\right)} dz \tag{C7}$$

Next, to obtain a comparison of the heat transfer mechanisms, the following steady state energy balance was constructed:

$$dq_k = \bar{k}dA \frac{dT}{dr} = dq_c = \bar{h}dA(T_s - T_b) \tag{C8}$$

where $\bar{h}$ is the average convective heat transfer coefficient of the laminar flowing gas, T_b is the bulk temperature of the gas in the bore of the dz increment, and q_c is the rate of heat transfer by convection. (To simplify the analysis, heat transfer by thermal radiation is neglected.) Upon inserting equation C7 and incorporating the appropriate ΔTs to maintain the balance, the equation may be rewritten as

$$\frac{2\pi\bar{k}(\Delta T_k)}{\ln\left(\frac{r_w}{r_s}\right)} dz = \bar{h}\ 2\pi r_s(\Delta T_c)dz \tag{C9}$$

If now

$$\bar{k}\Big]_{\text{quartz at } 900^{\circ}K} = 1.3\ Wm^{-1}\ {}^{\circ}K^{-1} \tag{C10}$$

and

$$\bar{h} \cong 500\ Wm^{-2}\ {}^{\circ}K^{-1} \tag{C11}$$

then by evaluating the respective ΔT's required for maintaining the balance for the dz element, it is found that

$$\Delta T_k << \Delta T_c \tag{C12}$$

Therefore, for the quartz connecting tube of Figure C-2, the vastly dominant mechanism of heat transfer is radial conduction through the tubing wall. Then for the entire connecting tubing length L, the assumption can be made that

$$T_s \cong T_w \tag{C13}$$

An energy balance can now be written for the heat transfer case as illustrated in Figure C-2. Specifically,

$$q = \bar{h}\, 2\pi r_s z \left[T_w - \left(\frac{T_o + T_b}{2} \right) \right] = \dot{m}\, c_p\, (T_b - T_o) \qquad \text{(C14)}$$

where T_o is the bulk temperature of the gas at z=0, $\dot{m}$ is the mass rate of flow, and c_p is the specific heat. If the flowing gas is air, then the properties of the flowing media at 900°K are as follows:

$$\left.\begin{aligned} \text{density, } \rho &= 0.393 \text{ kg m}^{-3} \\ \text{specific heat, } c_p &= 1.12 \text{ k J kg}^{-1}\, {}^{o}\text{K}^{-1} \\ \text{dynamic viscosity, } \mu &= 3.90 \times 10^{-5} \text{ kg m}^{-1}\, \text{s}^{-1} \\ \text{thermal conductivity, } \bar{k} &= 0.0628 \text{ Wm}^{-1}\, {}^{o}\text{K}^{-1} \\ \text{Prandt number, } N_{pr} &= 0.696 \end{aligned}\right\} \qquad \text{(C15)}$$

and as

$$\left.\begin{aligned} T_w &= 900°\text{K} \\ T_b\Big]_{z=0} &= 550°\text{K} = T_o \\ r_s &= 0.000215\text{m} \\ L &= 0.070\text{m} \end{aligned}\right\} \qquad \text{(C16)}$$

and the average linear gas velocity, $\bar{v}$, is

$$\bar{v} = 2.56\text{m s}^{-1} \qquad \text{(C17)}$$

then the Reynolds number is

$$N_{Re} = \frac{\rho \bar{v} 2 r_s}{\mu} = 11.09 \tag{C18}$$

With this low N_{Re}, along with a constant T_w, the Nusselt number (from Graetz's classical solution) is

$$N_{Nu} = 3.66 = \frac{\bar{h} 2 r_s}{\bar{k}} \tag{C19}$$

and therefore

$$\bar{h} = \frac{3.66 \bar{k}}{2 r_s} = 535 \ Wm^{-2} {}^{\circ}K^{-1} \tag{C20}$$

Also

$$\dot{m} = \rho \pi r_s^2 \bar{v} = 1.461 \times 10^{-7} \ kg \ s^{-1} \tag{C21}$$

Equation C14 can now be rewritten as

$$\frac{T_w - \left(\frac{T_o + T_b}{2}\right)}{T_b - T_o} = \frac{\dot{m} c_p}{\bar{h} 2 \pi r_s z} \tag{C22}$$

which for this particular case reduces to

$$z = \frac{(T_b - 550) \ 0.000453}{1250 - T_b} \tag{C23}$$

Using equation C23, a graph of T_b versus z was prepared and is shown in Figure C-3. This graph reveals that the flowing bulk air will experience a 350°K increase in the very short axial distance of 0.5 mm. This distance is considerably smaller than the axial length of the quartz barrier between the two heated zones (see the enlarged detail drawing of Figure C-1). Consequently, as a result of the above calculations, it is apparent that the major factors that affect this gas phase temperature increase are: 1) the axial length of the barrier between the heated zones and 2) the volume flow rate through this transition region. A simplified sketch of this particular heat transfer condition is presented in Figure C-4.

As was seen from Figure C-3, the axial distance required to attain thermal equilibrium is approximately 0.5 mm. Therefore, if this length is added to the barrier length, a worst case situation is presented. Now if it is assumed that the average temperature of the air in this transition region is 725°K, and as the interior volume, V_t, of this region is

$$V_t = \frac{1}{3}\left(A_1+A_2+\sqrt{A_1A_2}\right)z_1 + A_2z_2$$

$$= 1.130 \text{ mm}^3 \qquad \text{(C24)}$$

and the average air flow rate, F, corresponding to 725°K is

$$F = \frac{V_r}{\bar{t}_r}\left(\frac{725}{900}\right) = 300 \text{ mm s}^{-1} \qquad \text{(C25)}$$

where V_r is reactor volume and $\bar{t}_r$ is mean residence time. Then it is seen that the time required to displace the V_t transition volume is

$$t = \frac{V_t}{F} = 0.0038\text{s} \qquad \text{(C26)}$$

or 3.8 milliseconds.

From previous measurements and calibrations, the temperature of the central portion of the quartz tube reactor has been well established. And now, with the calculation of

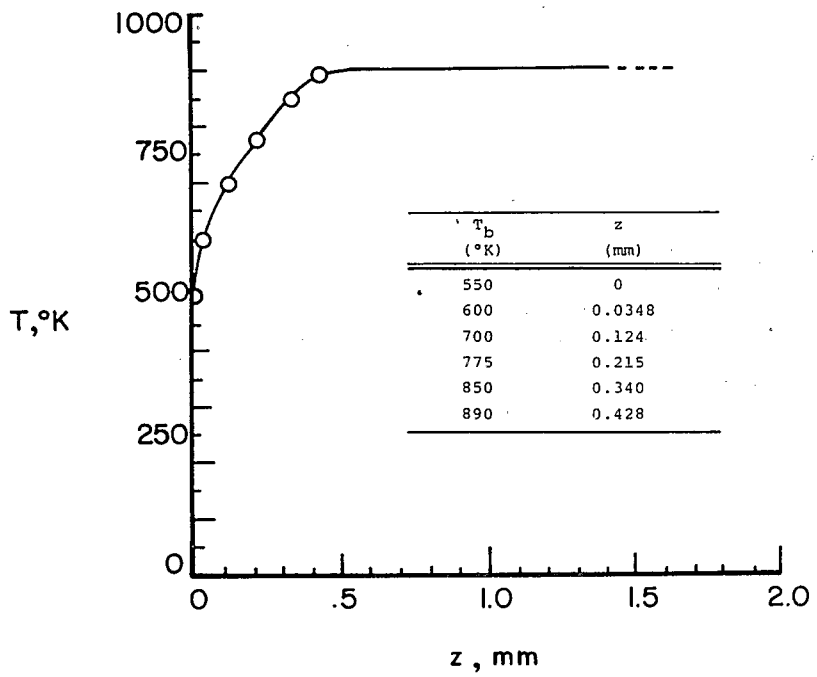

T_b (°K)	z (mm)
550	0
600	0.0348
700	0.124
775	0.215
850	0.340
890	0.428

Figure C-3. Graph of bulk temperature versus distance.

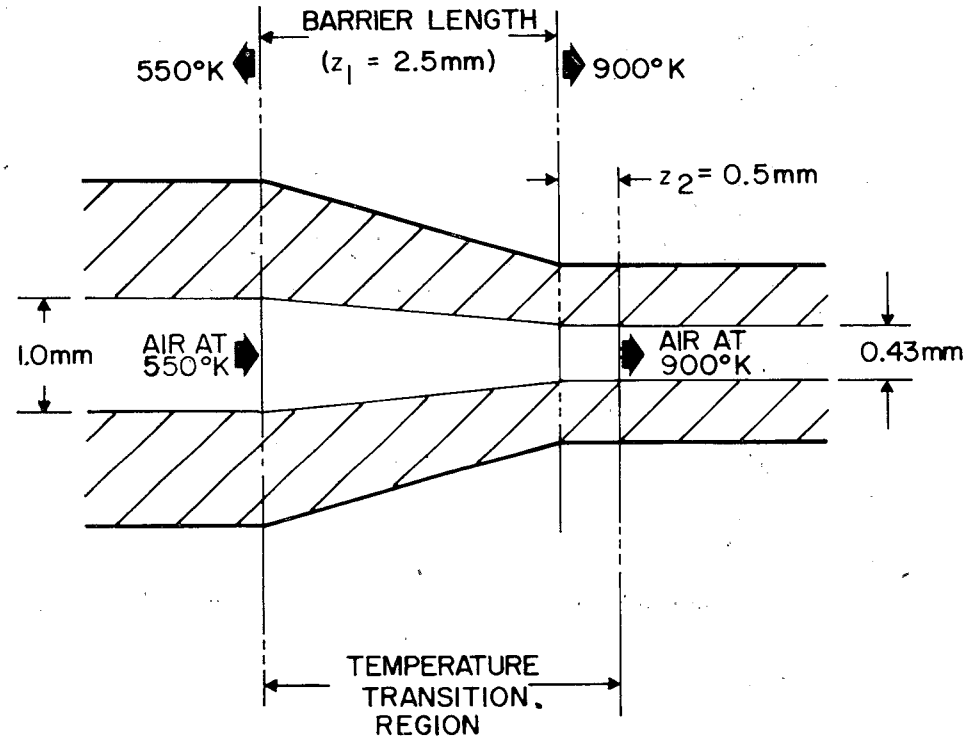

Figure C-4. Sketch of heat transfer condition.

the temperature rise time, the gas phase temperature can be represented relative to mean time as shown in Figure 25, which is presented in Section 6.

An even more abrupt temperature change occurs at the exit of the reactor. Specifically, the temperature of the gas emerging from the reactor changes almost instantaneously to the axial transport temperature. This very rapid change is attributed to the combination of induced mixing, greatly reduced axial velocity, and thermal quenching.

APPENDIX D

TDAS TRANSDUCER CALIBRATIONS

To obtain accurate measurements of the various thermal decomposition parameters, it is necessary to have precise measurement devices that have been accurately calibrated. Therefore, the individual TDAS measurement transducers have been calibrated using measuring equipment possessing traceability to the National Bureau of Standards. In this appendix, the callibration data and associated correction curves are presented for those transducers that were described earlier in Section 6 under the heading "TDU Instrumentation."

The differential pressure transducer calibration data are presented in Table D-1. This device was calibrated using a Merian Instruments 30-PA10 mercury manometer, which was calibrated for 22°C and 45° north latitude. The corresponding voltage readings were made with a Fluke 8300A digital voltmeter.

The calibration data for the mass flow transducer are presented in Table D-2 and Figure D-1. This particular calibration was conducted by the manufacturer. Both the pressure and flow transducer outputs were alternately registered with a Hewlett-Packard 3465A digital multimeter. Calibration data and corrective curves for this instrument are shown in Table D-3 and Figure D-2.

Many temperature measurement calibrations were performed. First, it was necessary to determine the longitudinal distribution of temperature throughout the reactor region. This was accomplished using a longitudinally movable unsheathed #24 AWG chromel-alumel thermocouple, and the actual temperature measurements throughout the reactor region are shown in Table D-4. Using this same unsheathed thermocouple, the temperature variations as a function of time at a given location were determined to be less than ±0.5°C over a 10-minute interval. For the actual measurement of the average temperature of the reactor, that is $\bar{T}_2$, a special calibrated sheathed thermocouple was purchased (Omega Engineering Inc.). This thermocouple was calibrated by the manufacturer at temperatures commonly used in the TDAS work. These temperature calibrations are shown in Table D-5. The readout device for the $\bar{T}_2$ thermocouple was an

TABLE D-1. DIFFERENTIAL PRESSURE TRANSDUCER CALIBRATION*

Transducer output (millivolts DC)	Differential pressure (in Hg)	or (mm Hg)	
0.527	0.20	10.34	
1.131	0.40	20.68	
1.743	0.60	31.02	correlation = 0.99991
2.379	0.80	41.37	slope = 0.0584
2.941	1.00	51.71	intercept = -0.0667
3.601	1.20	62.05	
4.148	1.40	72.39	
5.357	1.80	93.08	
5.80	2.00	103.4	
8.90	3.00	155.1	
12.2	4.00	206.8	
15.1	5.00	258.5	correlation = 0.99994
18.1	6.00	310.2	slope = 0.0599
21.2	7.00	361.9	intercept = -0.3764
24.4	8.00	413.6	
27.5	9.00	465.3	
30.7	10.00	517.14	

*Manufacturer: Statham Instruments, Inc.
Model #PL-295TC-15-350 Serial #316.

TABLE D-2. MASS FLOW TRANSDUCER CALIBRATION*

Transducer output (volts DC)	Actual air flow (STP, cm^3 min^{-1})
0.005	0
1.250	12.479
2.500	24.878
3.750	37.295
5.000	49.909
2.500	24.977
0.006	0

*Manufacturer: Brooks Instrument Division
Emerson Electric Company
Model #5810-1C214A Serial #7804 H52092

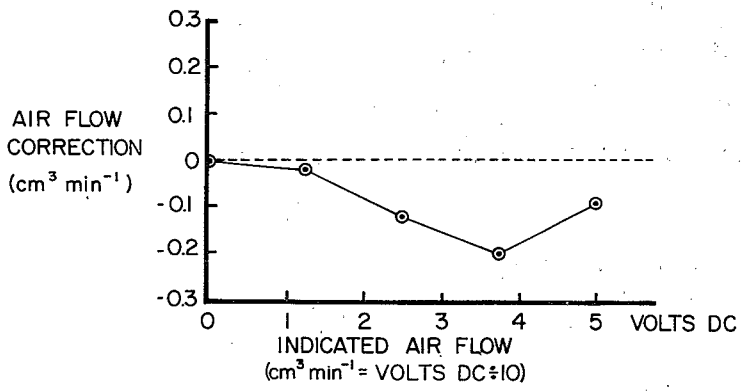

Figure D-1. Mass flow transducer calibration.

TABLE D-3. CALIBRATION OF HP-3465A DIGITAL MULTIMETER SERIAL 1521A00452

Standard (mv)	Meter reading (mv)
0.000	0.00
5.000	5.00
10.000	10.00
15.000	15.00
20.000	20.00
25.000	25.01
30.000	30.01
35.000	35.01
40.000	40.01
45.000	45.01
50.000	50.01
55.000	55.01
60.000	60.01
65.000	65.02
70.000	70.02
75.000	75.02

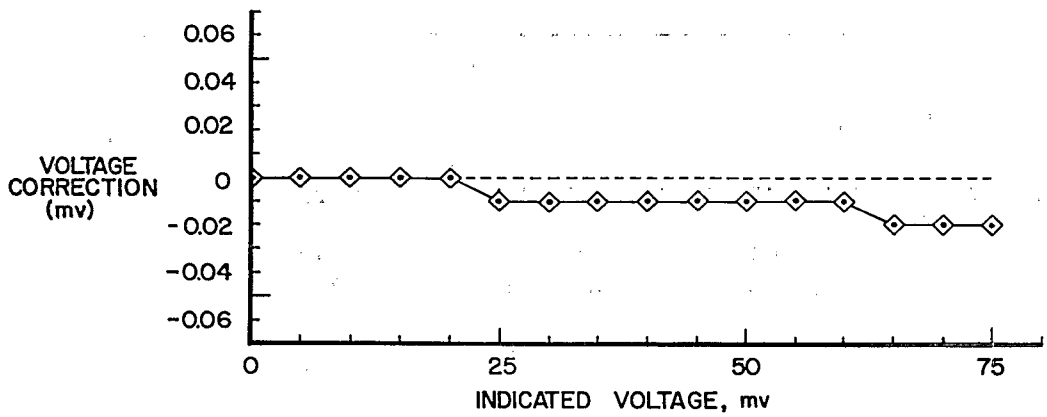

Figure D-2. Calibration of transducer readout instrument.

TABLE D-4. REACTOR TEMPERATURE MEASUREMENTS

Distance from reactor centerline (cm)	Measured temperature (°K) @ 599*	@ 903*	@ 1198*
-6	597	901	1195
-4	597	902	1196
-2	598	903	1197
0	599	903	1198
+2	599	903	1198
+4	599	903	1198
+6	599	902	1197

*Each of 3 zones of the furnace had the same dial setting.

TABLE D-5. OMEGA K-1 THERMOCOUPLE CHROMEL-ALUMEL

Actual temperature (°C)	Temperature deviation* (°C)
400	-0.75
600	-1.79
800	-2.24
950	-0.90

*When deviation is plus, add to actual reading. When negative, subtract from actual reading.

Omega Model 250 digital temperature indicator. The calibration of this instrument is presented in Table D-6 and Figure D-3.

Again, there are many temperature measurements made in the course of a single experiment with the TDAS. With the exception of the $\bar{T}_2$ measurement, these temperature measurements are selectively readout on a single Omega Model 175 digital temperature indicator. The calibration of this particular instrument is presented in Table D-7 and Figure D-4.

TABLE D-6. CALIBRATION OF OMEGA DIGITAL TEMPERATURE INDICATOR MODEL 250, TYPE K

Standard (°C)	(mv)	Meter reading (°C)
0	4.095	1
100	8.127	101
200	12.207	200
300	16.395	302
400	20.640	399
500	24.902	501
600	29.128	602
700	33.277	702
800	37.325	801
900	41.269	901
1000	45.108	1002
1100	48.828	1103
1200	52.398	1202
1300	54.125	1300

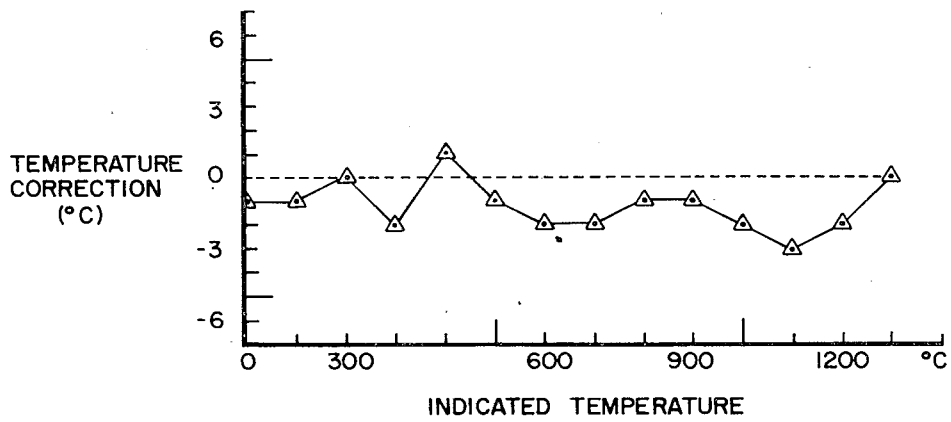

Figure D-3. Calibration of $\bar{T}_2$ readout instrument.

TABLE D-7. CALIBRATION OF OMEGA DIGITAL TEMPERATURE INDICATOR MODEL 175, TYPE K

Standard (°C)	(mv)	Meter reading (°C)
-200	-6.891	-197
-100	-4.553	-101
0	0.000	0
100	4.095	100
200	8.137	200
300	12.207	298
400	16.395	398
500	20.640	498
600	24.902	597
700	29.128	696
800	33.277	797
900	37.325	898
1000	41.269	998

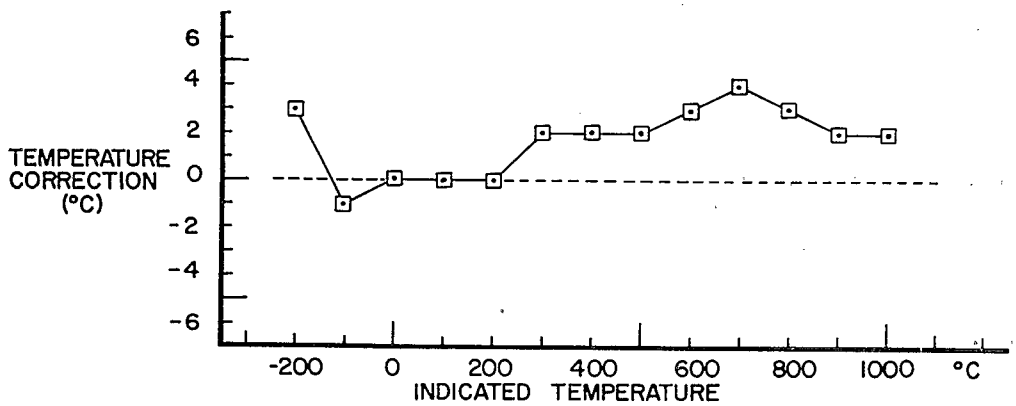

Figure D-4. Calibration of temperature selector readout instrument.

APPENDIX E

PREPARATION OF GAS CHROMATOGRAPHIC OPEN TUBULAR COLUMNS

A large number of chemical compounds can be formed upon the thermal decomposition of an organic material. Therefore, to analyze these complicated mixtures, high-resolution gas chromatographic columns are generally needed.

Before a sample is subjected to tests by the TDAS, it is screened by various GC's that contain high-resolution glass open tubular columns. And of course, the separation columns that are used in the TDAS must be capable of separating complex mixtures.

There are a number of procedures for preparing high-resolution OTC's. The preparation procedures that follow are those currently used in our laboratory for fabricating OTC's. These preparation procedures have evolved over a long period of time and are continually being updated. Our experience with fabricating and use OTC's dates back to the early 1960's when metal OTC's were used for the separation of complex petroleum-based hydrocarbon mixtures.

The selection of the tubing material is important, and only recently has information been presented that shows a clear advantage for borosilicate glass (Pyrex) over soda-lime (soft) glass. Specifically, it has been found that Pyrex is a better tubing material for high-temperature work, as there is less stationary phase bleed. The increased phase bleed with soft glass has been attributed to the composition of that material having a catalytic effect on the thin film of stationary phase. Consequently, at the present time, Pyrex is used almost exclusively as the glass tubing stock for our OTC's.

Once the anticipated dimensions of the finished OTC have been decided upon, the size of the glass tubing stock can be selected. For example, if the finished bore size of the OTC is to be approximately 0.25 mm ID, then a stock having a 2.5 mm ID can be used with a draw ratio of 100 to one. The actual wall thickness of the drawn tubing is of little importance, as most instrument installations can accommodate a wide variety of wall thicknesses.

After selecting the glass stock, it is necessary to clean the glass tubing before drawing. Some workers resort to cleaning with acids; however, it has been our experience that a simple cleaning with distilled water followed by acetone and drying with nitrogen gas is sufficient. The clean glass stock is next inserted into the glass drawing machine (Shimadzu Model GDM-1) and subsequently drawn to capillary bore diameters and tubing lengths of up to 150 meters.

After the capillary tubing has been drawn, it is necessary to determine the actual bore size of the finished tubing. This is accomplished by placing small sections of the tubing in a Nikon optical microscope, Model 43622. With the use of an optical filar micrometer, Nikon Model 66728, the bore diameters are measured to within ±0.01 mm ID. The length of the coiled capillary tubing is determined by merely counting the coils and multiplying by the circumference of an average coil of the drawn tubing.

At this point in the column fabrication process, it is necessary to select the stationary phase with which the tubing will eventually be coated. The selection of the stationary phase will govern much of the surface modification and de-activating procedures that will be applied to the tubing surface. For example, if a dimethylsilicone stationary phase is selected, then surface roughness is a relatively minor aspect, and surface deactivation is of major concern. These concerns are precisely reversed if a relatively polar stationary phase is to be coated on the tubing wall.

In our laboratory, the non-polar stationary phases are applied to tubing materials that have been treated with HCl gas at elevated temperatures. This is to etch or leach the surface of the glass. Specifically, this procedure involves filling the tube with HCl gas and then sealing the ends with a torch. The tubing is then heated in an oven at 380°C for approximately 15 hours. After removal from the oven and cooling to room temperature, the tube is vented and immediately flushed with nitrogen gas. Next, the tubing is mounted in the solvent cleaning apparatus shown in Figure E-1. It is then flushed with 5-ml quantities of methanol and methylene chloride, respectively. After cleaning with the solvents, the tubing is sealed and stored until ready for the deactivation process, which will be described later.

For medium polarity and polar stationary phases, the glass tubing bore is modified by a technique that produces whiskers on the interior surface. This is accomplished by decomposing in the tubing a specified amount (approximately 0.3 mm^3 cm^{-2}) of 2-chloro-1,1,2-trifluoroethyl methyl ether, or simply, etching ether. After drawing this quantity of liquid into the central part of the tubing length, a gentle vacuum is applied to the

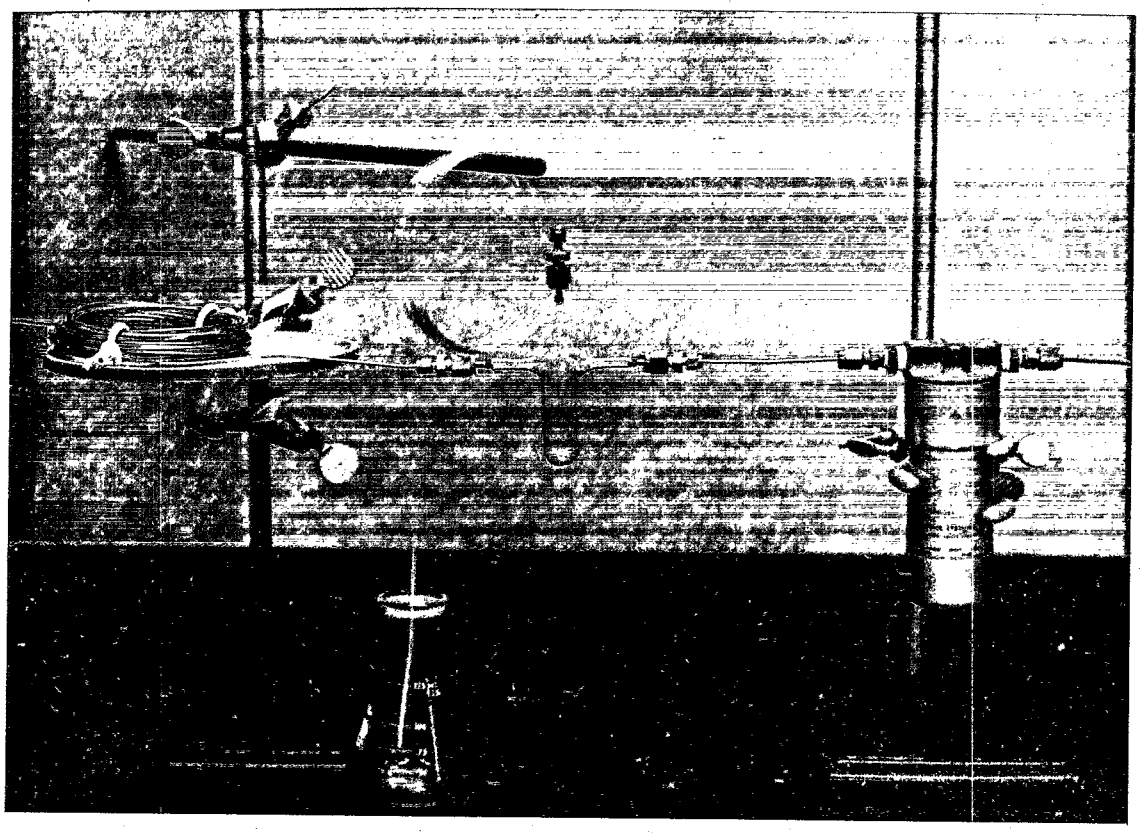

Figure E-1. Capillary cleaning apparatus.

ends of the tube to remove excess air, and the tubing is quickly sealed with a torch. The tubing is next subjected to 375°C for a period of 15 hours. It is then vented in a hood while still warm, and a vacuum is quickly applied to remove volatiles. Next, the tube is flushed with oxygen at 460°C for 15 hours in a special oven. After this, a whisker-textured surface is observed on the tubing interior wall. Figure E-2 is a scanning electron micrograph of these whiskers. Chemically, these whiskers are considered to be relatively pure SiO_2. After the flushing with oxygen at high temperature, the ends are sealed until the tube is ready for the deactivation step.

At present, there are just two deactivating procedures used in our laboratory. The first involves the chemical bonding of polyethylene glycol (Carbowax 20M) to the glass surface. This is accomplished by passing through the tube a 5% (w/v) solution of Carbowax 20M dissolved in methylene chloride. With a flow of dry nitrogen gas, the solvent is evaporated and the tubing dried. The tube is then sealed while containing a nitrogen gas atmosphere. Next, the tubing is heating for 15 hours at 280°C. After this thermal treatment, the tubing is removed from the oven and flushed sequentially with nitrogen gas and 5 ml quantities each of methanol and methylene chloride.

The second deactivation procedure involves the chemical N-cyclohexyl-3-azetidinol (CHAZ). This material is dissolved in methanol on a 5% (w/v) basis and is passed through the glass tubing. After removing the solvent and drying with a flow of nitrogen gas, the ends of the tube are sealed. It is then heated for 15 hours at 125°C and followed by the same thorough flushing and clean-up procedures as mentioned earlier with the Carbowax 20M. These deactivation procedures are applied to both the HCl-treated Pyrex tubing and whisker wall tubes.

The next step in the OTC preparation procedure is very important. It involves mounting the deactivated tube in an oven with a special "X" tubing connection that permits the heating of the glass tube interior while in a stream of dry nitrogen gas (see Figure E-3). This step is performed on each tube before it is coated with stationary phase. Specifically, the tube is mounted in the oven, and a flow of approximately 1.0 ml min^{-1} of nitrogen gas is established at the exit of the tubing. Next, the tubing is heated for approximately 3 hours at 150°C. This is to remove excess water from the tubing interior. After the tube has returned to room temperature, it is ready for filling with the stationary phase coating solution. It is important that this filling process be accomplished quickly so that moist atmospheric air will not back diffuse into the dried tubing.

A considerable amount of attention should be given to the selection of the stationary phase. Many workers have found that

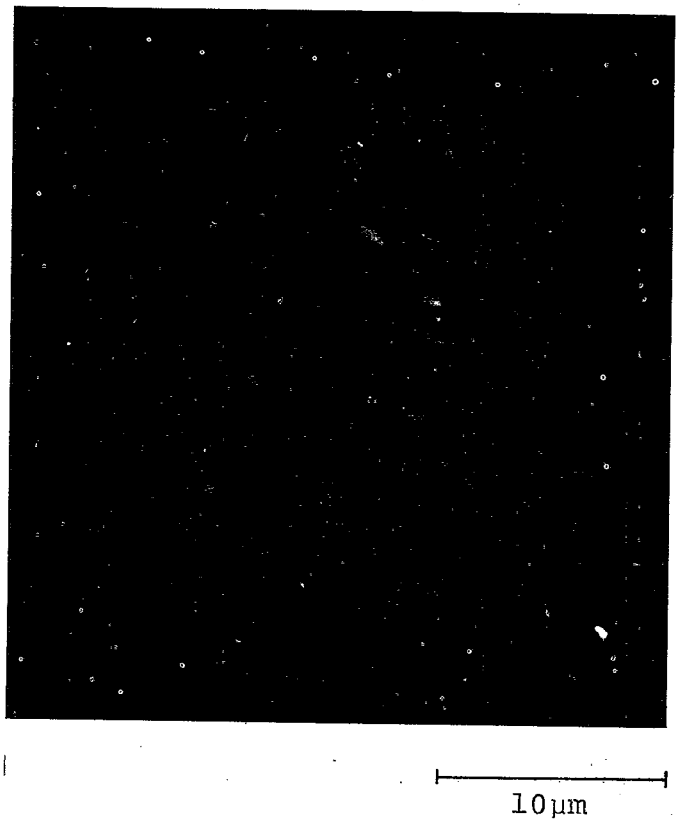

Figure E-2. Whisker-textured tubing bore.

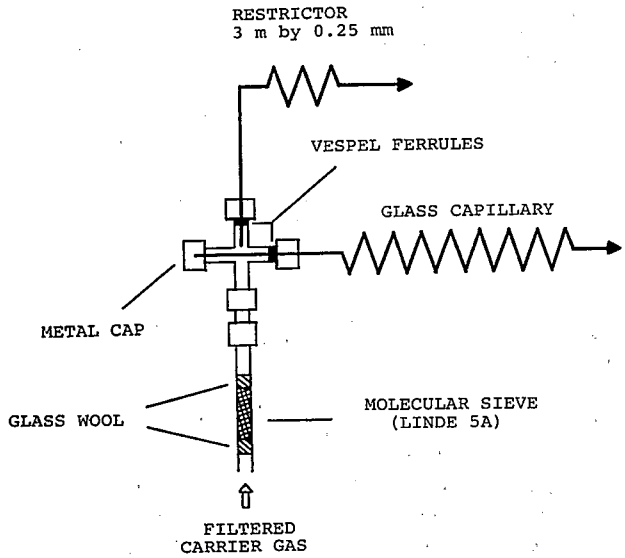

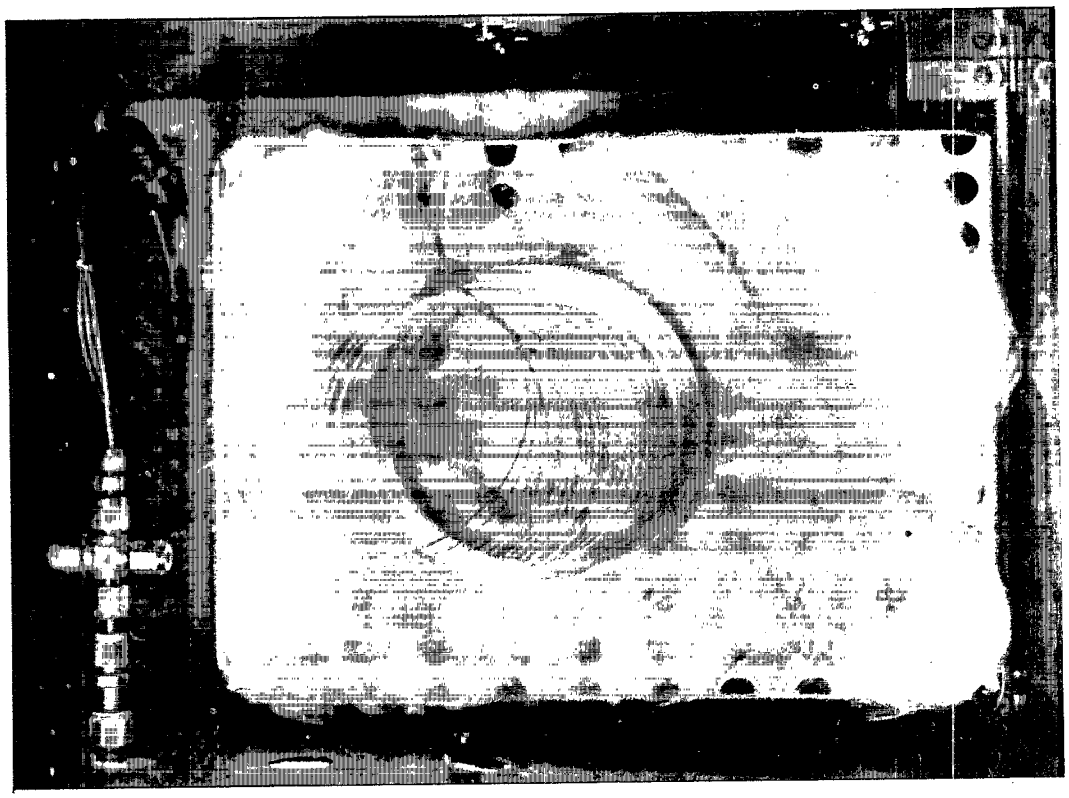

Figure E-3. Apparatus for drying glass tube interior.

for a thermally stable column of high efficiency, it is preferable to have a gum-type stationary phase, as opposed to the free flowing liquid phases. This presents some difficulties with respect to the actual coating of the stationary phase. However, it has been observed that not only is there an improvement in efficiency at the elevated temperatures with gum phases, but also, these columns seem to have somewhat higher thermal stability. In addition, there seems to be less adsorptivity with the gum-type stationary phases. The free-flowing liquid phases do have some advantages when one is trying to separate volatile substances at the lower chromatographic temperature regions, such as room temperature or less. The free-flowing coating solutions can be applied by the dynamic coating technique, or various modifications therefore (e.g., the mercury piston coating procedure). However, the gum-type stationary phases are normally best applied using the static coating procedures.

In any event, the preparation of the coating solution is an important step. Clean and filtered solvents are necessary. Also, the mercury used for the piston should be free of contaminants. The coating solution should be freshly prepared and placed in a Teflon screw-capped vial. When not in use, the coating solution should be stored in the dark.

Immediately after drying and returning to room temperature, the tubing is ready for application of the coating solution. For the dynamic coating procedure, approximately 10 percent of the tubing length is filled with the coating solution and immediately followed with about a 4 cm length of mercury, which acts as a piston. The tubing is filled by applying a partial vacuum at the exit and with the use of a rubber suction bulb connected to the capillary by silicone rubber tubing. The inlet end of the tubing is immersed in the coating solution, which readily fills the first 10 percent of the tubing length. Then a short length of clean mercury is pulled into the tube in the same manner. The tubing is next placed in the horizontal position. Silicone rubber tubing is attached to the tubing entrance, and a nitrogen gas pressure is applied that will push the liquid coating solution through the tube at an average velocity of approximately 0.5 cm sec^{-1}. At the exit end of the tubing, a short length of the same size capillary glass tubing is applied so that the solution coating plug will not be accelerated upon emerging from the main capillary. After this process, the solvent is evaporated by flowing nitrogen gas through the tube for approximately 1 hour. The tube is then ready for conditioning. This conditioning step will be described later.

For the static coating technique, the entire tube is filled with a relatively dilute degassed solution consisting of stationary phase in a volatile solvent (e.g., pentane or methylene chloride). It is then mounted on a rack, and a seal is made at one end of the tubing by pulling into the capillary bore

Apiezon "N". After the seal has been secured, the tubing assembly is mounted in a chamber located within a double-door cupboard in the temperature-controlled laboratory. Flexible tubing from a mechanical vacuum pump is attached to the open end of the filled tube, and the solvent is gently removed from the tubing bore, thus depositing a known and even film thickness of stationary phase along the tubing length. This static coating technique is a time-consuming process and can involve many days, depending on the length and bore diameter of the capillary tubing.

After the coating of the glass tube, it is mounted in the same oven arrangement as shown in Figure E-3 that was employed for the drying of the glass capillary tubing. The capillary is then purged with nitrogen gas as it is gradually heated to its elevated conditioning temperature. The conditioning time period for a newly prepared OTC is usually 15 hours.

After the conditioning of a column, it is mounted in a GC and evaluated with respect to its chromatographic performance. If the column meets established criteria of column efficiency, shape of elution profiles, and thermal stability, it is removed from the GC, and immediately the ends are sealed with a micro torch. The column is then stored on a special rack contained in a darkened cabinet. The column will remain stored in this manner until ready for use on a routine basis in one of the GC's, or in the GC that is an integral part of the TDAS.

APPENDIX F

APPLICATION OF THERMAL FOCUSING AND PROGRAMMED TEMPERATURE GAS CHROMATOGRAPHY IN THE TDAS

Appropriate application of temperature programming techniques is essential to the operation of the TDAS. Programmed increases of temperature with respect to time are applied sequentially to the sample insertion chamber, the effluent collection trap, and eventually the gas chromatographic column.

The transfer of thermal decomposition products from the collection trap and into the gas chromatographic column is a very important step and one that is crucial to the success of experiments conducted with the TDAS. This vitally important transfer is the subject of this appendix.

Chromatography is basically a dynamic separation process that uses the concept of differential migration. However, to obtain chromatographic separations, it is required that the unseparated mixture be deposited in a small locale at the start of the chromatographic process. Therefore, in the case of a mixture of widely different chemical compounds, which are emerging in somewhat random order from an effluent collection trap, it is necessary that the condensable compounds be concentrated in the inlet region of the gas chromatographic column. If the multicomponent sample can be placed within a low temperature region of a gas chromatographic column, it can subsequently be efficiently eluted, provided it is initially located in the column as a narrow longitudinal zone.

This thermal focusing process can be explained in fundamental migration terms. Specifically, the axial location of the centroid of like molecules migrating through a gas chromatographic column can be expressed as

$$z = \int_0^t v_m \left(\frac{1}{1+k}\right) dt \qquad \text{(F1)}$$

where z is the distance along the column axis, t is time, v_m is mobile phase velocity, and k is the partition ratio. The localized velocity of the migrating solute zone can then be written as

$$v_s = \frac{dz}{dt} = v_m \left(\frac{1}{1+k}\right) \tag{F2}$$

Even if k remains constant through the column length, it has been determined that the solute zone velocity experiences a very gradual increase as the zone migrates through the column. This small increase is due to the decompression of the carrier gas since

$$v_m = f(p) = \frac{p_o v_e}{p} = -\left(\frac{K}{\eta}\right)\frac{dp}{dz} \tag{F3}$$

where p is pressure, p_o is outlet pressure, v_e is mobile phase outlet velocity, K is column permeability, and η is the carrier gas viscosity. However, in usual GC practice, v_m does not change by more than a factor of two or three over the length of the column.

Now if k is initially very large and then diminishes with time, as in PTGC where it can eventually approach zero, it is seen from equation F2 that v_s experiences a many-fold increase with the passage of time. Therefore, if the given solute can be deposited in the column inlet while having a corresponding initial k or k_i such that

$$k_i \gg \bar{k}_e \tag{F4}$$

where $\bar{k}_e$ is the average partition ratio upon elution, it is evident that the initial v_s is very small indeed. Thus the time period over which the solute zone is deposited is of small consequence. If k_i is sufficiently large, the sample depositing time can be tens of minutes.

To capture a solute zone as a narrow distribution in the inlet portion of the chromatographic column, it is necessary that there be a pronounced longitudinal temperature gradient between the heated inlet block and the effective inlet portion of the chromatographic column. For this in-line thermal focusing of solute molecules to be efficient, it is important that the thermal gradient between the heated inlet block and the effective region of the column inlet be an even gradient. That is, there can be no intermediate cold spots or changes in the sign of the gradient. If this occurs, the chromatographic performance will definitely be affected, both qualitatively and quantitatively.

The selection of the liquid phase used for thermal focusing and subsequent PTGC is also important. A good liquid phase should have a broad liquid range. It should have low viscosity at the initial temperature of the program, and it should also have good thermal stability at the elevated final temperature. At no time should the stationary phase be allowed to solidify, because the solute will then be trapped by adsorption and not liquid partitioning. As a result of such capturing of sample, the resulting chromatographic peaks will be distorted. Also, the retention characteristics will be unknown, since the components experience undetermined extents of both adsorption and liquid partitioning during their subsequent migration.

APPENDIX G

APPROXIMATE COSTS OF TDU COMPONENTS

A number of companies have expressed an interest in the TDAS and its capabilities. Representatives from the following companies have visited the Research Institute facilities at the University of Dayton and observed the TDAS in various stages of its development:

Acurex Corporation
Babcock & Wilcox Company
Dow Chemical Company
Goodyear Tire & Rubber Company
Tennessee Eastman Company
TRW Incorporated
Shell Development Company
Union Carbide Corporation

There have been many inquiries about the cost of assembling a TDAS, particularly the costs of the various components that constitute the TDU. For this reason, this appendix was compiled showing a breakdown of the approximate costs (estimated 1978 prices) of the TDU components.

Gas purification filters	$ 395
Pressure regulators, flow regulators, and flow control valves	640
Tubing and tube fittings	480
Temperature programmed power supply	970
Digital voltmeter and mounting accessories	650
Pyrolysis probe power supply, probes, and accessories	1300
Console, instrumentation panels, name plates, etc.	680
Shielded thermocouple wire, thermocouple selector switch, and terminals	390
Digital temperature readout devices	510
Power switch boxes	130
Gas switching valves	360
Variacs, powerstats, and accessories	115
Pressure transducer and associated electronics	610
Mass flow transducer and associated electronics	645
Electrical terminals, switches, and wiring	75
Materials and machining of support brackets for sample inlet device	400

Fabricated heating blocks and cartridge heaters	$ 325
Heating tapes	150
Quartz stock	130
Quartzware fabrication costs	1100
High-temperature, 3-zone furnace and control console	2900
Rigid table for furnace and reactor	250
Glass insulating tape and adhesive glass tape	30
Vespel ferrules	25
High temperature insulation	15
Trapping media	50
Liquid nitrogen reservoir	30
Glass-lined stainless steel tubing	80
Valve oven	150
Support clamps and associated hardware	30
Calibrated sheathed thermocouple	90
Total estimated costs*	$13,705

*Minus assembly costs.

TECHNICAL REPORT DATA
(Please read Instructions on the reverse before completing)

1. REPORT NO. EPA-600/2-80-098	2.	3. RECIPIENT'S ACCESSION NO.
4. TITLE AND SUBTITLE DESIGN CONSIDERATIONS FOR A THERMAL DECOMPOSITION ANALYTICAL SYSTEM		5. REPORT DATE August 1980 (Issuing Date)
		6. PERFORMING ORGANIZATION CODE
7. AUTHOR(S) Wayne A. Rubey		8. PERFORMING ORGANIZATION REPORT NO.
9. PERFORMING ORGANIZATION NAME AND ADDRESS University of Dayton Research Institute 300 College Park Dayton, OH 45469		10. PROGRAM ELEMENT NO. SOS#4 Task#1 A73D1C
		11. CONTRACT/GRANT NO. R805117-01-0
12. SPONSORING AGENCY NAME AND ADDRESS Municipal Environmental Research Laboratory--Cin., OH Office of Research and Development U.S. Environmental Protection Agency Cincinnati, OH 45268		13. TYPE OF REPORT AND PERIOD COVERED
		14. SPONSORING AGENCY CODE EPA/600/14

15. SUPPLEMENTARY NOTES

Richard A. Carnes (Project Officer) 513/684-4303

16. ABSTRACT

Controlled high-temperature incineration is one of the most promising methods for obtaining safe and permanent disposal of highly toxic organic wastes. A sophisticated laboratory system has been designed and assembled to provide fundamental thermal decomposition data on a wide assortment of organic materials. This thermal decomposition analytical system (TDAS) is a specially designed, closed, continuous system consisting of a versatile and fully instrumented thermal decomposition unit which is connected to dedicated in-line gas chromatography, mass spectrometry, and data reduction equipment. The TDAS has been designed to generate fundamental thermal decomposition data rapidly, economically, and safely. These laboratory data should be instrumental in establishing acceptable criteria for controlled high-temperature incineration of toxic organic wastes.

17. KEY WORDS AND DOCUMENT ANALYSIS

a. DESCRIPTORS	b. IDENTIFIERS/OPEN ENDED TERMS	c. COSATI Field/Group
Organic Compounds Degradation Temperature Detoxification Recombination Reactions Research	Retention Time Excess Air	13B

18. DISTRIBUTION STATEMENT Release to Public	19. SECURITY CLASS *(This Report)* UNCLASSIFIED	21. NO. OF PAGES 158
	20. SECURITY CLASS *(This page)* UNCLASSIFIED	22. PRICE

EPA Form 2220-1 (9-73)

☆ U.S. GOVERNMENT PRINTING OFFICE: 1980--657-165/0054

United States
Environmental Protection
Agency

Center for Environmental Research
Information
Cincinnati OH 45268

Postage and
Fees Paid
Environmental
Protection
Agency
EPA-335

Official Business
Penalty for Private Use, $300

Special Fourth-Class Rate
Book

Please make all necessary changes on the above label, detach or copy, and return to the address in the upper left-hand corner.

If you do not wish to receive these reports CHECK HERE ☐; detach, or copy this cover, and return to the address in the upper left-hand corner.

EPA-600/2-80-098